SPARGER STUDY IN FLOTATION COLUMNS

Manqiu Xu

A thesis submitted to the

Faculty of Graduate Studies and Research

in partial fulfillment of the requirements for

the degree of Master of Engineering

Department of Mining and Metallurgical Engineering

McGill University

ABSTRACT

A technique of bubble size estimation in a bubble swarm is developed from drift-flux and Masliyah's hindered settling equation with the particular contributions of Dobby et al [24] and Yianatos et al [88]. The measurements required by the technique are superficial gas and liquid velocities and gas holdup. Predicted and measured (by photography) bubble sizes agree within 15% over the tested range 0.5-1.5 mm. The upper bound of applicability is a bubble Reynolds number approximately 500, or bubble size approximately 2 mm, making it well suited to flotation studies. In principle, there is no lower bound to applicability of the method (a practical limit with the present photographic measurements approximately 0.2 mm).

A scale-up model of spargers in column flotation is developed. The model provides an effective tool for the control of bubble size and insight in understanding the effect of sparger sizes on bubble diameter. Bubble size is shown to depend on the frother addition and the surface area of the sparger, with a minor contribution from sparger material. A sparger design criterion is suggested: the ratio of column cross-sectional area to sparger surface area (Rs) should be 0.5 to 1.

RESUME

On a développé une technique pour estimer la taille des bulles dans un essaim de bulles en se servant de l' analyse du flux de glissement et de l'équation de sédimentation retenue développée par Masliyah. Cette technique nécessite la mesure des vélocités superficielles du gaz et du liquide, et de la fraction gazeuse. La taille prédite des bulles par le modele est en accord avec la taille mesurée (par photographie) à ±15%, et ce pour des diamètres de bulle de 0.5 à 1.5 mm. La technique pourrait s'appliquer jusqu'à des nombres de Reynolds (des bulles) de 500, ou des bulles de 2 mm de diamètre. Elle convient donc parfaitement aux systèmes de flottation. En principe, il n'y a pas de limite inférieure à la taille des bulles qu'on peut mesurer avec cette technique (cette limite inférieure est de 0.2mm faites à partir de photographies).

Nous avons développé un modèle pour le dimensionnement des disperseurs de bulles. Ce modèle peut servir à obtenir la taille de bulles voulue et à mieux comprendre l'effet qu'a la dimension des disperseurs sur la taille des bulles. La taille de ces dernières dépend surtout de l'aire du disperseur et, dans une moindre mesure, du matériel duquel le disperseur est forme . On suggère que, pour dimensionner un disperseur , le ratio (Rs) diamètre de la colonne/aire du disperseur soit de 0.5 à 1.

ACKNOWLEDGEMENTS

I am indebted especially to two people:

My wife, Lilan, for her surpport and understanding throughout the past two years, and

Professor J.A. Finch, my supervisor, for his enthusiam, keen interest, excellent advice and constant encouragement.

As well, I gratefully acknowledge Dr. A.R. Laplante, Dr. G.S. Dobby (University of Toronto), Dr. M.H. Moys (University of Wittwatersand, South Africa) and Dr. S.R. Rao for helpful discussions.

I also want to thank my colleages Dr. J. Yianatos, Dr. R. Espinosa, Dr. R. del Villar, Mr. M. Kaya, Mr. R. Lastra and Mr. G. Shen for discussion and help.

The assistance of the following people is also gratefully acknowledged: M. Leroux and M. Knoepel for their help and assistance in the experimental set-up.

All funding is gratefully acknowledged.

Table of Contents

ABSTRACT.....i

RESUME.....ii

ACKNOWLEDGEMENT.....iv

TABLE OF CONTENTS.....v

NOMENCLATURE.....ix

LIST OF FIGURES.....xii

LIST OF TABLES.....xvi

CHAPTER 1 INTRODUCTION

1-1 Development of Flotation Column.....1

1-2 Objectives of Research Work.....2

1-3 Outline of the Thesis.....2

CHAPTER 2 GENERAL REVIEW OF COLUMN FLOTATION FUNDAMENTALS

2-1 Column Operating Variables.....4

2-1-1 Gas Holdup.....4
2-1-2 Bubble Size.....4
2-1-3 Gas Flowrate.....7
2-1-4 Wash Water and Bias Rate.....8
2-1-5 Slurry Downward Flowrate.....9
2-1-6 Residence Time.....9

2-2 Collection Zone.....10

2-2-1 Collection Efficiency and Rate Constant.....11
2-2-2 Mixing Characteristics and Recovery.....12
2-2-3 Total Recovery, and Froth Recovery.....17

2-3 Froth Zone.....18

2-3-1 Hydrodynamics.....18
2-3-2 Clean Action.....23
2-3-3 Selectivity.....28

2-4 Control Strategies: Current and Proposed.....28

2-4-1 Stabilizing Control.....28
2-4-2 Performance Control.....34
2-4-3 Novel Control Possibilities: Use of Temperature.....36

CHAPTER 3 PREVIOUS WORK ON BUBBLE FORMATION AT A SPARGER

3-1 Introduction.....39

3-2 Bubble Formation and Effect of Gas Flowrate.....39

3-2-1 Very Low Gas Flowrate.....42
3-2-2 Moderately High Gas Flowrate.....42
3-2-3 Very High Gas Flowrate.....43

3-3 Effects of Surfactants.....43

3-4 Effects of Sparger.....44

3-4-1 Orifice Size and Porosity.....45
3-4-2 Sparger Materials.....46

3-5 Effects of Flow of Continuous Fluid.....46

CHAPTER 4 THEORY: DEVELOPMENT OF BUBBLE SIZE ESTIMA TION TECHNIQUE AND SPARGER SCALE-UP MODEL

4-1 Bubble Size Estimation.....48

4-1-1 Dobby's Method.....48
4-1-2 Developed Method.....51

4-2 Development of Sparger Scale-up Model.....53

CHAPTER 5 EXPERIMENTAL

5-1 Laboratory Column Set-up.....57

5-1-1 Measurement of Gas Holdup.....57
5-1-2 Measurement of Bubble Diameter.....60
5-1-3 Morphology of Sparger Types.....61

5-2 Operation of Laboratory Column.....65

5-3 Experimental Design.....69

5-3-1 Verification of Bubble Size Estimation Technique.....69
5-3-2 Effects of Operating Variables on Gas Holdup and Bubble Size.....69
5-3-3 Testing Effect of Sparger Surface Area.....73

5-4 Plant Test of Pilot Unit.....73

CHAPTER 6 RESULTS: VERIFICATION OF BUBBLE SIZE ESTIMATION TECHNIQUE

6-1 Photographic Measurement of Bubble Size.....78

6-2 Comparison between Dobby's Method, Developed Method and Photographic Measurement.....79

6-3 In Flotation Columns.....84

6-4 In Mechanical Cells.....84

CHAPTER 7 RESULTS: EFFECTS OF OPERATING VARIABLES ON GAS HOLDUP AND BUBBLE SIZE

7-1 Gas Holdup and the Effect of Gas Flowrate and Frother Addition.....89

7-2 Bubble Formation and the Impact of Gas Flowrate and Frother Addition.....93

7-3 The Influence of Gas Sparger Types on Gas Holdup and Bubble Size.....97

CHAPTER 8 RESULTS: TESTING THE EFFECT OF SPARGER SIZE A SCALE-UP MODEL

8-1 Laboratory Studies.....106

8-1-1 Minimum Gas Flowrate, Gas Maldistribution and Bubble Coalescence.....106
8-1-2 Ceramic Sparger Series.....108
8-1-3 Steel Sparger Series.....112
8-1-4 Cloth Sparger Series.....112

8-2 Pilot Unit Tests.....119

CHAPTER 9 DISCUSSION

9-1 Bubble Size Estimation Technique.....122

9-2 Effects of Operating Variables on Gas Holdup and Bubble Size.....123

9-3 Sparger Scale-up.....126

CHAPTER 10 CONCLUSIONS AND SUGGESTIONS FOR FUTURE WORK

10-1 Summary of Conclusions.....130

10-1-1 Technique of Bubble Size Estimation.....130
10-1-2 Effects of Operating Variables on Gas Holdup and Bubble Size.....131
10-1-3 Sparger Scale-up Model.....131

10-2 Suggestions for Future Work.....131

10-2-1 Bubble Size Estimation Technique.....131
10-2-2 Sparger Design and Scale-up.....132
10-2-3 Wash Water Distributor Design.....132
10-2-4 Numerical Analysis of Flow Mechanism in a Flotation Column.....132

REFFERENCES.....134

APPENDIX A Complementary information for Fig.2-12 and Fig.2-13.....141

APPENDIX B Some experimental data selected.....142

APPENDIX C Computer program for the estimation of bubble size by the developed method.....144

APPENDIX D Regression program for the experimental data processing.....145

APPENDIX E Derivation of $F(\varepsilon_l) = \varepsilon_l^{m-1}$ 148

APPENDIX F Flowmeter calibration.....150

APPENDIX G CARRYING CAPACITY IN COLUMNS - GAS RATE AND BUBBLE SIZE EFFECTS (manuscript).....152

APPENDIX H Computer program for the maximum bubble/particle aggregate density.....175

NOMENCLATURE

a	parameter in Eq.[2-16]
Ac	column cross-sectional area, cm^2
Ao	opening area of an orifice of a sparger, cm^2
As	sparger surface area, cm^2
Br	bias ratio
C	constant in Eq.[4-15]
C_D	orifice discharge coefficient, dimensionless
C_o	parameter in Eq.[4-7]
db	bubble diameter, cm
dbi	individual bubble diameter measured by photography,
dbs	Suater mean diameter defined in Eq.[6-1], cm
dbv	volumetric mean diameter defined in Eq.[6-2], cm
db^{cr}	critical bubble diameter defined in Eq.[2-2], cm
dc	column diameter, cm
do	orifice diameter of a sparger, cm
Ek	collection efficiency, fractional or percentage
E_l	liquid axial dispersion coefficient
F	bubble formation frequency, s^{-1}
g	acceleration due to gravity
K	flotation rate constant
Ko	parameter in Eq.[4-7]
L	collection zone length, cm or m
M	parameter in Eq.[4-8]

n	constant in Eq.[4-15]
N	number of orifices of a sparger
m	parameter defined in Eq.[4-3]
Nd	dimensionless vessel dispersion number
P	parameter in Eq.[4-8]
ΔP_o	orifice pressure drop defined in Eq.[4-22], kg/m^2
Q_B	bias flowrate, cm^3/s
Q_g	volumetric gas flowrate into a column, cm^3/s
Q_F	feed flowrate, cm^3/s
Q_T	tailing discharge flowrate, cm^3/s
Q_o	orifice gas flowrate, cm^3/s
R	recovery
Rc	collection zone recovery
Rf	froth zone recovery
Rt	total recovery of a flotation column
Rs	ratio of column cross-sectional area to sparger surface
Re	Reynolds number defined in Eq.[4-5]
Reb	bubble Reynolds number defined in Eq.[4-10]
Ti	induction time, ms
Ui	interstitial liquid velocity, cm/s
U_p	particle settling velocity, cm/s
U_T	terminal velocity of a bubble, cm/s
Us	slip velocity. cm/s
Vg	superficial gas velocity, cm/s
V_l	superficial liquid velocity, cm/s
V_{sl}	superficial slurry velocity, cm/s

Vb	superficial bias flowrate, cm/s
Vc	superficial concentrate rate, cm/s
Vw	superficial wash water rate, cm/s
Vo	superficial orifice gas flowrate, cm/s
Weo	Weber number based on orifice defined in Eq.[3-1]

GREEK SYMBOLS

α	constant in Eq.[4-13]
β	constant in Eq.[4-13]
π	pi number
μ	liquid viscosity, g/cm·s
ψ	parameter in Eq.[4-21]
φ	parameter in Eq.[4-21]
ε_c	fractional concentate at the top of a column
ε_g	fractional gas holdup
ε_l	fractional liquid holdup
τ	norminal or liquid (slurry) retention time, s
τ_p	solid particle retention time, s
δ	surface tension, kg/s^2
ρ_b	bubble/particle aggregate density, g/cm^3
ρ_l	liquid density, g/cm^3
ρ_s	particle density, g/cm^3
ρ_g	gas density, g/cm^3
ρ_{susp}	suspension density in liquid, g/cm^3
ϕ_o	porosity, number of orifices per unit sparger area

LIST OF FIGURES

Fig.2-1 General illustration of a flotation column

Fig.2-2 Simulation example of effect of gas rate on db, Ek and K for operating system where $db = C\ Vg^n$ n=0.53, dp=10 μm, Ti=30 ms, V_l =0 [17]

Fig.2-3 Collection efficiency vs. particle size and induction time for the flotation model db=0.1 cm, Ui=10 cm/s, μ =0.01 poise particle s.g. = 4.0, gas holdup ε_g = 0 [17]

Fig.2-4 Froth bed expansion in a laboratory flotation column [80]

Fig.2-5 Bubble surface loss along froth zone [80]

Fig.2-6 Froth structure in a flotation column [80]

Fig.2-7 Concentration vs. time - response curve of tracer test [80]

Fig.2-8 The nature of the relationship between recovery rate of hydrophilic particles and water due to entrainment (after Lynch et al [45])

Fig.2-9 Dependence of flotation rates of valuable sulphide (galena), gangue sulphide (marmatite) and non-sulphide gangue on the flotation rate of water (after Lynch et al [45])

Fig.2-10 The mass transfer in a flotation column a) positive bias b) negative bias

Fig.2-11 Retention time vs. feed flowrate under different control loops [78] conditions: column 0.9m x 0.9m x 10 m bias = 0.2 m/min at Gaspe ratio = 1.2 at Gibraltar

Fig.2-12 Wash water flowrate vs. feed flowrate. under different control loops [78] conditions: the same as in Fig.2-11

Fig.2-13 Effect of changes in gas rate and level setpoint on level measurement [51]

Fig.2-14 Effect of measurement methods on the accuracy of level measurement (from Moys et al [51])

Fig.3-1 Bubble formation on rigid sparger: the effect of gas flowrate

Fig.5-1 Laboratory Experimental Set-up

Fig.5-2 A special design of sparger system for the scale-up study of spargers

Fig.5-3 General illustration of a sparger surface

Fig.5-4 Microscopical observation of stainless steel sparger surface

Fig.5-5 Microscopical observation of rubber sparger surface

Fig.5-6 Microscopical observation of ceramic sparger surface

Fig.5-7 Microscopical observation of filter cloth sparger surface

Fig.5-8 Pilot Unit Set-up in plant

Fig.6-1 A typical bubble size distribution in a column

Fig.6-2 The typical relationship betweem gas holdup and superficial gas velocity

Fig.6-3 The drift-flux plot to estimate the terminal rise velocity of bubbles. the data is based on Fig.6-2

Fig.6-4 Bubble size vs. superficial gas velocity, the comparison of measured bubble size with those estimated by the developed and Dobby's methods.

Fig.6-5 Comparison of measured (Sauter mean) with predicted bubble size by the developed method in flotation columns

Fig.6-6 Comparison between calculated and measured bubble size in mechanical flotation machines

Fig.7-1 Gas holdup vs. superficial gas velocity

Fig.7-2 Gas holdup vs. superficial gas velocity

Fig.7-3 Gas holdup vs. frother addition

Fig.7-4 Bubble size vs. superficial gas velocity

Fig.7-5 Photographies showing the effect of frother addition on bubble size

Fig.7-6 Bubble size vs. superficial gas velocity

Fig.7-7 Bubble size vs. gas flowrate per unit area of sparger [Rs.Vg]

Fig.7-8 Bubble size vs. superficial gas velocity (bubble size is measured by photography)

Fig.7-9 Bubble size distribution for the four type of spargers used in this work without frother Vg = 1 cm/s

Fig.7-10 Bubble size distribution for stainless steel sparger with frother addition frother concentration: 15 ppm

Fig.7-11 Gas holdup vs. superficial gas velocity for the four type os spargers used in this work

Fig.7-12 Bubble size vs. superficial gas velocity

Fig.7-13 Bubble size vs. gas flowrate per unit area of sparger [Rs.Vg]

Fig.8-1 Minimum available superficial gas velocity: the effect of sparger surface

Fig.8-2 The effect of gas maldistribution on gas holdup

Fig.8-3 The effect of bubble coalescence on gas holdup

Fig.8-4 Gas holdup vs. superficial gas velocity for ceramic sparger series [Tests No.1-No.7]

Fig.8-5 Bubble size vs. superficial gas velocity

Fig.8-6 Bubble size vs. gas flowrate per unit area of sparger for ceramic sparger series

Fig.8-7 Gas holdup vs. superficial gas velocity for steel sparger series [Tests No.8-No.13]

Fig.8-8 Bubble size vs. gas flowrate per unit area of sparger for steel sparger series

Fig.8-9 Gas holdup vs. superficial gas velocity for cloth sparger series [Tests No.14-No.20]

Fig.8-10 Bubble size vs. gas flowrate per unit area of sparger for cloth sparger series

Fig.8-11 Bubble size vs. gas flowrate per unit area of sparger for the three type of spargers

Fig.8-12 Mass recovery vs. superficial gas velocity

Fig.8-13 Concentrate recovery vs. superficial gas velocity: the effect of sparger size

Fig.9-1 The relationship between parameter α and ratio Rs

Fig.9-2 Log[db] vs. Log[Rs.Vg], the regression line and 90% confidence interval limits for ceramic sparger

Fig.9-3 Log[db] vs. Log[Rs.Vg], the regression line and 90% confidence interval limits for filter cloth sparger

LIST OF TABLES

TABLE	2-1	Stabilizing control strategies in use
TABLE	2-2	Performance control strategies in use
TABLE	5-1	Description of spargers used in this work
TABLE	5-2	Column characteristics for verification of bubble size estimation technique
TABLE	5-3	Test conditions for verification of bubble size estimation technique
TABLE	5-4	Test conditions for the effect of operating variables on gas holdup and bubble size
TABLE	5-5	Sparger sizes for testing sparger scale-up
TABLE	5-6	Sparger and column combinations for testing sparger scale-up
TABLE	6-1	Bubble size measured and predicted
TABLE	6-2	Test conditions and results

CHAPTER 1

INTRODUCTION

1-1 Development of Flotation Column

Extensive research work has been done recently on flotation columns [15, 17-26, 73-88], some 20 years after the column was first introduced in Canada [4, 9-10]. Industrial applications of flotation columns are now widespread [12, 14-15, 26]. Following the work of Sastry and Fuerstenau [60], Flint and Howarth [27] and Rice et al [57], Dobby and Finch investigated extensively particle collection in a flotation column and the requirements for flotation column modelling and scale-up [17-23]. Subsequently, Yianatos, Finch and Laplante directed attention to flotation column froth behaviour since the froth has a significant effect on column performance [80-85]. Three aspects were stressed: froth hydrodynamics, cleaning action (rejection of hydraulically entrained particles) and selectivity (separation between particles of different hydrophobicity). Meanwhile, Espinosa and Finch conducted work on slime flotation by column [25-26]. Some fundamental research concerning flotation kinetics [47, 76] and aerosol frother addition and column control [28, 51, 87] has been conducted around the world.

1-2 Objectives of the Research Work

The study is to investigate bubble generation using spargers (bubble generating devices) by determining the effects of sparger material and sparger size (surface area) on gas holdup and bubble size. In order to be able to conduct this work, a novel method to estimate bubble size was developed from the contributions of Dobby et al [24] and Yianatos et al [88]. Using this technique the problem of photographic measurement of bubble size was eliminated, permitting the effect of operating variables on gas holdup and bubble size to be extensively investigated. The ultimate objective is to provide a methodology of sparger sizing for flotation columns.

1-3 Outline of the Thesis

The thesis consists of 10 chapters. Chapter 1 is the general introduction and description of the research objectives. The operating fundamentals and new developments in flotation columns are briefly reviewed in chapter 2. Column operating variables, particle collection kinetics, column froth characteristics, and column control strategies are described and discussed.

In chapter 3, previous work related to bubble formation and the effects of some parameters on gas holdup and bubble size are reviewed. Chapter 4 proposes a technique for the estimation of bubble size which was used in the next chapters.

Finally, a scale-up model for spargers is developed.

In chapter 5, the experimental system and column operation are described. In particular, the experimental design is presented in some detail. All the experimental results are presented in chapters 6, 7 and 8. The data used to verify the bubble size estimation technique is presented in chapter 6. It is shown that the bubble size estimation technique gives a very close prediction of bubble size. Chapter 7 presents the results concerning the effect of operating variables on gas holdup and bubble size. It is found that the major factors affecting gas holdup and bubble size are frother concentration, gas flowrate and sparger size. In chapter 8, the proposed scale-up procedure for spargers is examined. It is demonstrated that the model provides a rational explanation for the effect of sparger size on bubble size.

Finally, all the results are critically discussed in chapter 9. In chapter 10, thesis conclusions, with suggestions for future work, are presented.

CHAPTER 2

GENERAL REVIEW OF COLUMN FLOTATION FUNDAMENTALS

2-1 Column Operating Variables

For a flotation column as shown in Fig.2-1, there are two readily identifiable zones: the collection zone (also known as recovery or bubbly zone) and froth zone (cleaning zone). There exist a large number of variables which affect column performance. A brief description of these variables are given below.

2-1-1 Gas Holdup

Gas holdup is defined as the volumetric fraction of air in the air/slurry mixture and is used to characterize the hydrodynamics of the column [61]. It is a combined function of bubble size and gas rate and varies directly with gas rate and inversely with bubble size. Consequently, gas holdup can not be adjusted independently of bubble size and gas rate.

2-1-2 Bubble Size

Bubble size is considered to be the most important variable for the physical optimization of flotation [8,35]. For example, recent evidence suggests that fine bubbles are able to float fine particles more effectively than coarse

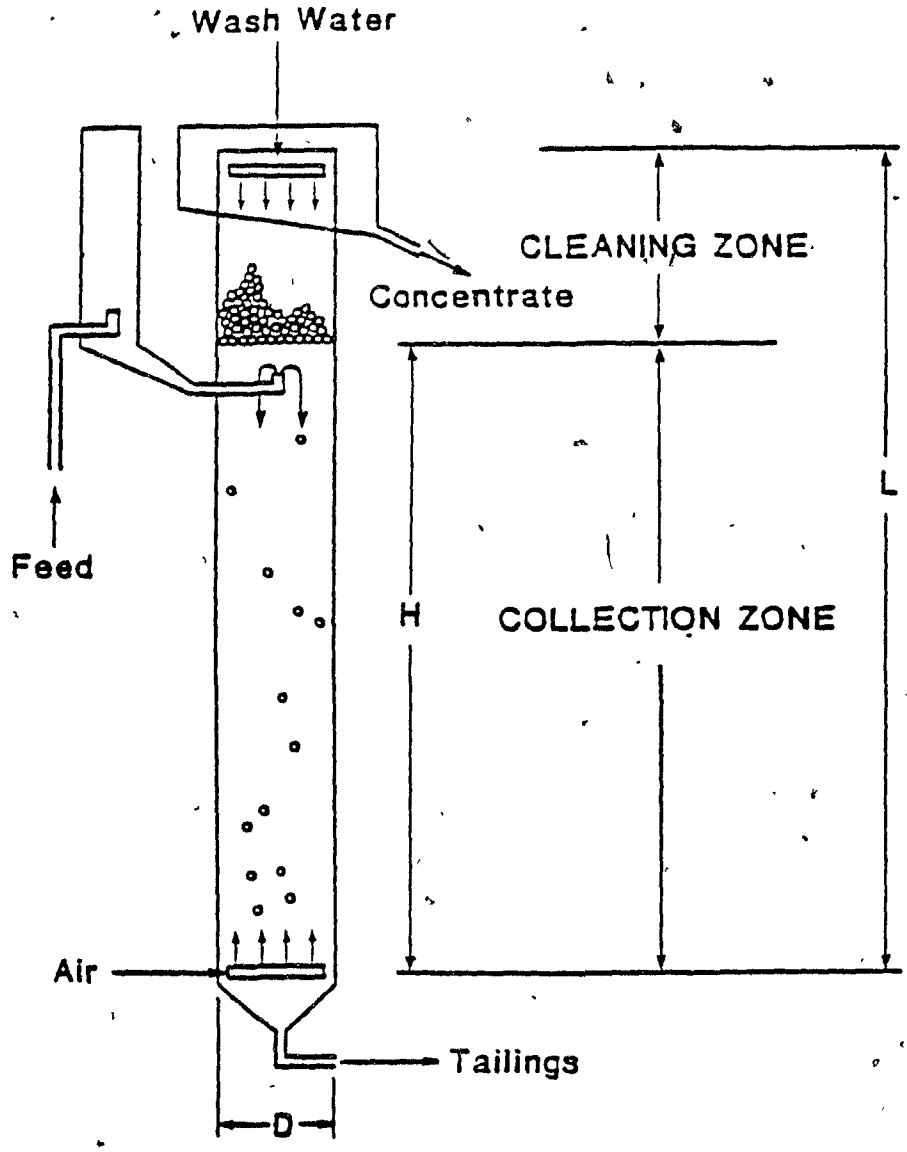

Fig.2–1 General illustration of a flotation column

bubbles. Szatkowski et al [63-65] investigated the flotation kinetics with fine bubbles and claimed that critical bubble size can be determined as a function of particle size and density:

$$\rho_l\, g\, (db^{cr})^3 - \pi\, dp\, g\, (\rho_s - \rho_l)\, (db^{cr})^2 - 18\, db^{cr}\, \mu\, Vs_l - 36\, dp\, \mu\, Vs_l = 0 \qquad [2\text{-}1]$$

where V_l is the average net downward velocity of slurry.

The critical bubble size is defined as the diameter of the smallest mineral-laden bubbles which still rise to the froth against an opposite pulp flow in the flotation system. In stationary water, Eq.[2-1] can be simplified as follows:

$$db^{cr} = \frac{\pi\, (\rho_s - \rho_l)\, dp}{\rho_l} \qquad [2\text{-}2]$$

Ahmed and Jameson [1] investigated the effect of bubble size on the rate of flotation of fine particles and found that the rate of flotation of fines can be accelerated considerably using very small bubbles less than 100 μm in diameter.

Bogdanov et al [8] investigated the flotation of martite fine particles by different sized bubbles and found that without mixing, the flotation rate of - 10 μm particles was lowered when bubble size decreased from 0.5 to 0.2 mm.

The theoretical work by Dobby and Finch [22] suggests that small bubbles [db<o.5mm] are not effective in flotation columns because reducing bubble size means the gas flowrate must be reduced. The effect is that an optimum bubble size exists to maximize flotation rate. Recent work conducted in parallel with this thesis showed [77] that for particles $2\mu m < dp < 25\ \mu m$, the optimum bubble size to maximize carrying capacity is about 1-1.5 mm.

There are a large number of factors affecting bubble size in a flotation column. Among them gas rate and frother addition are the most important. In general, uniform bubbles with diameter db=1-1.5 mm can be readily achieved in flotation columns with gas flowrates Vg=1-3 cm/s in the presence of frother.

2-1-3 Gas Flowrate

Gas is introduced into a flotation column as bubbles usually generated by an internal sparger. Superficial gas velocity will be used to describe gas rate since it is independent of column dimensions. It is defined as the volumetric gas flowrate per unit column cross-sectional area per unit time. Typical range is Vg=1-3 cm/s [86]. (Gas rates are always given here at standard conditions)

Gas flowrate is one of the most important variables for flotation column operation. The required gas flowrate must be determined in each case. Gas rate has direct and indirect

effects. For example, gas rate directly affects rate constant and indirectly affects it by affecting bubble size. Gas flowrate has been used for flotation control in some Finnish and Australian conventional flotation plants [41].

2-1-4 Wash-Water and Bias Flowrate

Wash water added at the top of flotation column has two functions: (1) to provide a downward flow of water which prevents hydraulic entrainment of non-floatable minerals, (2) to increase froth stability and allow a deep froth bed to be built [83].

An estimate of the wash water requirement, (superficial wash water rate Vw, cm/s), is given by [86];

$$Vw = \frac{Vg\,\varepsilon_c}{1 - \varepsilon_c} + Vb \qquad [2-3]$$

where

$$\varepsilon_c = \frac{Vc}{Vc + Vg} \qquad [2-4]$$

and represents the fractional holdup of concentrate at the top of the column; Vb is the superficial bias flowrate, Vc the superficial concentrate rate, and Vg, the superficial gas flowrate.

A positive bias flowrate, Q_B, is obtained by having a tailing volumetic flowrate, Q_T, slightly greater than that of

the feed, Q_F. One way to control this is to maintain:

$$Q_B = Q_T - Q_F = \text{constant} > 0 \qquad [2\text{-}5]$$

Superficial bias rates Vb = 0.1-0.6 cm/s are used in plant practice.

Another way of achieving a positive bias is to maintain a ratio of tailing flowrate to that of feed constant at some value greater than one. This is a "bias ratio", Br, i.e.:

$$Br = \frac{Q_T}{Q_F} = \text{constant} > 1 \qquad [2\text{-}6]$$

Br values from 1.01 t0 1.15 are typically recommended [18]. The relative merits of both bias strategies for control are explored in some detail in section 2-4.

2-1-5 Slurry Downward Flowrate

A flotation column is operated in the countercurrent bubbly regime. The slurry downward flowrate is mainly determined by the required residence time of solids. In general, the superficial slurry downward flowrate V_l is in the range 1-2 cm/s. The downward slurry velocity has a significant effect on gas holdup.

2-1-6 Residence Time

Solids residence time governs recovery. The typical

range of slurry residence time is 2-10 minutes in laboratory and 10-20 in plant operations [86]. The mean residence time of slurry, , can be estimated as:

$$\tau = \frac{Ac\ L\ (1 - \varepsilon g)}{Q_T} \qquad [2\text{-}7]$$

where Ac is the column cross-sectional area, L represents the collection zone length (the distance between pulp/froth interface and air input level).

In a flotation column particle residence time, τ_p, is a function of the particle settling velocity (Up) and interstitial liquid velocity (Ui) [19,84]:

$$\frac{\tau_p}{\tau} = \frac{Ui}{Ui + Up} \qquad [2\text{-}8]$$

where Up is the particle settling velocity in a swarm of bubbles and particles. To estimate Up the equation of Masliyqh for hindered settling in a multispecies particle system can be used [84].

2-2 Collection Zone

A flotation column consists of two flow regimes: the collection zone (also known as recovery or bubbly zone) and

froth zone (cleaning zone). The two zones have different functions.

2-3-1 Collection Efficiency and Rate Constant

A mineral particle is recovered by a gas bubble in the collection zone of a column by one of two mechanisms: (1) particle-bubble collision followed by attachment due to the hydrophobic nature of the mineral surface (the true collection process), or, (2) entrainment of the particles within the boundary layer and in the wake of the bubbles. In a flotation column, tracer tests have shown that there is virtually no feed water entering the concentrate [19]. This is due to the wash water added at the top of a flotation column. Consequently there is no entrainment of particles to the concentrate [33, 45-46, 72].

The collection process in the collection zone is that of countercurrent bubble/particle collision and attachment. Dobby and Finch [23] have modelled the process. Collection efficiency, Ek, defined as the fraction of all particles swept out by the projected area of the bubble that collide with, attach to and remain attached to the bubble until reaching the cleaning zone was calculated. For a given system, the collection efficiency is a complex function of many parameters among which the most obvious are: particle size, bubble size and particle hydrophobicity. Collection rate constant, K, is

related to Ek by [36]:

$$K = \frac{1.5\ Vg\ Ek}{db} \qquad [2\text{-}9]$$

If Ek does not vary with solids content and bubble loading, the collection rate mechanism is first-order with respect to particle concentration. It is intuitive that Ek is constant only for a narrow range of particle size and for a single value of hydrophobicity.

Fig.2-2 is the simulation results from Dobby [17] and shows the effect of gas rate on collection efficiency, rate constant and bubble size. There exists a peak in collection rate constant for a range of gas flowrate. Fig.2-3 shows the effect of induction time and particle size on collection efficiency. As induction time decreases, collection efficiency Ek increases.

2-2-2 Mixing Charateristics and Recovery

Recovery is determined by three factors: the rate constant, the mean residence time of solid particles and the mixing conditions in the collection zone of a flotation column.

One extreme of mixing is plug flow, where the residence time of all elements of the fluid and all mineral particles is

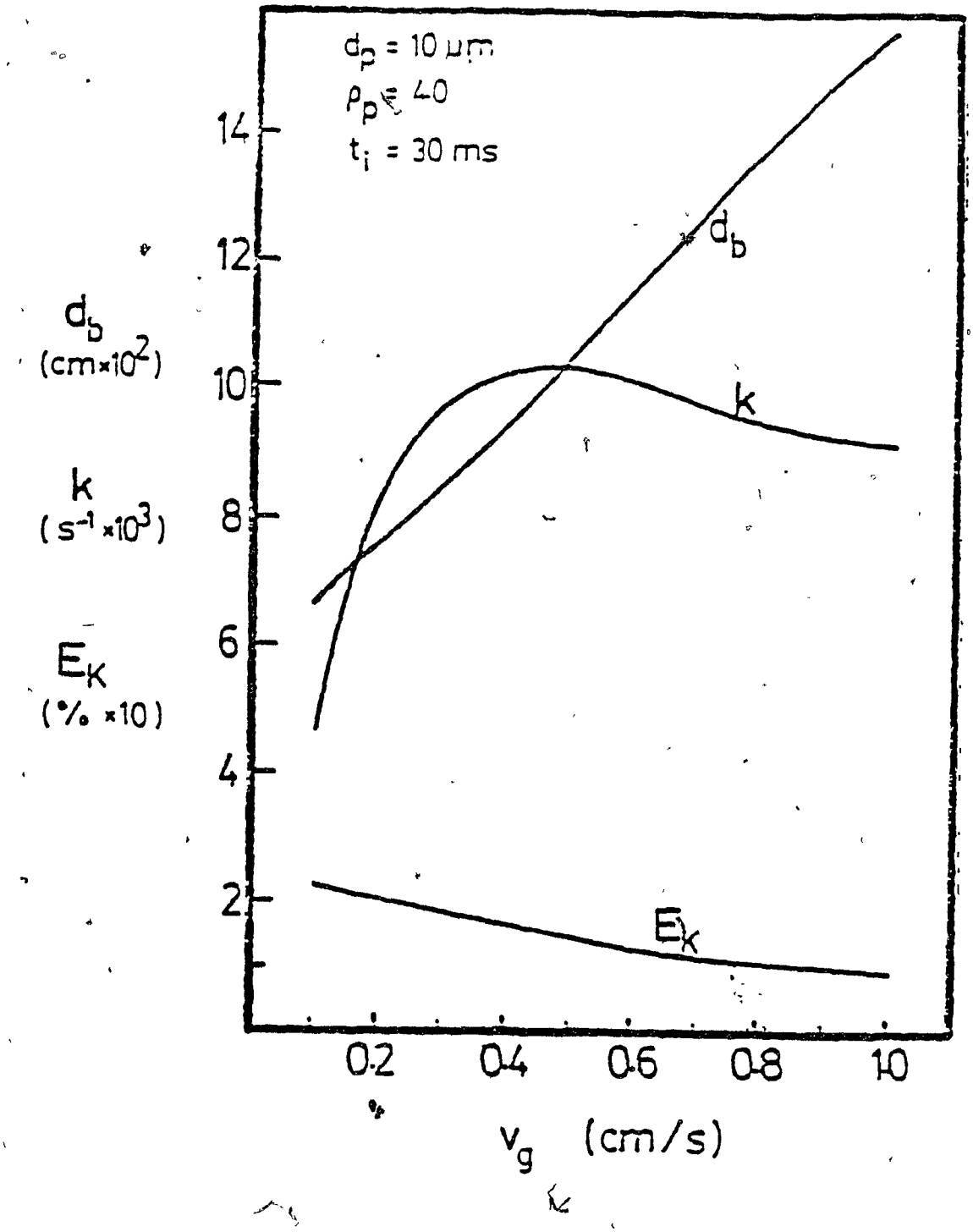

Fig.2-2 Simulation example of effect of gas rate on db, Ek and K for operating system where $db = C \cdot Vg^n$ n=0.53, dp=10 μm, Ti=30 ms, V_l =0 [17]

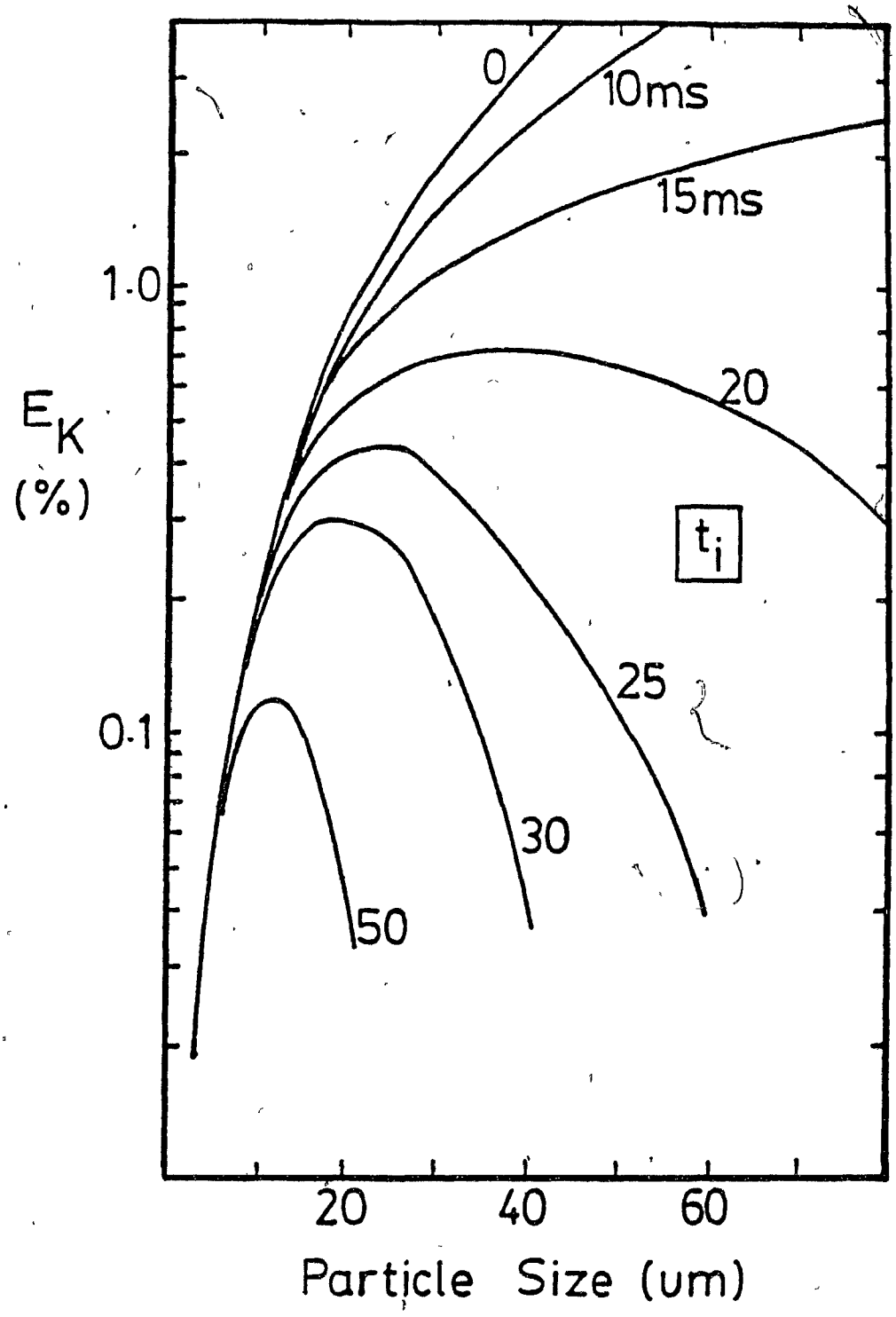

Fig.2–3 Collection efficiency vs. particle size and induction time for the flotation model db=0.1 cm, Ui=10 cm/s, μ=0.01 poise particle s.g. = 4.0, gas holdup $\varepsilon_g = 0$ [17]

the same. Consequently a concentration gradient of floatable mineral along the axis of the column exists. The other extreme is perfectly mixed flow in which there is a distribution of particle residence time and the solid concentration is the same throughout the system. For a first-order rate system having plug flow and a retention time, τ ,

$$R = 1 - \exp (- K\tau) \qquad [2\text{-}10]$$

and for a perfectly mixed first-order system having a mean retention time, τ ,

$$R = \frac{K\tau}{1 + K\tau} \qquad [2\text{-}11]$$

The flow conditions in a laboratory flotation column would approximate plug flow, while the mixing conditions in industrial columns would be between plug flow and perfectly mixed flow. The difference in performance between plug flow and perfectly mixed flow is significant. Therefore, it is important to know the degree of mixing of industrial flotation columns and to relate that mixing to recovery.

A dimensionless vessel dispersion number, Nd, and liquid axial dispersion coefficient, E_l , have been used to describe mixing in bubble columns, where,

$$Nd = \frac{dc\ E}{Ui\ L} \qquad [2\text{-}12]$$

and,

$$Ui = \frac{V_l}{1 - \varepsilon_g} \qquad [2\text{-}13]$$

where dc is the column diameter. Nd = 0 correspods to plug flow and Nd = ∞ corresponds to perfectly mixed flow.

The effect of various physical and operating parameters upon the liquid axial dispersion coefficient in bubble columns has been reviewed by Shah et al [62]. They conclude that for cylindrical columns E is essentially independent of liquid velocity and liquid properties such as viscosity, surface tension and density.

Dobby and Finch examined the mixing charateristics of industrial flotation column and proposed [19]:

$$E_l = 0.63\ dc \qquad [2\text{-}14]$$

with dc in meters, E_l in m /s. Further, they showed from particle tracer studies that;

$$Ep \approx E_l \qquad [2\text{-}15]$$

where Ep is the particle axial dispersion coefficient. E_l (and therefore Ep) is linked with Nd by the following

equation:

$$E_l = \frac{Nd\ L}{60\ \tau} \qquad [2\text{-}16]$$

For the purpose of scale-up and design of flotation columns Eq.[2-14] is quite adequate.

The objective of measuring the mixing parameters is to quantify the effect of mixing on recovery. For a first-order rate system, the recovery is given by [44]:

$$R = 1 - \frac{4\ a \exp\left(\frac{1}{2\ Nd}\right)}{(1+a)^2 \exp\left(\frac{a}{2\ Nd}\right) - (1-a)^2 \exp\left(-\frac{a}{2\ Nd}\right)}$$

where

$$a = \left(1 + 4\ K\ \tau^{\alpha} Nd\right)^{1/2} \qquad [2\text{-}17]$$

2-2-3 Total Recovery and Froth Recovery

Recovery in the previous discussion is the recovery of collection zone. Since a deep froth bed exists in a flotation column, some particles which have already entered the froth zone may drop back to the collection zone due to detachment. The work done by Yu [79] an Yianatos [80] shows that the recovery in froth zone can be lower than 50% depending on the froth depth.

Defining the froth zone recovery Rf as the recovery to the concentrate of particles entering the froth zone from collection zone then, for a collection zone recovery Rc, the total column recovery Rt is [17]:

$$Rt = \frac{Rc\ Rf}{1 - Rc\ (1-Rf)} \qquad [2-18]$$

2-3 Froth Zone

2-3-1 Hydrodynamics

The froth in a mechanical flotation cell is unstable and different from cell to cell. The froth in a flotation column is relatively stable due to the wash water added at the top of the flotation column. The chemical structure of the various types of frothers exerts a marked influence on frothing power and froth stability [43] in conventional froths, and this may be the case in column froths.

Fig.2-4 shows the froth bed expansion of a water-air system in a laboratory flotation column [83]. As wash water rate increases, froth depth increases. Thus, wash water addition is an important factor for the stablization of column froth. Yianatos et al [83] investigated the effect of gas rate and liquid downward flowrate on the local gas holdup and they found that an increase of either gas or liquid flowrate significantly increases the liquid content in the froth zone [81]. The higher liquid holdup in the froth zone will increase

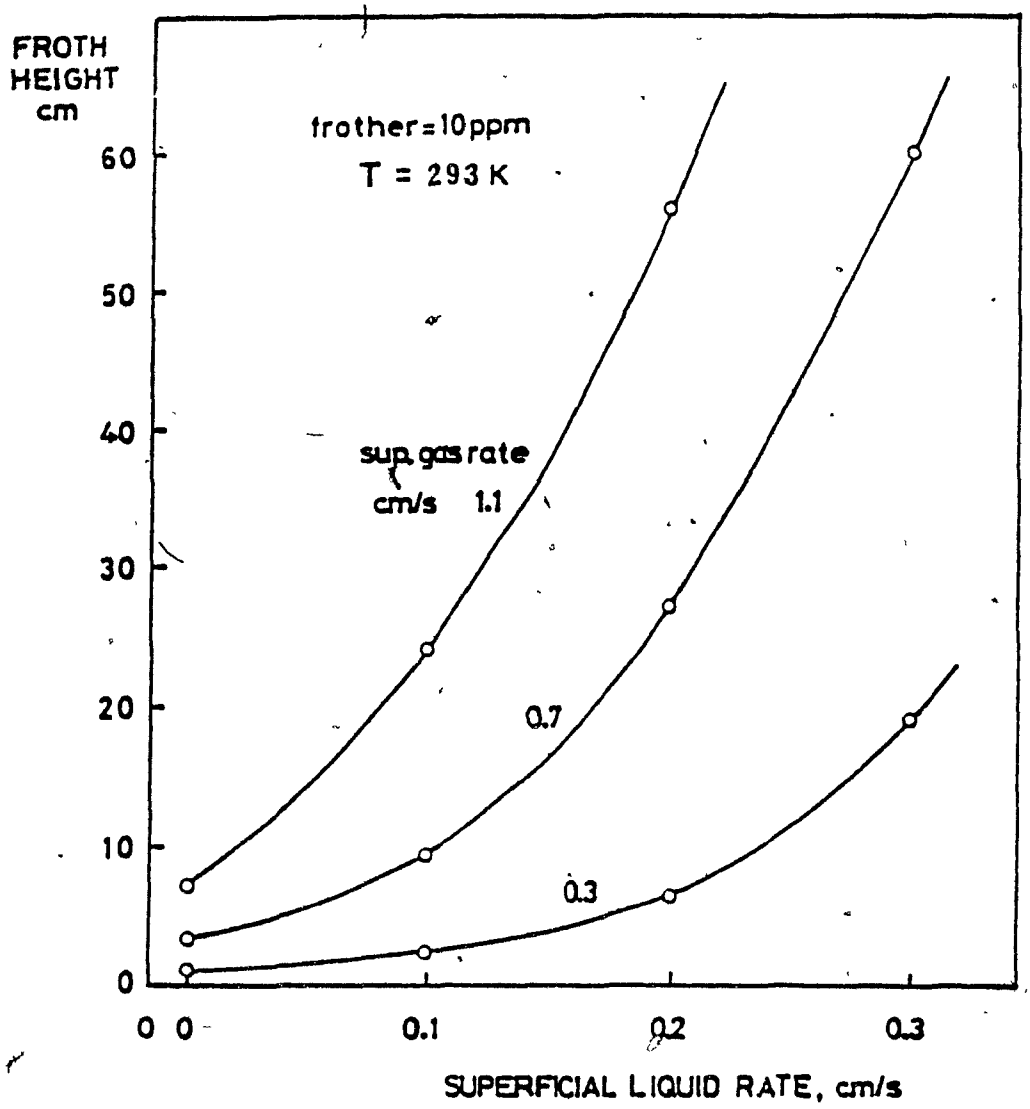

Fig.2–4 **Froth bed expansion in a laboratory flotation column [80]**

the internal liquid drainage and entrainment, which may cause an increase in the internal circulating load of gangue and weakly hydrophobic minerals. It has also been observed that a strong increase in wash water flowrate will drastically change the near plug flow regime of the bubble bed to a more heterogeneous behaviour including severe channelling and recirculation.

The experimental data show that the bubbles remain nearly spherical as coalescence increases bubble size to about 2-3 mm. Fig.2-5 shows the surface loss of bubbles due to the coalescence [81]. In this figure, "fractional surface" is used which is defined as the ratio between the total bubble surface per unit time crossing the bubble bed at a certain level and the total bubble surface per unit time entering the froth zone at the interface level.

Based on the experimental observation and measurement in the two dimensional column, the froth structure shown in Fig.2-6 has been proposed [83]. Basically, this structure consists of three sections: (1) an expanded bubble bed, (2) a packed bubble bed, and (3) a conventional draining froth.

(1) the expended bubble bed: Bubbles travel upward from the collection zone with very high rise velocity and enter the expanded bubble bed section after collision with the first layer of bubbles which define a very distinct interface. At this stage bubbles have a quite homogeneous and small size (similar to that of the collection zone, 1-2 mm) and remain spherical. Bubble collisions against the interface generate a

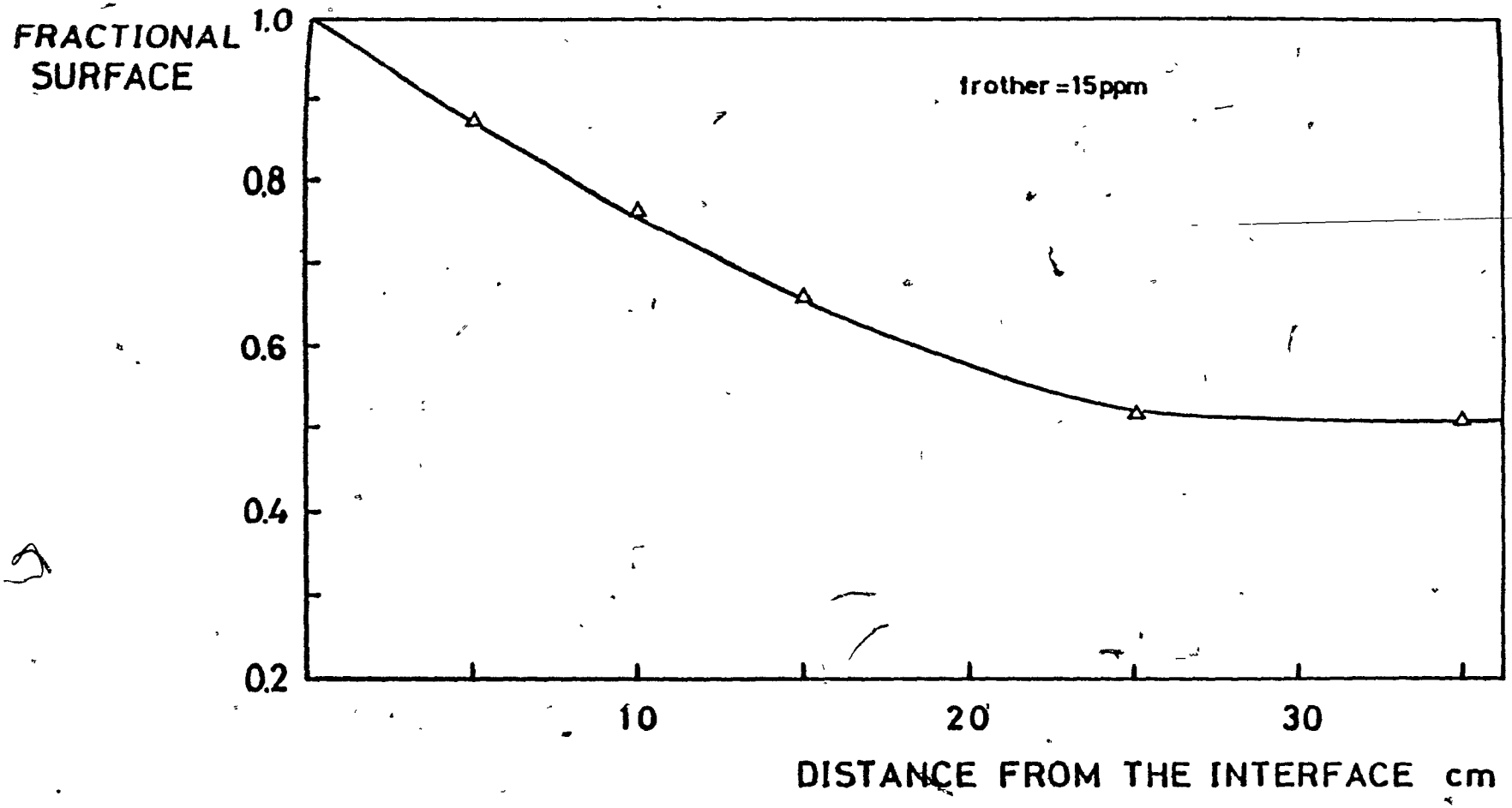

Fig.2–5 Bubble surface loss along froth zone [80]

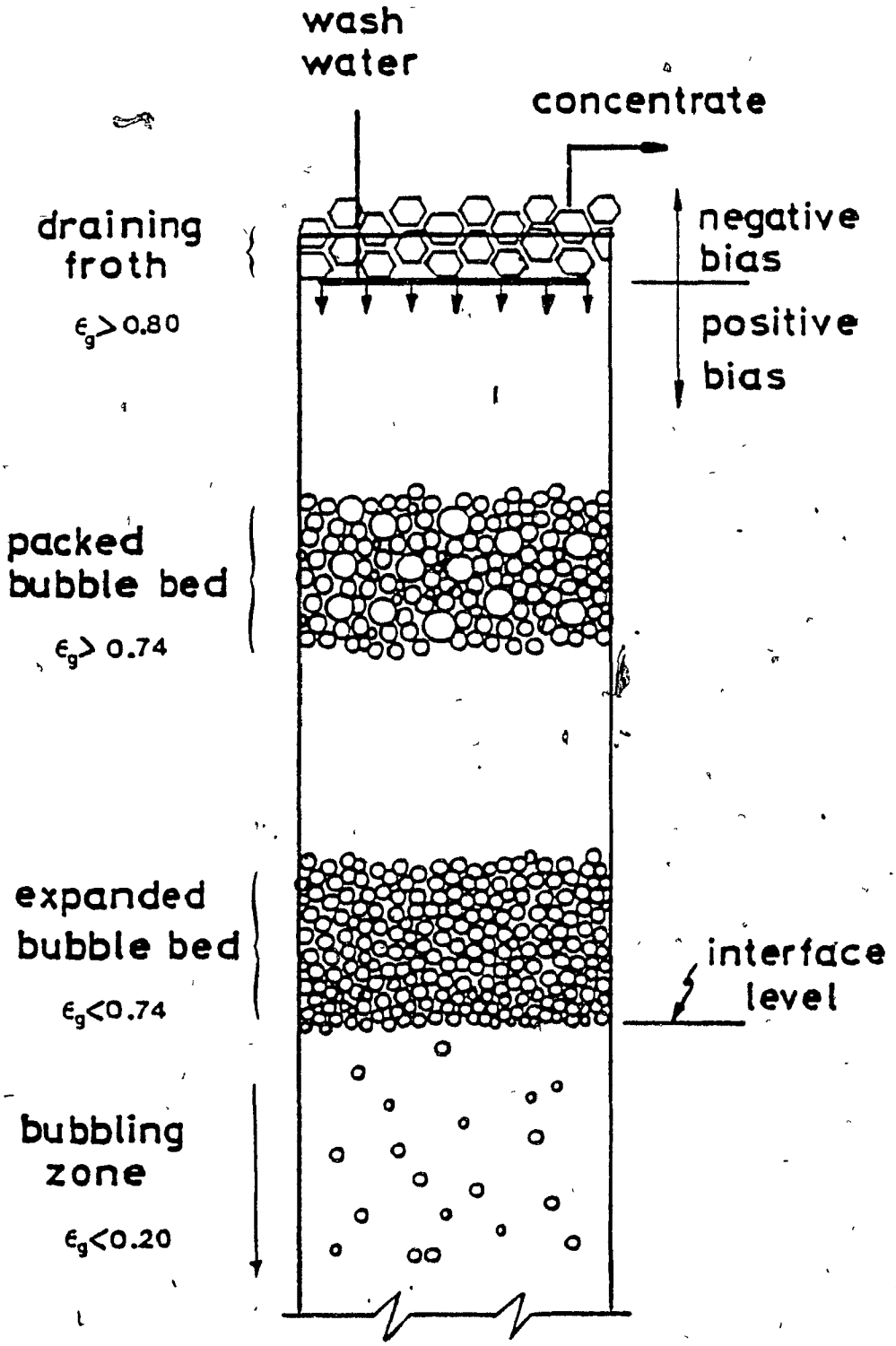

Fig.2–6 **Froth structure in a flotation column [80]**

shock pressure wave which promote additional collisions above the interface. This phenomenon seems to be the main cause of bubble coalescence in a zone where high fractonal liquid content (ε_l >0.26) makes natural drainage unlikely as the primary cause of film thinning and rupture.

(2) the packed bubble bed: The section just above the expanded bubble bed, called a packed bubble bed, extends until the wash water additional level. The fractional liquid content is lower than 0.26 and bubbles remain nearly spherical. Most bubbles move upward close to plug flow against a well distributed flow of wash water. In this bed the rate of coalescence is lower and is mainly due to collisions caused by the motion of larger bubbles, which travel upward at a velocity higher than the average.

(3) the conventional draining froth: This section occurs immediately above the wash water input level and consists of a coventional draining froth. Typical fractional liquid contents are lower than 0.2 .

2-3-2 Cleaning Action

Hydraulic entrainment and entrapment of fine particles into the froth decrease concentrate grade in mechanical flotation cells. Flotation column froths prevent hydraulic entrainment by maintaining a net downward flow of water through the froth. In a flotation column, tracer tests have shown that there is virtually no feed water entering the concentrate [19,82], indeed little even crosses the interface,

as shown in Fig.2-7. The entrainment mechansim of fine particles are due to feed water recovery into the concentrate. Lynch et al [45] discuss this point in some detail for mechanical flotation cells. Fig.2-8 shows the linear relationship between water and gangue recovery rates [45]. This implies that an increase in feed water recovery results in an increase in gangue recovery. In Fig.2-9, there is also some evidence to suggest that an approximate relationship exists between the recovery rate of valuables and water [45]. Elimination of feed water prevents fines recovery by hydraulic entrainment [33,45,46,73]. Yianatos et al [83] studied the effect on cleaning action of three variables: gas rate, froth depth and bias rate. One conclusion was that to have an effective cleaning action 1 m froth depth is essential and gas rate must be not higher than 3-4 cm/s. As gas rate increases, more water in the collection zone will entrain into the froth zone and decrease cleaning efficiency. An increase in bias rate (Vb>0.2-0.5 cm/s) is detrimental due to increased mixing in the froth. The following recommendations were made:

(1) superficial gas rate less than 1.5-2.0 cm/s

(2) froth depth be at least 1 m

(3) superficial bias rate less than 0.2-0.4 cm/s

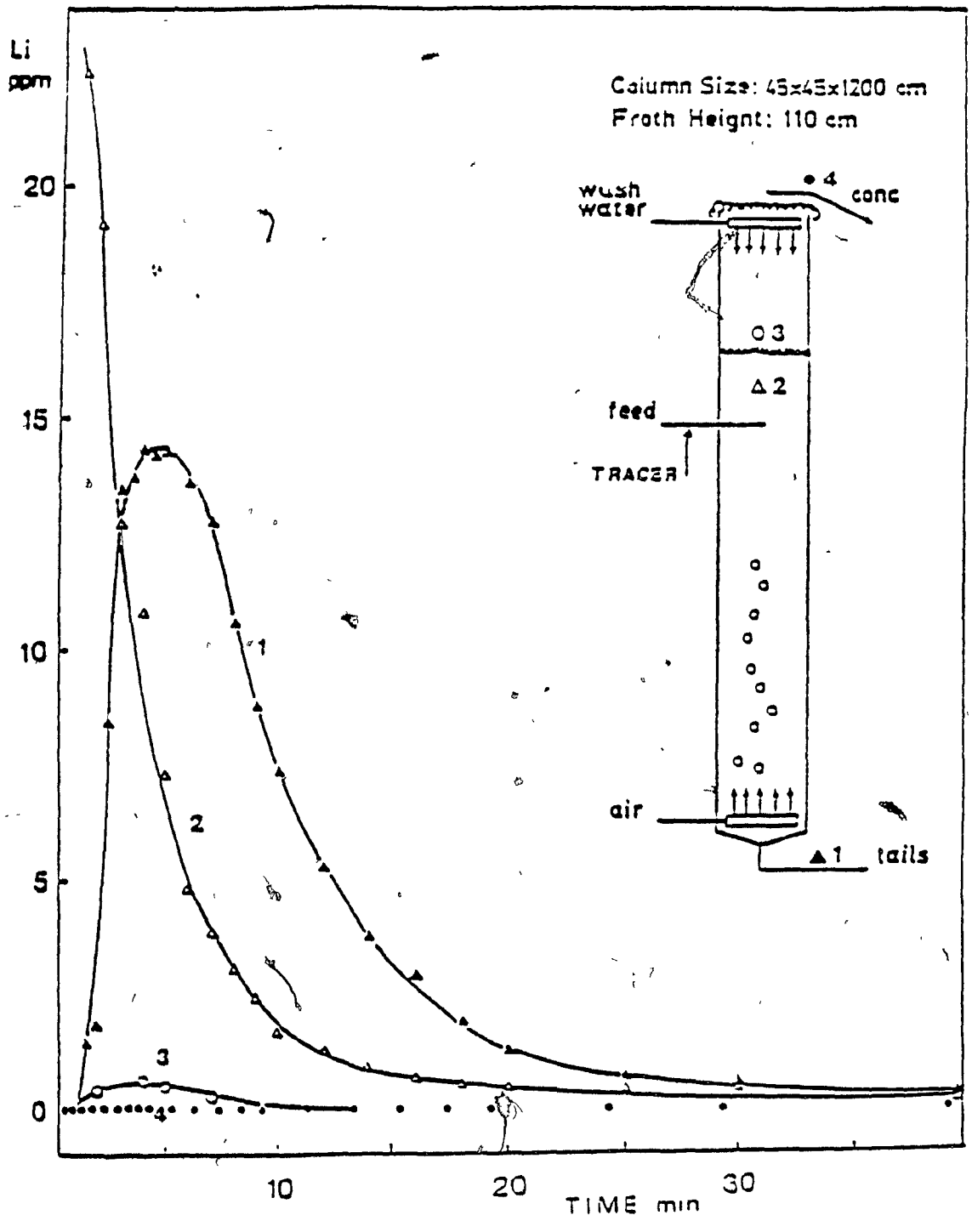

Fig.2–7 Concentration vs. time – responce curve of tracer test [80]

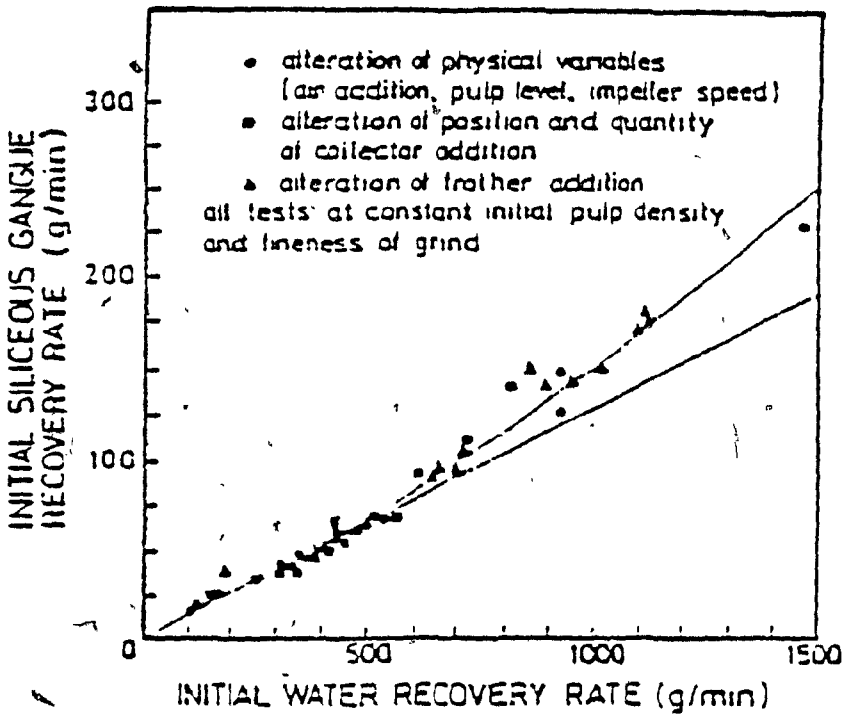

Fig.2–8 **The Nature of the Relationship between Recovery Rate of Hydrophilic Particles and Water due to Entrainment (after Lynch et al [45])**

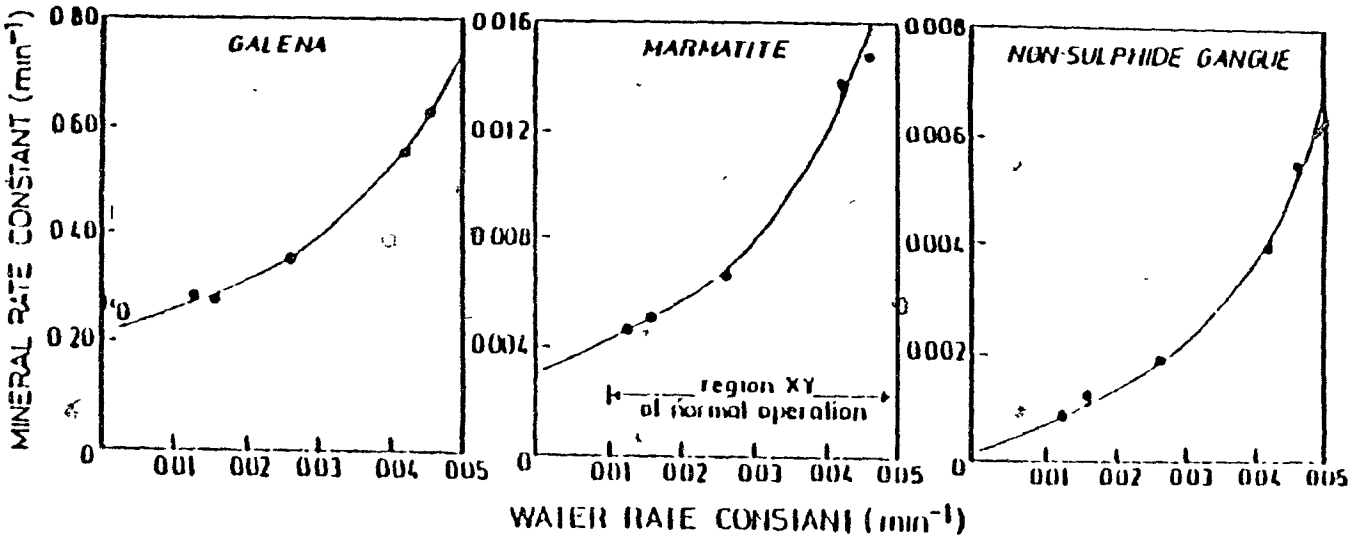

Fig.2–9 Dependence of the Flotation Rates of Valuable Sulphide (galena), Gangue Sulphide (marmatite) and Non–sulphide Gangue on the Flotation Rate of Water (Lynch et al [45])

2-3-3 Selectivity

Selectivity in the froth zone of two industrial flotation columns has been examined [53,85] and in froths deeper than 1 m absolute molybdenite grade increase of 10% to 15% were observed [85]. In shallow froths (less than 50 cm) little grade increase was found. The difference in upgrading between deep and shallow froths is due to the shallow froth being almost completely mixed.

2-4 Control Strategies: Current and Proposed

Process control in a flotation column can be essentially divided into two aspects: Stabilizing control and performance or optimizing control. Recently, Moys and Finch reviewed the developments in the control of flotation columns [51]. They concluded that the major deficiency of the methods currently used for the control of flotation columns is that those methods rely entirely on inaccurate and indirect measurements of slurry-froth interface and bias flowrate. Thus, a new technique is being developed by which more accurate measurement of slurry-froth interface and bias flowrate can be obtained.

2-4-1 Stabilizing Control

Current stabilizing control has two objectives: first to maintain a net downward flow of wash water (called positive bias) shown in Fig.2-10, and second to maintain a known froth

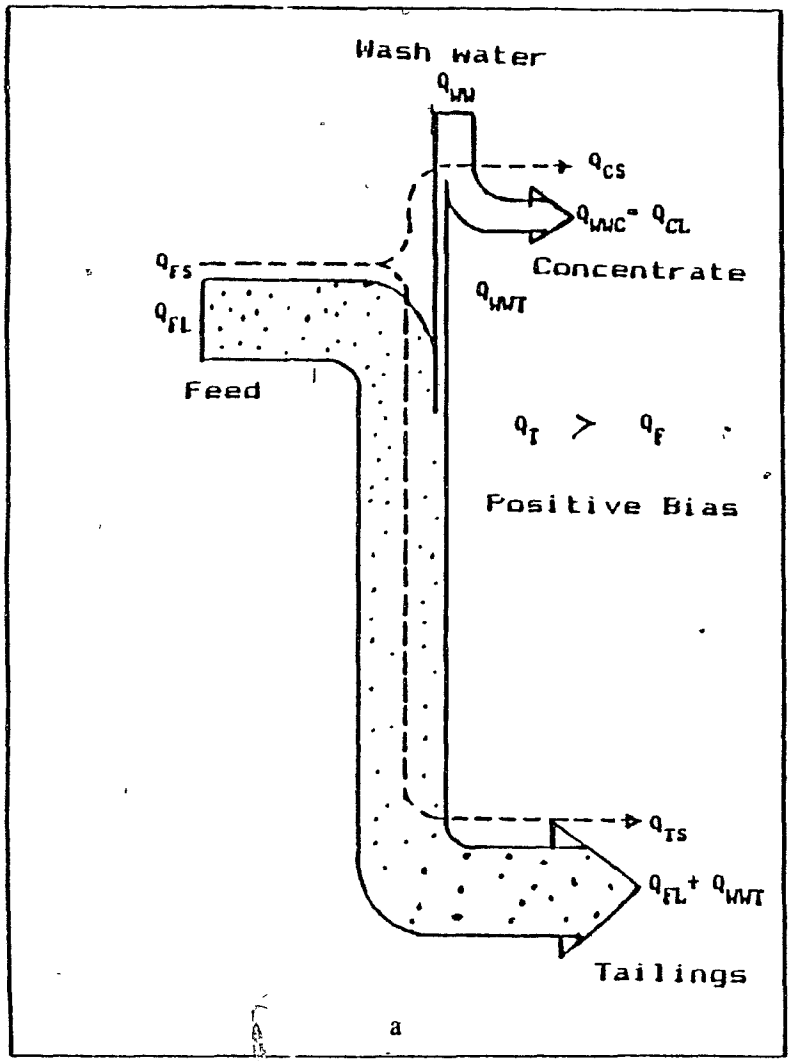

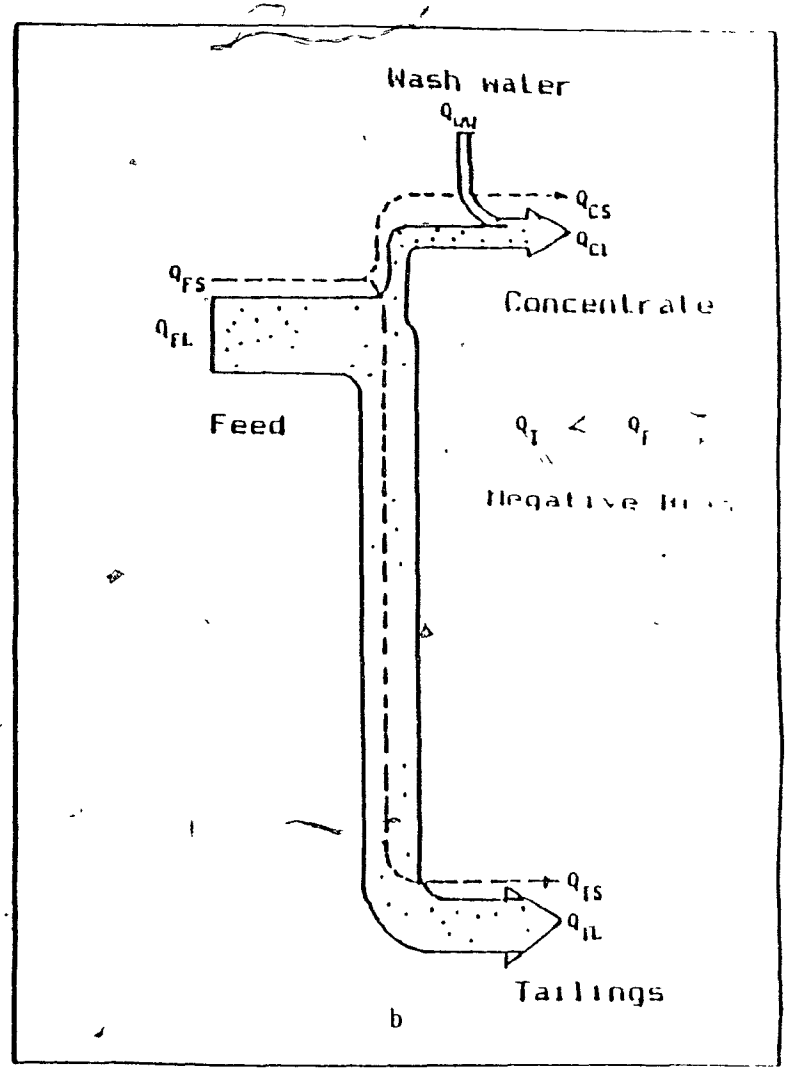

Fig.2–10 The Mass Trancfer in a Flotation Column
a) positive bias b) negative bias

depth. The net downward flow of wash water must be positive to ensure cleaning action, but must not be too large otherwise unnecessary dilution of the underflow occurs. The interface level must be maintained near a pre-specified setpoint. If the level is too high, insufficient cleaning volume will exist and concentrate grade will be reduced, while if the level is lower than required, collecting volume is reduced unnecessarily and recovery may be reduced. In any case level must be controlled within limits for stable operation. There are three stabilizing control strategies which have been used and are summarized in Table 2-1 [3,15,49,72]

To control bias, Mines Gaspe [15] sets a constant difference ($Q_T - Q_F > 0$), while Gibraltar [3] sets a constant ratio ($Q_T/Q_F > 1$). Lornex ignores the bias control [49]. The difference may be significant. For instance, the Gibraltar strategy means a varying water flowrate which could influence cleaning action. No systematic evaluation of these alternative control strategies has been conducted and it is necessary to clarify a situation which confuses users. Fig.2-11 is a plot of retention time vs. feed flowrate for the two bias control strategies [78]. It is evident that as feed flowrate increases, the retention time in the case of Gibraltar decreases faster than in the case of Gaspe. Retention time is directly related to the recovery and the change in retention time may affect recovery, especially, if the system is capacity constrained. Fig.2-12 [78] is a plot of wash water flowrate as a function of feed flowrate and shows as feed

TABLE 2-1

STABILIZING CONTROL STRATEGIES IN USE

USERS	CONTROLLED VARIABLES	
	BIAS/RATIO	FROTH DEPTH
GASPE	DIFFERENCE * TAILINGS	WASH WATER
GIBRALTAR	RATIO ** TAILINGS	WASH WATER
LORNEX	NON	TAILINGS

* $Q_T - Q_F > 0$
** $Q_T / Q_F > 1$

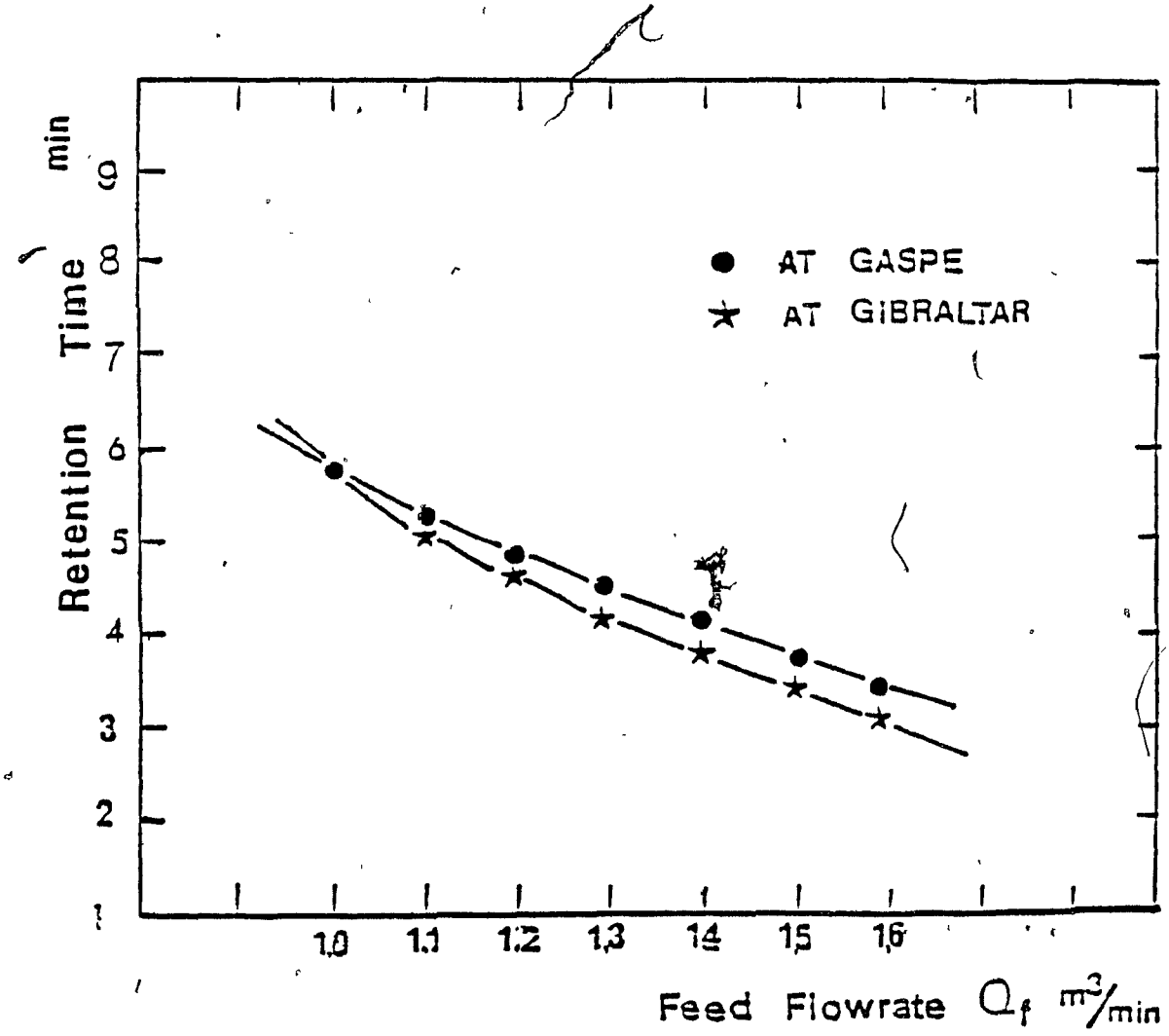

Fig.2–11 Retention Time vs. Feed Flowrate Under Different Control Loops [78]
conditions:
column 0.9m x 0.9m x 10 m
Bias = 0.2 /min at Gaspe
Ratio = 1.2 at Gibratar

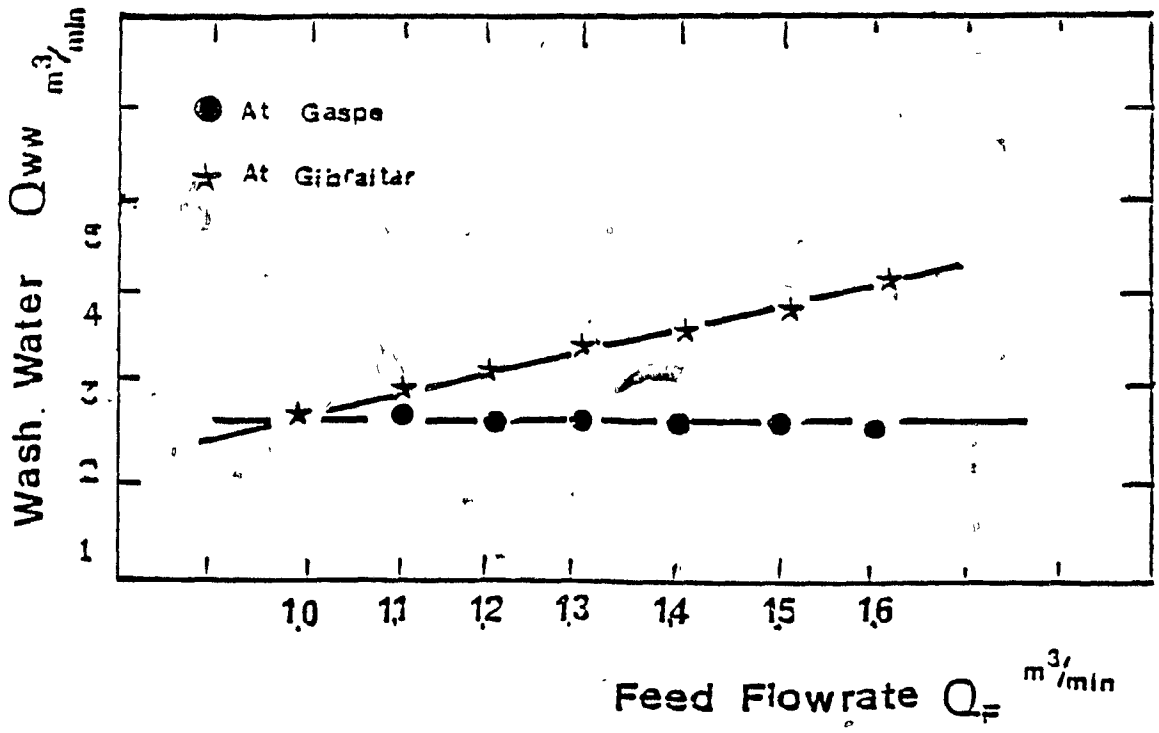

Fig.2–12 Wash Water Flowrate vs. Feed Flowrate Under Different Control Loops [78]
conditions:
column 0.9m x 0.9m x 10 m
Bias = 0.2 m /min at Gaspe
Ratio = 1.2 at Gibratar

flowrate increases the wash water flowrate does not change in the case of Gaspe but increases in the case of Gibraltar.

To control slurry-froth interface level, wash water is used as a controlled variable at Mines Gaspe and Gibraltar, tailings flowrate is used at Lornex [49].

As pointed out by Moys and Finch [51], the current control strategies rely on inaccurate infered measurements for the control variables: bias rate and interface level, and the control configurations are inherently susceptible to control loop interactions. For example, wash water is used both for bias and interface control.

2-4-2 Performance Control

The objective of performance control or optimizing control is to control the metallurgical performance (i.e. grade/recovery). Preliminary work toward this objective has been reported [3,16]. Attention was focussed on recovery because columns, compared to conventional machines, already give higher grades. Two different control loops have been used at present and are summarised in Table 2-2. There is not much evidence to evaluate whether a better relationship between gas holdup and recovery exists than that between gas rate and recovery. However, it is expected that gas holdup may be a better indicator since the effect of bubble size are included and bubble size does influence recovery.

TABLE 2-2

PERFORMANCE CONTROL STRATEGIES IN USE

USERS	CONTROLLED VARIABLE
GASPE	GAS RATE
GIBRALTAR	GAS HOLDUP

2-4-3 Novel Control Possibilities: Use of Temperature

The common technique for level measurement is the use of transducers near the interface sensitive to hydrostatic pressure. However, the pressure at a fixed point below the overflow lip is a function not only of interface level (if the interface is above the measurement point) but also of several other important variables such as gas rate and bubble size (which affect the holdup of liquid) and solids loading (solids holdup). Thus, this measurement is subject to substantial errors. The error in the manometric measurement at a given level can be as high as 30% [51].

A new method for measuring interface and bias rate based on measurements of the temperature profile in the cleaning zone is being developed. It is based on the assumption that the wash water (which is generally recirculated from a tailing dam, but could be plant make-up water) will be significantly cooler than the feed which has passed through a grinding mill and perhaps a bank of a conventional stirred flotation cells. Several measurements made on plants in Canada revealed temperature differences of 2-10 C in the spring and summer months: these differences are expected to increase in winter. When this assumption holds, the temperature distribution on the froth zone will be a function of the relative flowrate through it. Fig.2-13 and Fig.2-14 show the close agreement between true level and measured by temperature [51].

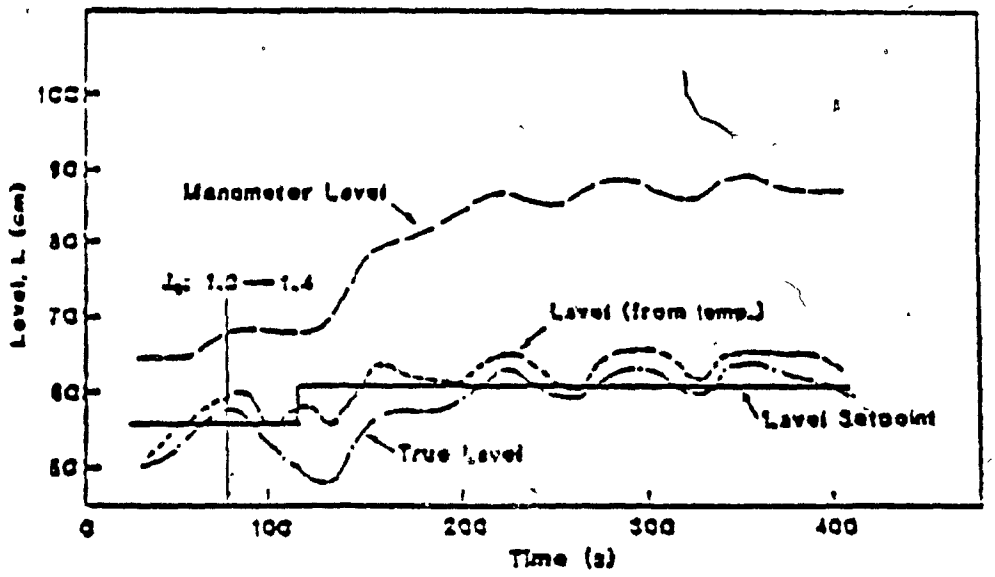

Fig.2–13 Effect of Changes in Gas Rate and Level Setpoint on Level Measurement [5-1]

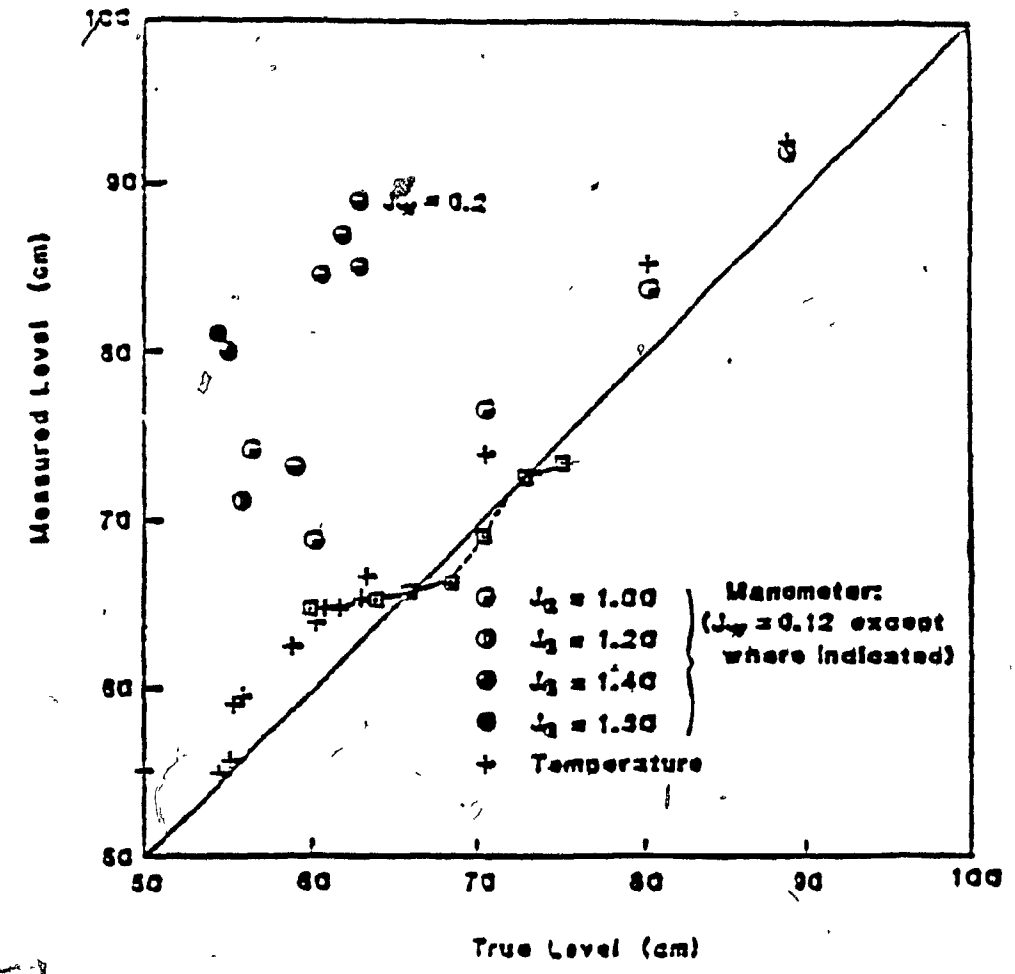

Fig.2-14 Effect of measurement methods on the accuracy of level measurement (from Moys et al [51])

CHAPTER 3

PREVIOUS WORK ON BUBBLE FORMATION AT A SPARGER

3-1 Introduction

The bubble formation process is a complex phenomenon. Many studies on bubble formation from a single orifice and a large number of models to describe this formation process have been proposed [11, 13].

The main objective of sparger design and scale-up for flotation columns is to produce uniform bubbles since non-uniform bubbles induces mixing, and larger bubbles rising more rapidly causing downflow of liquid and smaller bubbles. The second objective of sparger design is to avoid the build-up of solids particles on the surface of spargers.

Little attention has been paid to the problem of how spargers influence bubble size and what governs the formation mechanism of bubbles on the surface of a sparger in a flotation column. This chapter gives a brief review of previous work on this subject.

3-2 Bubble Formation and Effect of Gas Rate

Gas bubbles suspended in fluids usually tend to agglomerate (coalesce) and lose their identity, and the existence of small bubbles is only transitory. When gas is

forced through the orifices of a sparger, bubbles are formed; a process affected by a large number of factors. In general, the formation process is mainly controlled by the properties of liquid, particularly frother addition in the case of water, gas velocity and sparger design [29,58,67-69,84]. There exist a large number of theoretical models proposed to describe bubble formation in liquids. All are based on a sequence of events from photographic observation and depend on some form of force balance for predicting one or more stages in bubble growth. Many assumptions are made for those models, such as that bubbles remain spherical. In fact, this assumption is most closely approched in flotation since frother is added. Fig.3-1 presents the general view of gas bubble formation on the surface of a rigid sparger. There are two processes affecting bubbles: the formation and the subsequent passage through the continuous liquid. A good generation of uniform bubbles can be achieved only if the gas passes through all the possible holes. This condition can be satisfied if the Weber number based on the diameter and the gas density is equal to or greater than 2 [2]:

$$We_o = \frac{Q_o^2 d_o \rho_g}{\delta} \geq 2 \qquad [3\text{-}1]$$

where do, Qo are the hole diameter, the gas flowrate per hole, respectively. ρ_g is the gas density and δ is the surface tension of the liquid.

Bubble Formation Mechanism

effect of gas rate

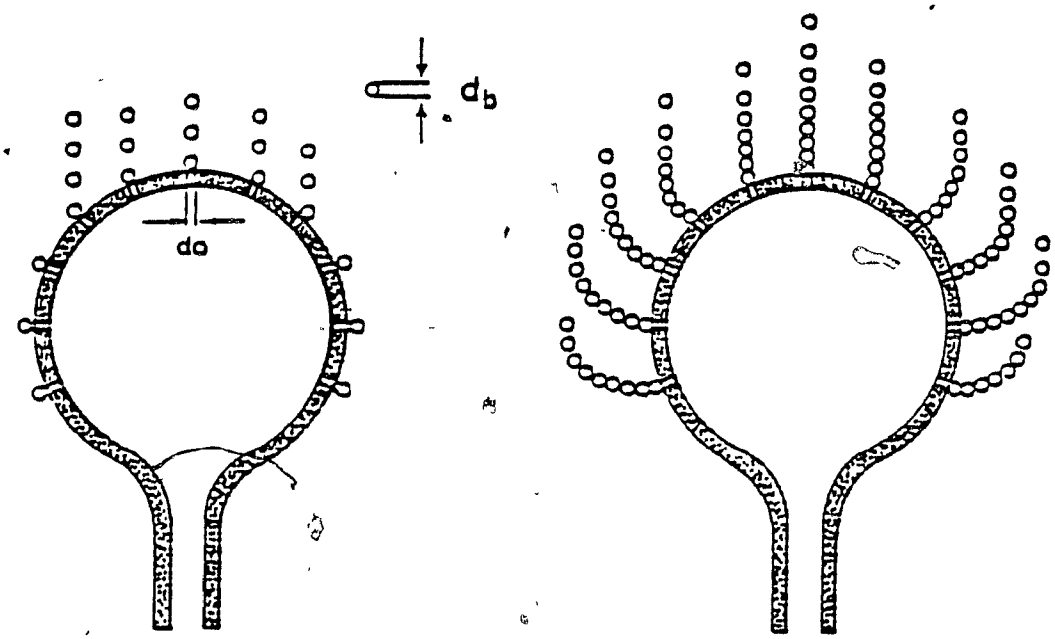

Low gas flowrate

High gas flowrate

$$W_{eo} = \frac{W_o^2 \, d_o \, \rho_g}{\delta} \geqslant 2$$

Fig.3–1 Bubble Formation on Rigid Sparger the Effect of Gas Flowrate

van Krevelen and Hoftijzer [69] divided bubble formation process into two types: the formation of separate bubbles and the formation of bubbles in series. They proposed several empirical correlations for bubble size, superficial gas velocity and orifice diameter. Recently, Bhavaraju et al [11] conducted a more detailed discussion on this subject. On the basis of gas flowrate, three distinct regimes of bubble formation can be defined.

3-2-1 Very Low Gas Flowrate

In this regime, bubbles of constant volume are formed and there is no interaction between bubbles. (i.e. the distance between one bubble and another is larger than the bubble size). The bubble size is found to be a function of orifice diameter, surface tension and buoyancy. The bubble grows until its buoyancy force exceeds the suface tension force. A balance between buoyancy and surface tension forces yields the following relation for the bubble diameter [11]:

$$db = \left[\frac{6 \ \delta \ do}{g \ (\rho_l - \rho_g)} \right]^{1/3} \qquad [3-2]$$

where ρ_l is liquid density and g is acceration due to gravity.

3-2-2 Moderately High Gas Flowrate

With further increase in gas velocity, surface tension

becomes less important (even negligible), and bubble size is determined by a balance of buoyancy, inertial and viscous forces. In this regime, a mass balance results in the relationship [11]:

$$db = \left[\frac{6\ Qo}{\pi\ F}\right]^{\frac{1}{3}} \qquad [3-3]$$

where F is the bubble formation frequency.

The moderately high gas flowrate case corresponds to the flowrate used in flotation columns, with superficial gas velocity typically around 0.5-3 cm/s [86].

3-2-3 Very High Gas Flowrate

At very high gas flowrate, the formation process of bubbles is complicated. However, flotation columns do not operate in this condition since flooding, breakup and coalescence of bubbles occur [69] which are undesirable for column operation. It is observed that the bubbles are not uniform and a number of large bubbles are formed. These large bubbles are enriched at the column center and very effectively collect small bubbles in their wake. This situation leads to excessive turbulance which should be avoided.

3-3 Effect of Surfactants

Gas holdup increases considerably when water contains some surfactants. For example, the gas holdup increases in

the following order [40]:,

n-butanol > n-propanol > i-propanol

> ethanol > methanol > water

The decrease in surface tension in the presence of alcohols was not sufficient to explain this phenomenon. Kelkar et al discussed this subject in some detail and found that the number of carbon atoms in the straight chain of the surfactant is an important factor affecting gas holdup [40]. For flotation columns, in the presence of alcohols (frother), the bubbles become more rigid and hence have low rise velocities resulting in a bubbly flow regime up to surprising high superficial gas velocities (8-10 cm/s) [40]. It is also noted that in flotation columns the interaction of frother and collector may affect gas holdup and the stability of froth bed.

3-4 Effects of Spargers

The effects of sparger material and orifice diameter on bubble formation and bubble size have been studied by many investigators for bubble columns in chemical engieering. Typically those investigators use perforated plates with few orifices and with diameters greater than 0.5 mm. Consequently, bubble size is essentially dependent on the dynamic equilibrium among the buoyancy, drag and the gravitational forces through the continous liquid. In contrast, for flotation columns, the spargers usaully have a large number of

orifices with diameters less than 100 um. There is relatively little data on these type of spargers.

3-4-1 Orifice Size, Shape and Porosity

When bubbles are formed from a sparger adjacent orifices may affect the bubble size formed at any single orifice. For example, several holes may contribute to a single bubble. Attempting to use the correlations developed for single orifices is rendered difficult, for example, at low gas rates when not all the orifices are active, and because in typical spargers there is a range in orifice size and shape [5]. There is no systematic work reported to evaluate the effect of orifice size, shape and porosity on bubble formation and bubble size for flotation columns.

The influence of orifice shape may not be so important for spargers compared with single orifices. For very low gas flowrates, where the surface tension effect is dominant, bubbles appear to form from an equisided orifice, such as an equilateral triangle or regular hexagon, as from the inscribed circular orifice. At higher flow rates, an orifice with a shape not too far from circular gives roughly the same bubble size as the circular orifice of the same area at the same flowrate. Irregular goeometries, such as elongated rectangular slots, show more complex behaviour [13].

Porosity is the number of orifices per unit area of sparger surface. In general, the porosity of a perforated

plate is quite low (less than 5). In contrast, the porosity of a sparger used in flotation columns is considerably higher (more than 50 and up to 150). The effect of porosity on bubble size is not known.

3-4-2 Sparger Materials

The effect of sparger materials on bubble size has been reported by many investigators [13,17,22,58-59,70]. The flexibility and hydrophobicity of sparger materials may have an effect on bubble formation. After studying the effect of rigid and flexible spargers on gas holdup and bubble size, Rice et al [58] concluded that rubber spargers are inherently self-regulating, with hole area increasing in direct relation to the pressure drop across the sparger. The rubber sparger can ocsillate and deform, thus preventing fine particle build-up on the sparger which is important in mineral processing. Recently, Rice et al [59] examined thin elastic membrance spargers. It seems that high gas holdup and small bubble size can be achieved with this type of sparger. On the other hand, if the surface of a sparger is poorly wetted with water, the bubbles will remain on it longer and this may result in an increase in bubble size [13].

3-5 Effects of Flow of Continuous Fluid

If the continuous fluid has a net vertical velocity

component, the additional drag causes earlier or later detachment of bubbles and hence reduces or increases bubble size formed according to whether the drag force assists or impedes the detachment. Significantly smaller bubbles can be produced by causing the continuous fluid to flow cocurrently with the dispersed phase [13]. Horizontal component of velocity also tends to affect the bubble size produced at an orifice. At low flowrates, there is little effect, but larger bubbles tend to be formed as the horizontal mean velocity is increased [13].

CHAPTER 4

THEORY: DEVELOPMENT OF BUBBLE SIZE ESTIMATION TECHNIQUE AND SPARGER SCALE-UP MODEL

4-1 Bubble Size Estimation

Several methods for measuring bubble size have been proposed. The most frequently used is photography either used directly or to calibrate a proposed alternative method [62]. Photography is tedious and restricted to vessels with transparent walls and relatively low bubble concentrations. Thus, for flotation column work, it is necessary to have an alternative way to estimate bubble size.

The technique described in this chapter is a further development of the bubble size estimation technique proposed by Dobby et al [24]. In that technique the terminal velocity (U_T) of a single bubble is first estimated and U_T is then related to bubble size. A variety of relationships were tested, which, over the range of interest, gave similar results. The technqiue developed here is similar but gives a direct estimate of db.

4-1-1 Dobby's Method

This method used the concept of drift-flux introduced by Wallis [74] to relate phase flow rates and gas holdup to physical properties of a two-phase system.

For counter-current flow of gas bubbles and water in a bubble column the slip velocity Us is:

$$Us = \frac{Vg}{\varepsilon_g} + \frac{V_l}{1 - \varepsilon_g} \qquad [4-1]$$

where Vg and V are the superifical gas and liquid velocities. respectivley (both positive quantities). Wallis [72] also postulated that Us is a function of terminal rise velocity U_T of a single bubble and the gas holdup, in the follwing form:

$$Us = U_T (1 - \varepsilon_g)^{m-1} \qquad [4-2]$$

As noted by Bhaga [6] this form of the relationship satisfies two boundary conditions:

1) as $\varepsilon_g \longrightarrow 0$, $Us \longrightarrow U_T$, and

2) as $\varepsilon_g \longrightarrow 1$, $Us \longrightarrow 0$.

m is a parameter defined according to Richardson and Zaki [56], for 1<Re<200

$$m = [4.45 + 18 \frac{db}{dc}] Re^{-0.1} \qquad [4-3]$$

and For 200<Re<5oo

$$m = 4.45 \ Re^{-0.1} \qquad [4-4]$$

and the Reynolds number is defined [56] as:

$$Re = \frac{db\ U_T\ \rho_l}{\mu} \qquad [4-5]$$

Combining Eq.[4-1] and Eq.[4-2] gives:

$$U_T = \frac{Vg}{\varepsilon_g\ (1-\varepsilon_g)^{m-1}} + \frac{V_l - Vg}{(1-\varepsilon_g)^{m-1}} \qquad [4-6]$$

Eq.[4-6] is derived assuming a uniform flow profile and uniform bubble concentration across the column cross-section. For large columns, this a reasonable assumption. For small columns, correction factors are required and given by Bhaga [7]:

$$Ko\ U_T = \frac{Vg}{\varepsilon_g\ (1-\varepsilon_g)^{m-1}} + \frac{Co\ (V_l - Vg)}{(1-\varepsilon_g)^{m-1}} \qquad [4-7]$$

When gas holdup is uniform over the cross section, Ko = Co = 1 Gas holdup measurements are made at varying levels of V_l for constant Vg. Since bubble diameter increases with gas rate, Vg must be held constant. A plot of $Vg/\varepsilon_g(1-\varepsilon_g)^{m-1}$ vs $(V_l - Vg)/(1-\varepsilon_g)^{m-1}$ results in an intercept = Ko U and slope = - Co. In counter-current flow, it is difficult to estimate Ko, which Bhaga [7] has discussed in detail. Considering the relatively low gas rate and small bubble size common to flotation columns, the theoretical predictions of Bhaga [7] suggest

$0.95<Ko<1$. For this work it is assumed that $Ko=0.97$, thus, U_T can be estimated.

Concha and Almendra [16] developed an equation for the terminal velocity U_T of a spherical particle for hindered settling, which can be rewritten for a single bubble because of the similarity in behaviour between small rigid bubbles and solid particles.

$$U_T = \frac{20.52\ M}{db}\left[\left[\ 1 + 0.092\ \left(\frac{db}{P}\right)^{3/2}\ \right]^{1/2} - 1\right]^2$$

where

$$M = \frac{\mu}{\rho_l}$$

$$P = \frac{3}{4}\left[\frac{\mu^2}{\rho_l \cdot g}\right] \qquad [4\text{-}8]$$

Knowing U_T, it is easy to solve Eq.[4-8] for bubble size.

4-1-2 Developed Method

Masliyah derived a general expression for relative particle to fluid velocity (or slip velocity) for hindered settling of spherical particles in a multi-species system [52]. Bubbles and rigid spheres in water have virtually equivalent drag coefficient up to Reynolds number (Re)

approximately 500 [55]. Thus, for Re less than 500, an analogous expression for bubbles can be written;

$$Us = \frac{g\ db^2\ F(\varepsilon_l)\ (\rho_b - \rho_{susp})}{18\ \mu\ [\ 1 + 0.15\ Reb^{0.687}\ ]} \qquad [4-9]$$

where

$$Reb = \frac{db\ Us\ \rho_l\ \varepsilon_l}{\mu} \qquad [4-10]$$

and (see appendix E for clarification)

$$F(\varepsilon_l) = \varepsilon_l^{m-2} = (1 - \varepsilon_g)^{m-2} \qquad [4-11]$$

where m is defined according Richardson and Zaki in Eq.[4-3] and Eq.[4-4]. Eq.[4-9] can be simplified for a two phase (gas liquid) system, since $\rho_b \cong 0$, to:

$$Us = \frac{g\ db^2\ (1-\varepsilon_g)^{m-1}(-\rho_l)}{18\ \mu\ (\ 1 + 0.15\ Reb^{0.687}\ )} \qquad [4-12]$$

where - sign means the bubbles are rising.

The solution for db is by repeated substitution of estimates of db in Eq.[4-12] until the calculated Us in Eq.[4-12] is equal to the measured Us in Eq.[4-1]. (see appendix C for the numerical analysis of the solution in detail or refer

Fig.1 in appendix G).

4-2 Development of Sparger Scale-up Model

The relation between gas holdup and superficial gas velocity, Vg, for a certain range of operating conditions, is given by:

$$\varepsilon_g = \alpha\ Vg^{\beta} \qquad [4\text{-}13]$$

where α, β are empirical constants. The value of β reflects the flow regime in the system [33,61]. A flotation column should operate in the bubbly regime where β is between 0.7 and 1.2 [33,61].

It has been empirically established that bubble size is a function of superficial gas velocity [22]:

$$db = C\ Vg^{n} \qquad [4\text{-}14]$$

where C and n are constants. A modification is here proposed to account for the sparger size effect, namely:

$$db = C\ [\ Rs \cdot Vg\ ]^{n} \qquad [4\text{-}15]$$

where Rs is the ratio of column cross-sectional area to sparger surface area,

$$Rs = \frac{Ac}{As} \qquad [4\text{-}16]$$

and Ac, As are the cross-sectional area of a column and sparger surface area, respectively. It is observed that Rs.Vg is the volumetric gas rate per unit area of sparger.

Eq.[4-15] can be derived theoretically. Assuming that the orifices are uniformly distributed on the surface of a sparger and have a diameter, do, then any change in sparger surface area will not affect the orifice diameter and porosity, ϕ_o , For a single orifice, the following equation can be obtained from the gas volume balance:

$$Qo = \frac{\pi F \, db^3}{6} \qquad [4-17]$$

where Qo is orifice volumetric gas flowrate, i.e. the volumetric flowrate Qg into a column divided by the total number of orifices N:

$$N = \phi_o \, As \qquad [4-18]$$

Defining a superficial orifice gas velocity:

$$Vo = \frac{Qo}{Ao} \qquad [4-19]$$

and noting that,

$$\frac{Qg}{As} = \frac{Ac}{As} \frac{Qg}{Ac} = Rs \; Vg \qquad [4-20]$$

thus,

$$\frac{Rs\ Vg}{\rho_n} = \frac{\pi\ F\ db^3}{6} \qquad [4\text{-}21]$$

From experimental observation, it is not possible to measure F. However, the bubble formation frequency is mainly determined by the orifice gas velocity, Vo, orifice pressure drop, ΔPo and surface tension, δ. It is here proposed that F as a function of Vo, ΔPo and δ and can be expressed as follows:

$$F = \psi \frac{\mu\ Ao\ Vo^{\varphi}}{\delta\ \Delta Po} \qquad [4\text{-}22]$$

where ψ, φ are constants.

The pressure drop across a single orifice is [29]:

$$\Delta Po = \frac{\rho_l}{2\ g\ C_D^2} Vo^2 \qquad [4\text{-}23]$$

where C_D is the orifice discharge coefficient.

Combining all the equations from Eq.[4-17] to Eq.[4-23], the following expression can be achieved:

$$db = \left[\frac{3\ \rho_l\ \delta}{\psi \pi \mu g\ C_D\ (Ao\ \phi_o)^{3-\varphi}}\right]^{\frac{1}{3}} \left[Rs \cdot Vg\right]^{\frac{3-\varphi}{3}} \qquad [4\text{-}24]$$

Comparing Eq.[4-15] with Eq.[4-24], then

$$C = \left[\frac{3\,\rho_l\,\delta}{\psi\,\pi\,\mu\,g\,g_D^2\,(Ao\,\phi_o)^{3-\varphi}}\right]^{\frac{1}{3}} \qquad [4\text{-}25]$$

$$n = \frac{3 - \varphi}{3} \qquad [4\text{-}26]$$

From Eq.[4-25] and Eq.[4-26], it can be seen that for constant operating conditions, a change of sparger surface area will not affect constants, C and n, since the change of sparger surface area does not affect any term in the two equations, Eq.[4-25] and Eq.[4-26].

CHAPTER 5

EXPERIMENTAL

5-1 Laboratory Column Set-up

Fig.5-1 shows the laboratory column set-up. The column was constructed from Plexiglas tubing. For most of the tests, water was the only feed and was fed through the wash water inlet. Water flow rate was controlled by a variable speed pump (Masterflex), and the discharge flowrate was controlled by a Moyno pump. Compressed air was introduced into the column through a variety of spargers. A flowmeter, calibrated at 20 psi, was used to regulate gas flow. In order to investigate the scale-up of gas spargers, four columns of different dimensions were constructed: 3.8 cm, 5.71 cm, 10.16 cm (circular) and 2.5*10 cm (rectangular). Various combinations of the sparger type, size and column size were obtained to test the effects on gas holdup and bubble size. Fig.5-2 shows a particular design of sparger system for the scale-up study of spargers.

5-1-1 Measurement of Gas Holdup

Gas holdup is one of the most important parameters which characterize the hydrodynamics of bubble columns [61,62]. The techniques for the measurement of gas holdup can be classified

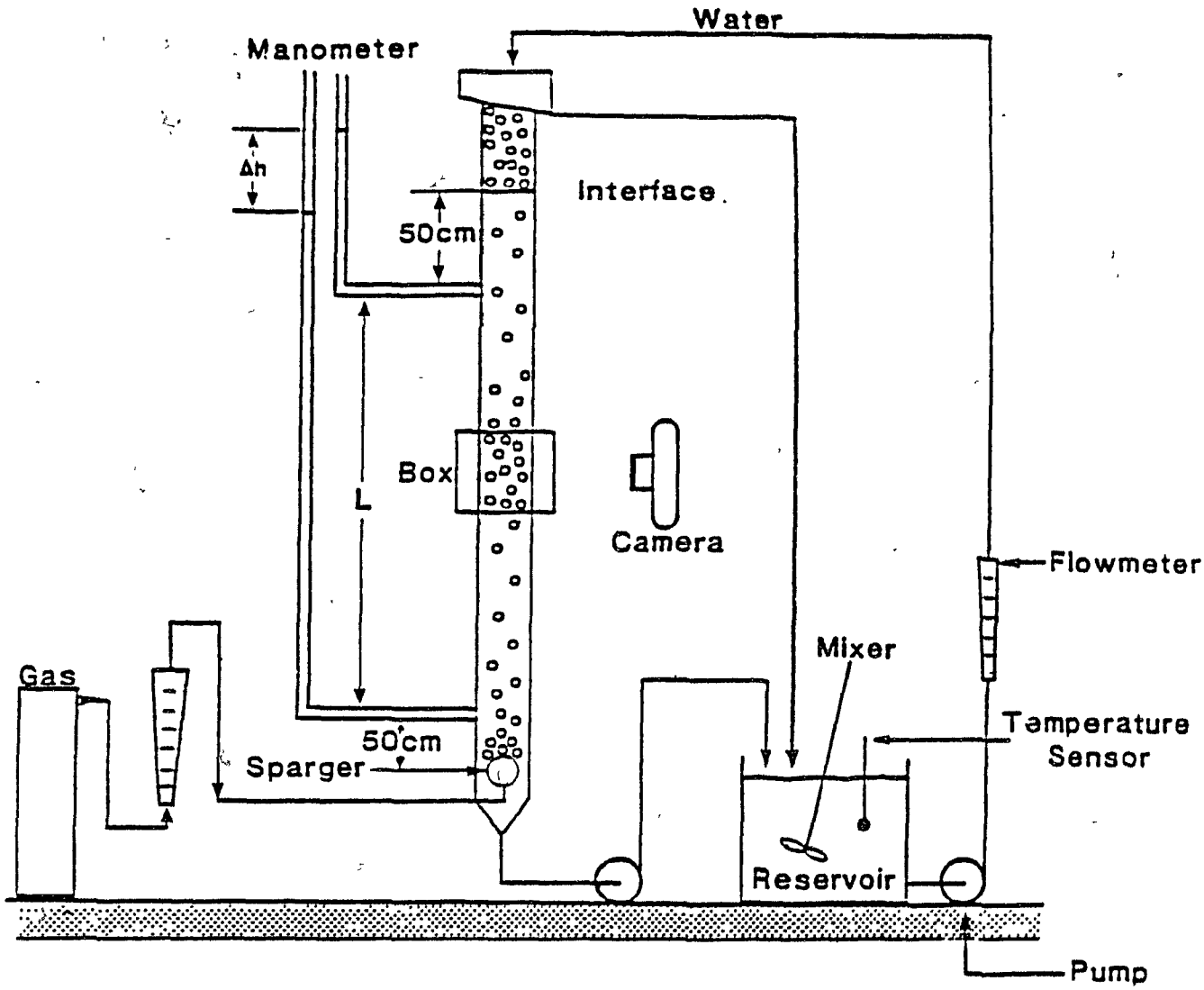

$$\text{Gas Holdup} \quad g = \frac{\Delta h}{L} \times 100\%$$

Fig.5-1 Laboratory Experimental Set-up

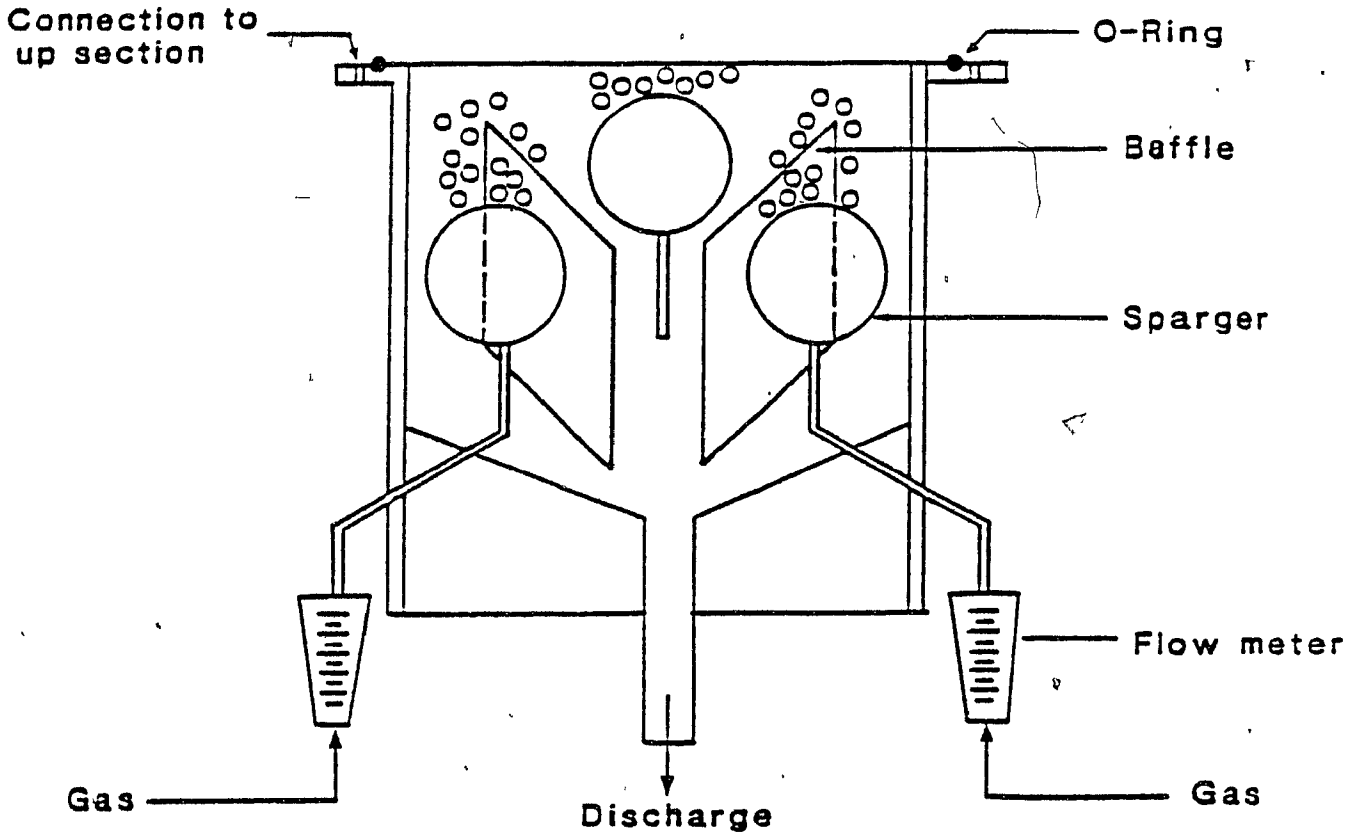

Fig.5–2 A Special Design of Sparger System for the Scale–up Study of Spargers

into two categories: local and global measurements.

Of the local measurement techniques, the most frequently used are based on either electrical conductivity or X-ray absorption which depend on the concentration of each phase. There are two global methods, bed expansion and the manometric technique based on pressure drop along the column. In this study, global measurement were used. Each measurement of gas holdup was repeated at least three times and the average is presented in all the following figures. It was found that when no froth zone exists at the top of the column, the two global methods are in good agreement (within 3%). All experiments were performed at room temperature (293±2K).

5-1-2 Measurement of Bubble Diameter

The common way to measure bubble size is by photography which is accurate only with dilute bubble systems and which can not be used with slurries. A Plexiglas box filled with water was placed around the column for photographic measurement of bubble size. The water-filled box reduces optical distortion due to the curved wall of the column. Bubble size distribution and bubble shapes were determined using 4-5 times enlargement. Counting and measurement of bubble size was done manually or automatically using a Zeiss Digitizer. Accuracy was better than +0.1 mm. A minimun of 400-600 bubbles were counted.

5-1-3 Morphology of Sparger Types

Scanning electron microscopical analysis of each sparger was conducted. This gave an idea of morphology and permitted pore size and porosity to be estimated. Fig.5-3 presents a general illustration of the surface and shape of spargers used in this work.

(1) Steel Sparger

This type of sparger is made from stainless steel and is available through the Flotation Column Co. of Canada Limited. Fig.5-4a shows the holes and the distribution of holes. The number of orifices per unit area (porosity) is quite low with respect to the dead area and the orifices are distributed randomly. The enlargement (Fig.5-4b) indicates the holes are not circular and there is a distribution of hole sizes. The average diameter is approximately 50 μm. The number of holes per unit area is difficult to estimate.

(2) Rubber Sparger

This type of sparger was recommended by Wheeler [73]. For example, it is used at Mines Gaspe. Fig.5-5 shows the regular distribution of holes. The estimated porosity is around 42 and average orifice diameter is around 80 μm.

(3) Ceramic Sparger

This sparger was obtained from Fisher Scientific Inc and

General Illustration of Spargers

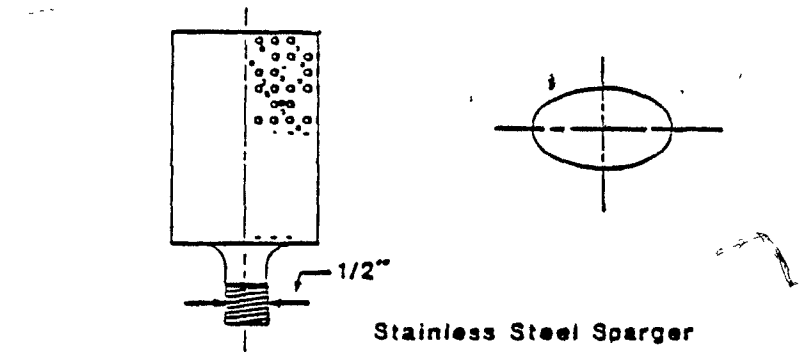

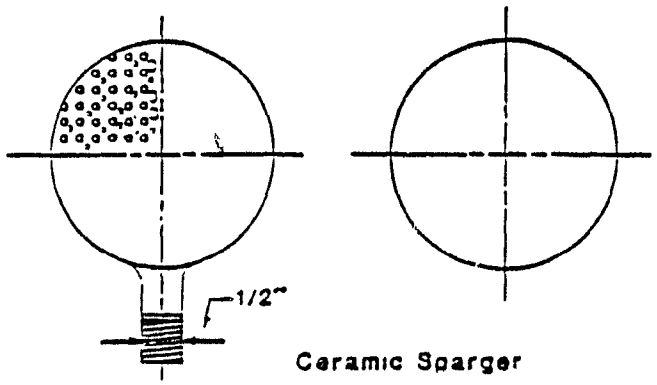

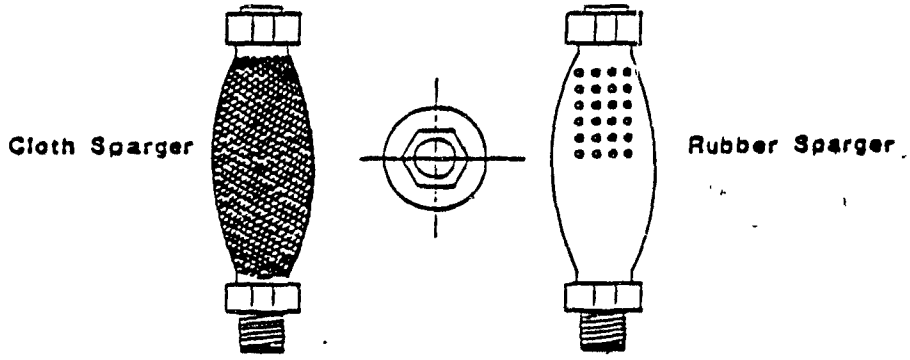

Fig.5-3 General Illustration of Sparger Surface

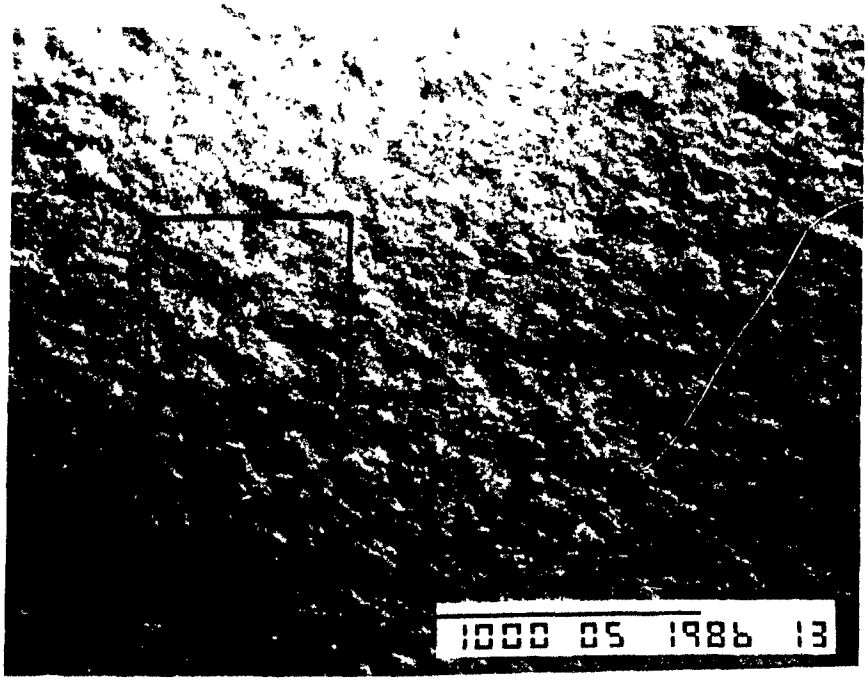

(a)

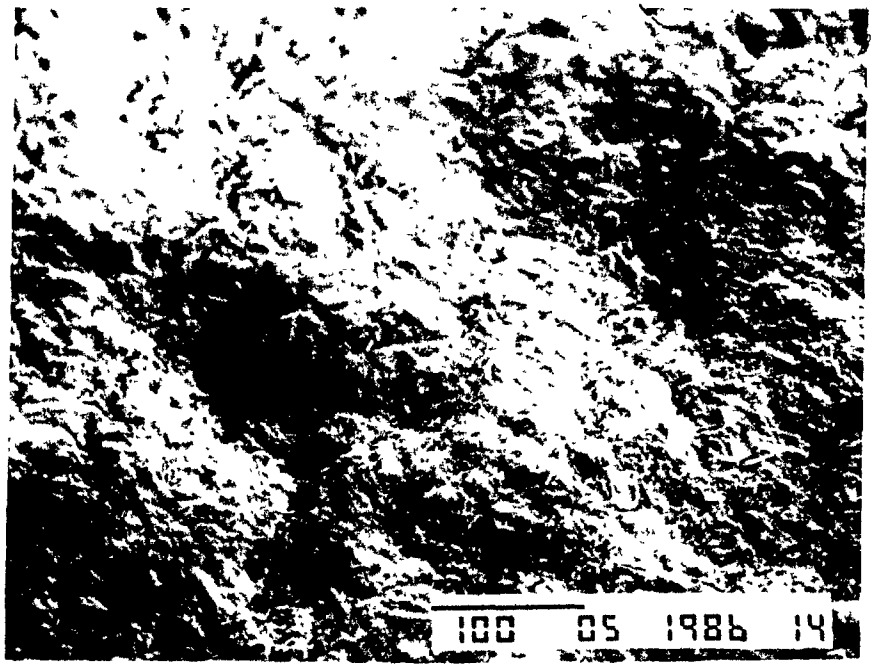

Fig.5-4 Microscopical Observation of Stainless Steel Sparger Surface

(a)

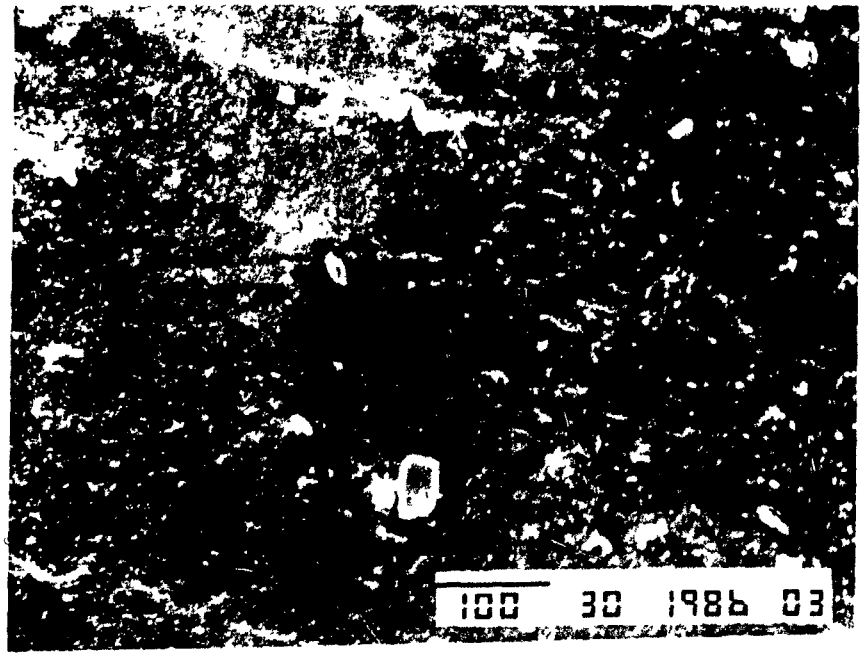

Fig.5—5 Microscopical Observation of Rubber Sparger Surface

is often used in laboratory columns [86]. The average orifice diameter is 60 μm. Fig.5-6a shows that the distribution of orifices is random and porosity is higher in comparison with steel and rubber spargers. Fig.5-6b indicates the shape of orifices is not circular.

(4) Filter Cloth Sparger

This type of sparger is common in "home-made" columns (e.g. Gilbraltar). It has the attraction of being cheap and easy to build. Fig.5-7 shows, as expected, the structure is completely different. It is not possible to estimate hole size; it is interesting to note that there is no identifiable hole at all.

From this microscopical observation of the sparger surface, some information was obtained and is summarized in Table 5-1.

5-2 Operation of Laboratory Column

The laboratory operation of a column is relatively simple. Manual control of froth/slurry interface is realised by adjusting wash water flowrate with tailing discharge flowrate at a set value. If wash water flowrate has to be set constant, tailing discharge flowrate can be regulated to control the interface level. Before taking any measurements, steady state operation has to be reached.

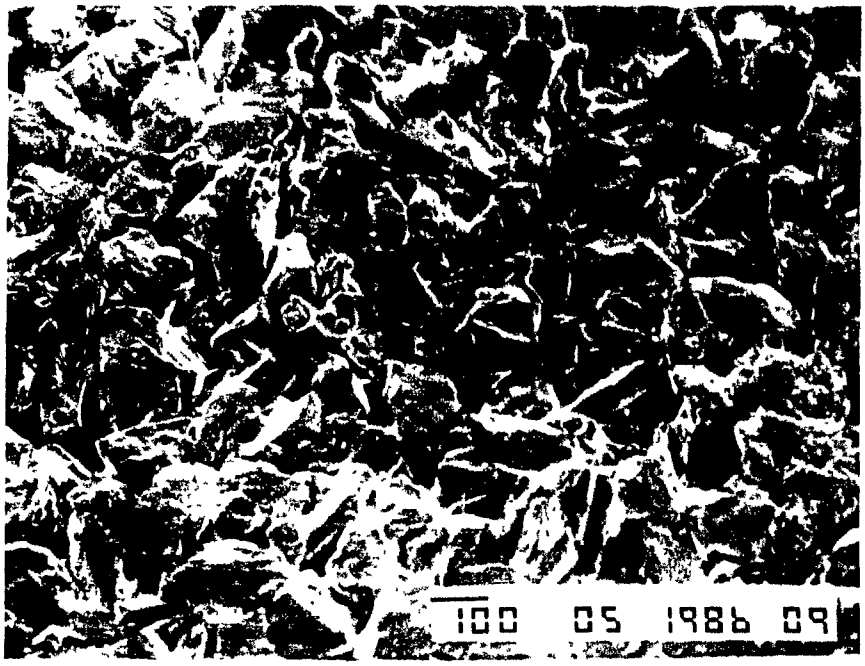

(a)

Fig.5–6 Microscopical Observation of Ceramic Sparger Surface

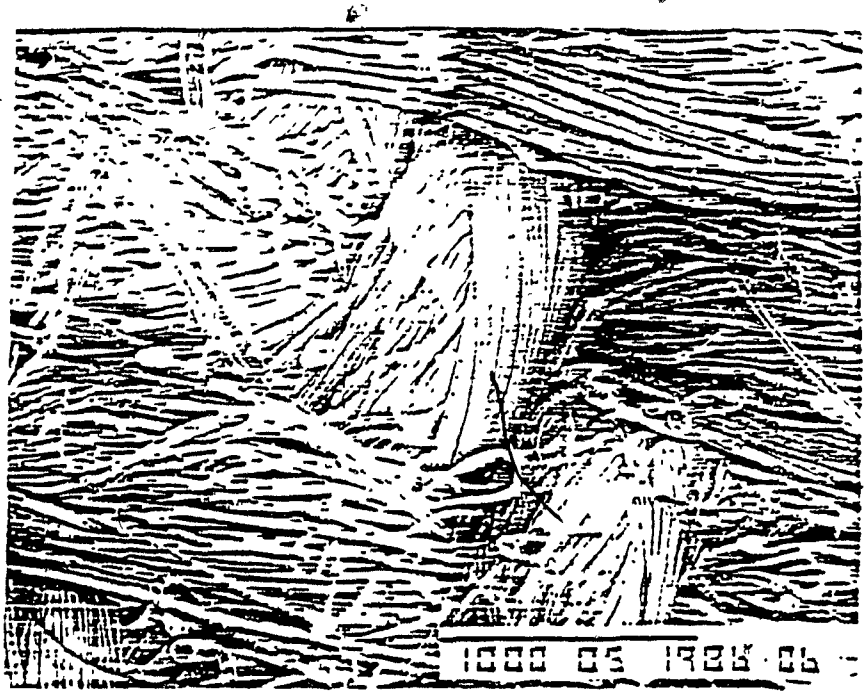

(a)

Fig.5-7 Microscopical Observation of Filter Cloth Sparger Surface

TABLE 5-1

DESCRIPTION OF SPARGERS

USED IN THIS WORK

TYPE	ORIFICE DIAMETER μm	SURFACE AREA cm^2 (*)	POROSITY $1/cm^2$
STEEL	50	20 - 60	10
RUBBER	80	56	42
CLOTH	**	37.8-213.63	**
CERAMIC	60	19 - 57	140

* the range of sparger surface area tested

** impossible to estimate

5-3 Experimental Design

The experimental work was essentially divided into three individual parts. The first dealt with the bubble size estimation technique, second with the effects of operating variables on gas holdup and bubble size, and the last with testing the sparger scale-up methodology.

5-3-1 Verification of Bubble Size Estimation Technique

For the verification of the bubble size estimation technique, three columns were used. A summary of these column characteristics is given in Table 5-2. Bubbles were generated either with porous stainless steel or ceramic spargers, and bubble size was controlled by a variety of frothing agents. The test range of superficial gas velocity and liquid velocity with different frother is summarized in Table 5-3. For each test series, pressure drop (gas holdup) was manometrically measured and bubble size was measured from photographies.

5-3-2 Effect of Operating Variables on Gas Holdup and Bubble Size

After the bubble size estimation technique was developed, the effect of operating variables on gas holdup and bubble size was extensively investigated. The test conditions are summarized in Table 5-4. All the work was carried out in two columns: the 3.81 cm and 5.71 cm diameter columns.

TABLE 5-2

COLUMN CHARACTERISTICS FOR VERIFICATION OF BUBBLE SIZE ESTIMATION TECHNIQUE

COLUMN	SHAPE	DIAMETER (cm)	HEIGHT (cm)	SPARGER	TEST SERIES (*)
1	circular	3.81	200	ceramic	1,4,5
2	circular	5.71	200	ceramic	3
3	rectangular	2.5X10	180	steel	2

* Test series number is presented according to the type of frothers and different column dimensions (refer to Table 7-1 results)

TABLE 5-3

TEST CONDITIONS FOR VERIFICATION OF

BUBBLE SIZE ESTIMATION TECHNIQUE

TEST SERIES	FROTHER (*)	ppm	Vg (cm/s)	V_l (cm/s)
1	DOW	5-25	1.0	0.7-1.0
2	DOW	10-25	1.5-2.1	0.3
3	DOW	15	0.5-1.8	0.3-1.3
4	TEB	5-25	1.0	0.8-1.0
5	MIBC	20-75	1.0	0.9-1.0

* DOW : Dowfroth 250C (polypropylene glycol methyl ether)

TEB : Tri ethoxy butane

MIBC: Methylisobutyl carbinol (methylamyl alcohol)

TABLE 5-4

TEST CONDITIONS FOR THE EFFECT OF OPERATING VARIABLES ON GAS HOLDUP AND BUBBLE SIZE

SPARGER	FROTHER CONCEN. PPM *	Vg (cm/s)	V_l (cm/s)
steel	15	0.5-1.8	1.0
ceramic	5-30	0.5-1.8	0.9-1.0
cloth	15	0.5-1.8	1.0
rubber	15	0.5-1.8	1.0

* Dowfroth 250C

5-3-3 Testing Effect of Sparger Surface Area (Sparger Scale-up)

In order to examine systematically the effect of sparger design on gas holdup and bubble size and to test the sparger scale-up model (refer to Chapter 4), various sizes of spargers were constructed from three type of materials: ceramic, stainless steel and filter cloth. Table 5-5 presents the sparger surface areas. In the case of ceramic spargers, two or three individual spargers were combined (Fig.5-2) and called, respectively, sparger #2 and sparger #3. For the stainless steel sparger, part of sparger surface was sealed with tape to generate different surface areas. Filter cloth spargers were home-made and various sizes were built.

The important purpose of the experimental design here is to obtain a wide range of Rs -- the ratio of column cross-sectional area to sparger surface area. Table 5-6 summarizes the column and sparger combinations.

For all the test work in this part, froth depth was 0.5 m and collection zone length was 1.5 m. The frother concentration was 15 ppm (Dowfroth 250C) and superficial liquid downward flowrate (discharge flowrate) was 0.3 cm/s. All the test work was carried out in three columns: 3.81 cm, 5.71 cm and 10.18 cm in diameter.

5-4 Plant Test of Pilot Unit

In order to see the effect of sparger surface area on the metallurgical performance of column, plant tests were

TABLE 5-5

SPARGER SIZES FOR TESTING SPARGER SCALE-UP

CERAMIC SPARGER	#1 (*)	#2	#3
SURFACE AREA (cm^2)	19.00	38.00	57.00
STEEL SPARGER	#4	#5	#6
SURFACE AREA (cm^2)	20.00	40.00	60.00
CLOTH SPARGER	#7	#8	#9
SURFACE AREA (cm^2)	37.80	81.07	113.10
CLOTH SPARGER	#10	#11	
SURFACE AREA (cm^2)	144.51	213.63	

* sparger number for identification

TABLE 5-6

SPARGER AND COLUMN COMBINATIONS

FOR TESTING SPARGER SCALE-UP

Rs	COLUMN #1	COLUMN #2	COLUMN #3
sparger #1	No.1 (*) 0.6	N0.2, 1.35(**)	No.3, 4.23
sparger #2		No.4, .675	No.5, 2.13
#3		No.6, o.45	No.7, 1.42
#4		No.8, 1.28	No.9, 4.05
#5		No.10, 0.64	No.11, 2.03
#6		No.12, 0.43	No.13, 1.35
#7		No.14, 0.68	No.15, 2.14
#8		No.16, 0.316	No.17, 1.00
#9			No.18, 0.72
#10			No.19, 0.56
#11			No.20, 0.38

* : test number, will appear in results analysis

** : Rs

conducted at Brunswick Mining and Smelting. Fig.5-8 shows the column set-up in plant. The total length of column was 7.5 m and the column diameter was 5,71 cm. The plant operation was relatively difficult due to difficulties in observing the froth/slurry interface.

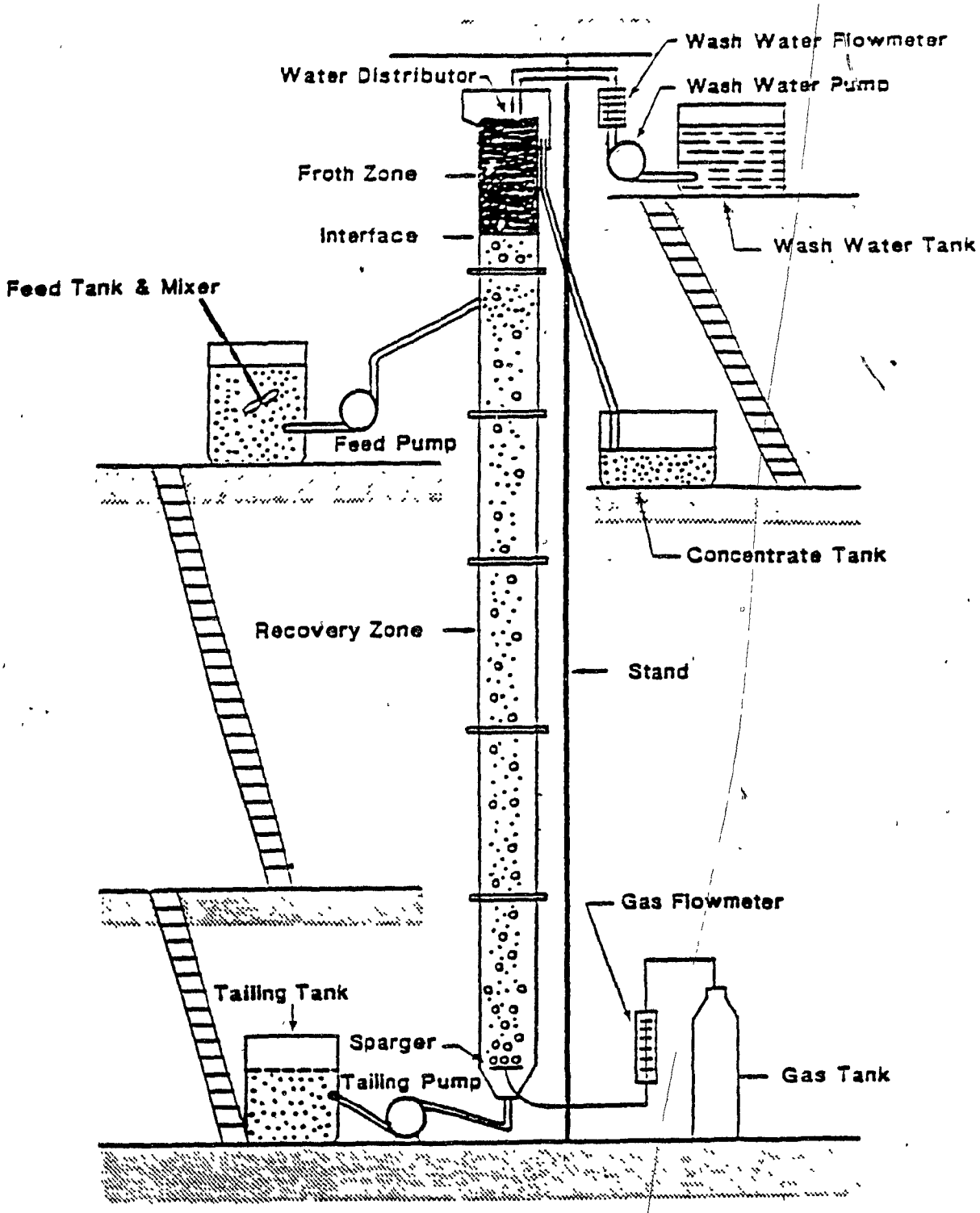

Fig.5-8 Pilot Unit Set-up in Plant

CHAPTER 6

RESULTS: VERIFICATION OF BUBBLE SIZE ESTIMATION TECHNIQUE

6-1 Photographic Measurement of Bubble Size

Since bubbles generated by spargers in flotation columns usually have a size distribution rather than a unique size, there are a number of ways to define the mean bubble diameter [61].

Sauter mean diameter: the Sauter mean diameter is the most consistent representation of mean bubble diameter obtained from various techniques according to Shah et al [61] and is defined as the volume-to-surface mean diameter:

$$dbs = \frac{\sum ni \ \ dbi^3}{\sum ni \ \ dbi^2} \qquad [6\text{-}1]$$

Volumentric mean diameter: the volumentric mean diameter is also used to present mean bubble diameter [17] and is defined:

$$dvs = \sqrt[3]{\frac{\sum ni \ \ dbi^3}{ni}} \qquad [6\text{-}2]$$

Fig.6-1 shows the bubble size distribution obtained by photography in the collection zone. Little difference was noted between two mean diameters. This is expected since the range in size distribution is small, typical relative standard deviation is about 20%.

6-2 Comparison between Dobby's method, Developed Method, and Photographic Measurement

For the estimation of bubble size by drift-flux analysis, gas holdup measurement has to be made at varying values of liquid downward velocity at constant gas velocity. A typical plot of gas holdup vs superficial gas velocity for different liquid velocity is shown in Fig.6-2. Plotting $Vg/\varepsilon g(1-\varepsilon g)^{m-1}$ vs $(V_l - Vg)/(1-\varepsilon g)^{m-1}$, as shown in Fig.6-3, the intercept can be estimated. Therefore, the terminal velocity of a single bubble can be calculated by assuming Ko = 0.97. Using Concha and Almendra' equation [16] (Eq.[4-8]), bubble size is computed.

Fig.6-4 presents the comparison of the bubble sizes by Dobby's method, the developed method and photography. There is little difference noted between the two methods and both are in good agreement with photographic measurement.

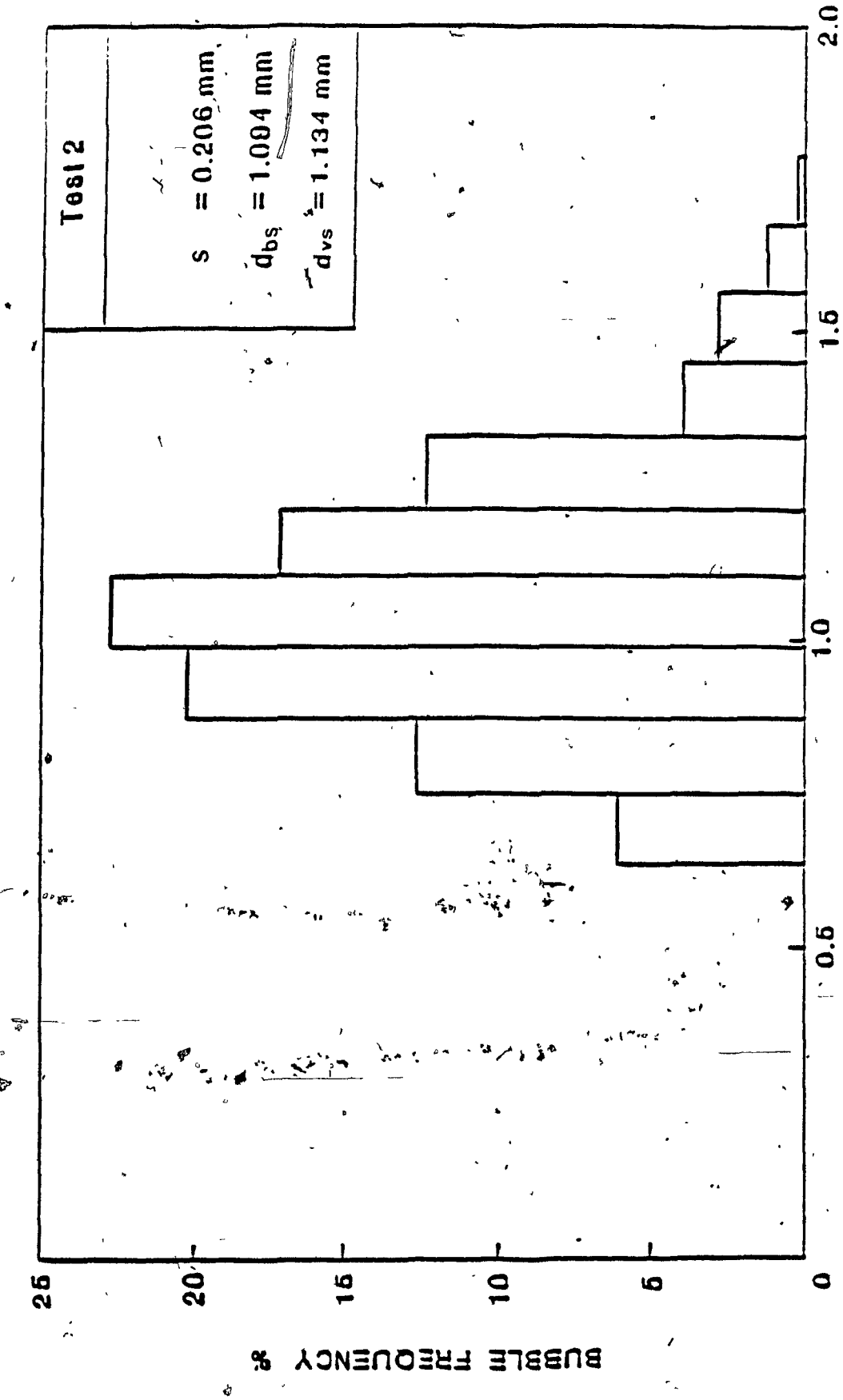

Fig.6–1 A Typical Bubble Size Distribution in a Column

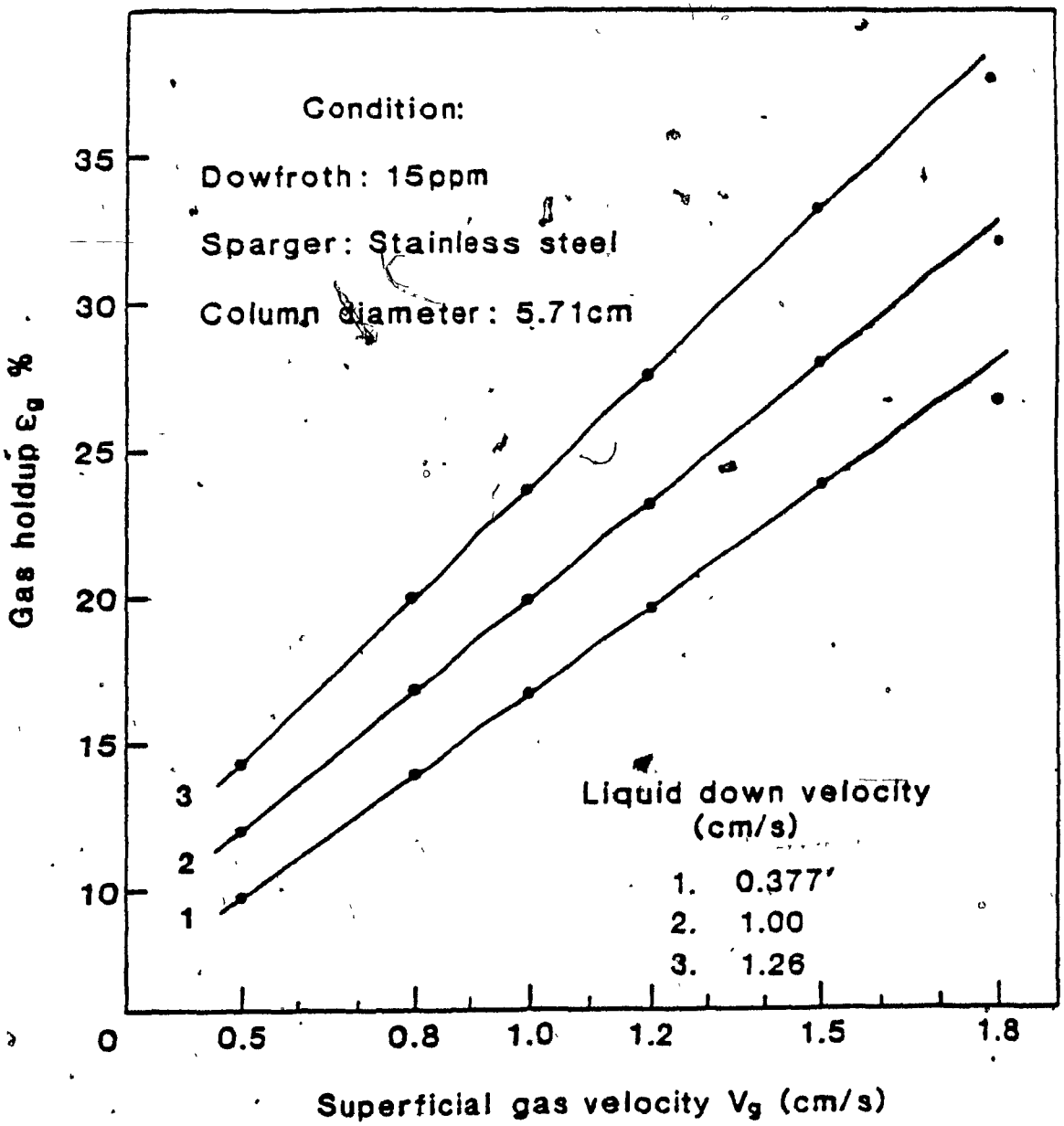

Fig.6–2 The Relationship between Gas Holdup and Superficial Gas Velocity

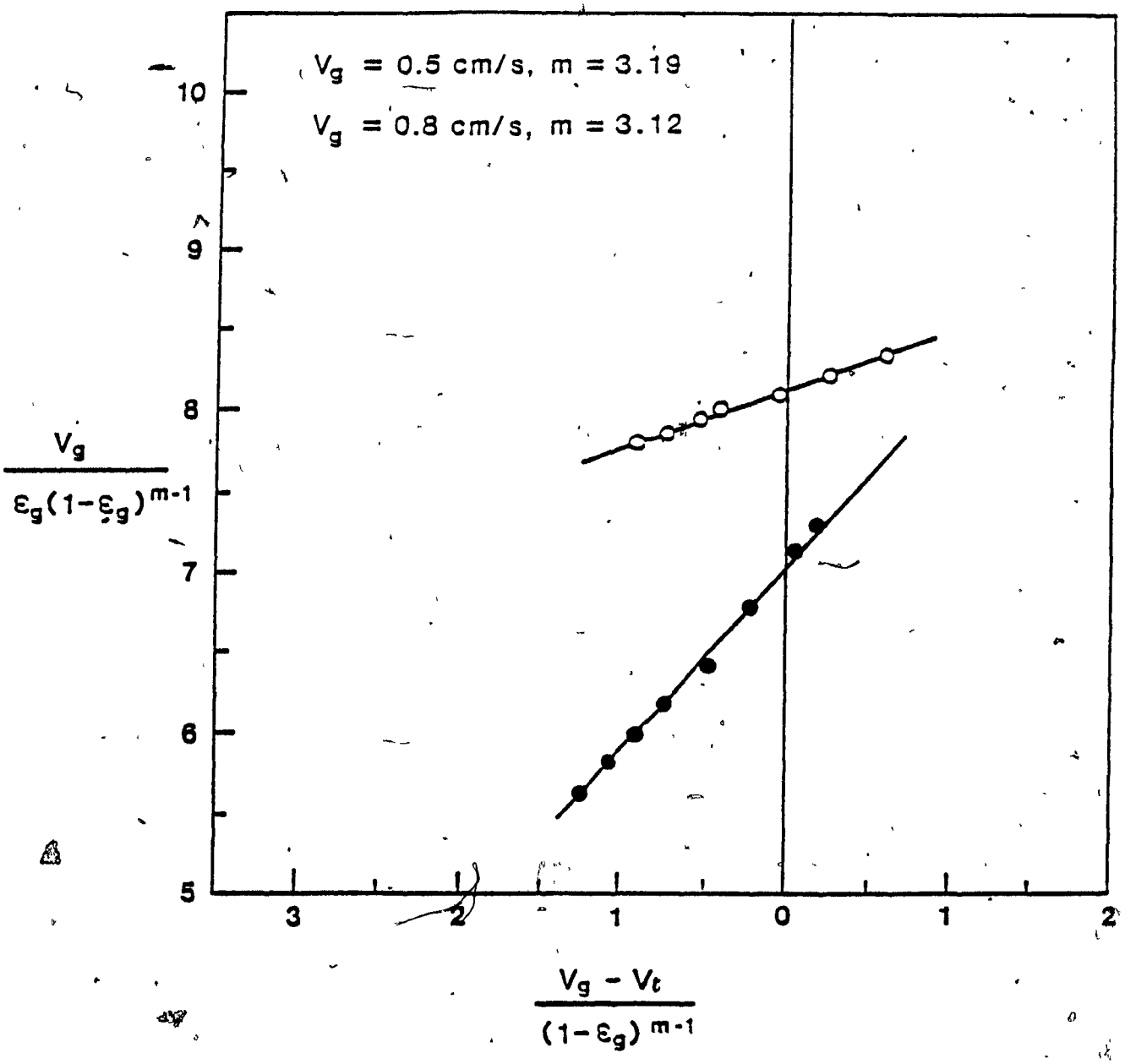

Fig.6—3 The Drift—flux Plot to Estimate the Terminal Rise Velocity of Bubbles. condition: the same as Fig.4—1

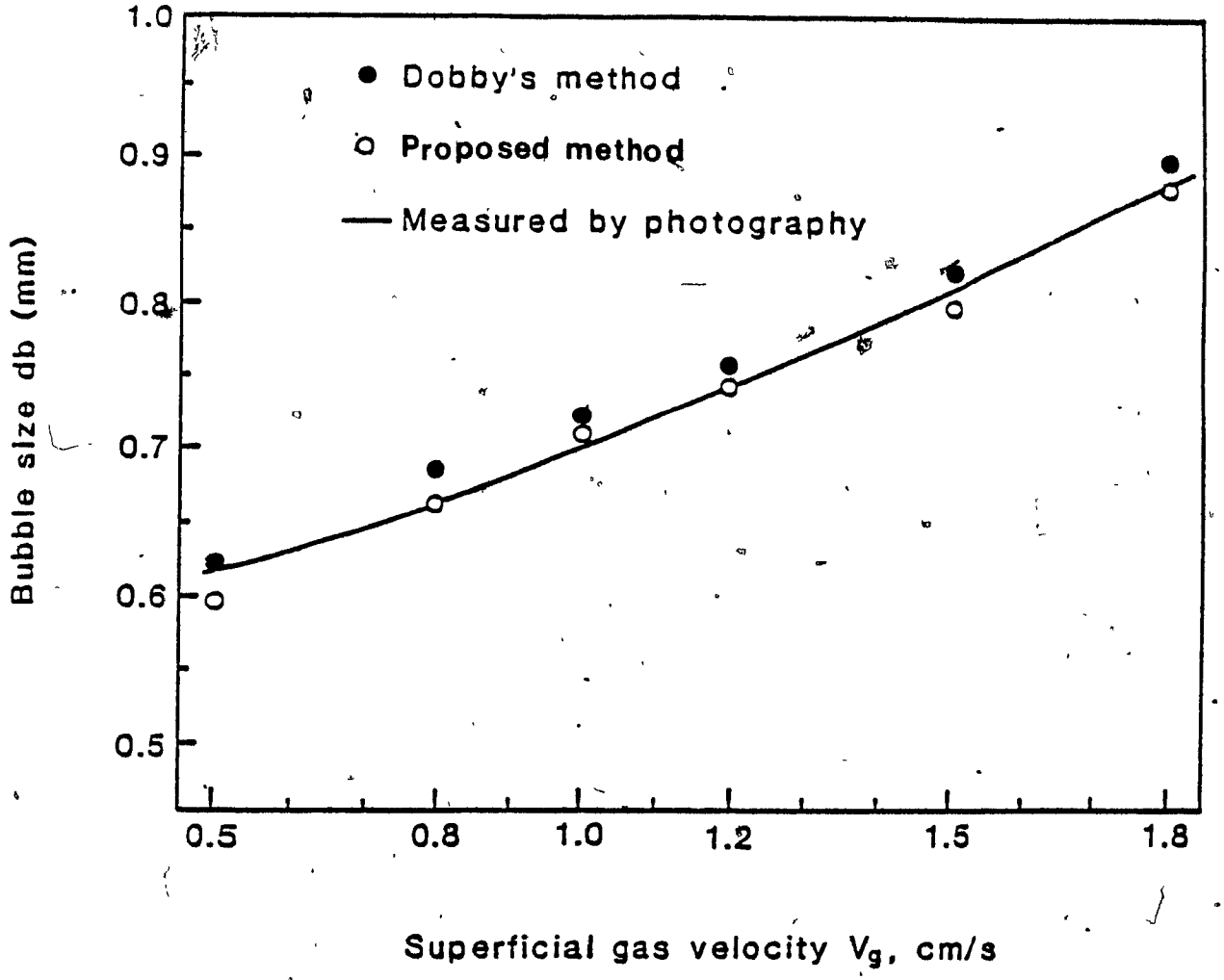

Fig.6-4 Bubble size vs. superficial gas velocity, the comparison of measured bubble size with those estimated by Masliyah's equation and Dobby's method. Conditions shown in Fig.6-2

6-3 In Flotation Columns

Table 6-1 compares measured bubble size with that calculated by the developed method and the method used by Dobby [24]. Fig.6-5 summarizes the excellent agreement between measured and calculated bubble size in flotation columns.

6-4 In Mechanical Cells

Table 6-2 presents the data obtained from a mechanical cell by Szatkowski [65]. The liquid downward velocity in this case is zero (batch system). This table provids all the information necessary for computation of bubble size. The calculated bubble size is presented in Table 6-2 and compared with the measured bubble size. Fig.6-6 plots measured vs. calculated bubble size and shows a good agreement between values.

TABLE 6-1

BUBBLE SIZE MEASURED AND PREDICTED

TEST SERIES	FROTHER †	ppm	V_g cm/s	V_L cm/s	ε_g %	Re	Reb	BUBBLE SIZE, mm MEASURED dbs	PREDICTED †† De-Hrooec	Dabo.
1	DOW	5	1.0	0.91	9.5	157	120	1.20	1.11	
		10	1.0	0.85	12.9	97	66	0.96	0.87	
		15	1.0	0.82	15.9	77	47	0.77	0.76	
		20	1.0	0.85	15.5	79	49	0.69	0.77	
		25	1.0	0.77	16.2	74	44	0.73	0.74	
2	DOW	10	2.1	0.30	15.7	265	171	1.51	1.40	
		15	1.5	0.30	14.0	165	111	1.13	1.11	
3	DOW	15	0.5	1.00	12.3	37	25	0.62	0.55	0.61
		15	0.8	1.00	17.0	55	31	0.67	0.64	0.69
		15	1.0	1.00	20.0	66	33	0.70	0.69	0.73
		15	1.2	1.00	23.4	78	36	0.74	0.74	0.75
		15	1.5	1.00	28.0	98	39	0.81	0.80	0.82
		15	1.8	1.00	32.0	122	42	0.88	0.87	0.90
4	TEB	5	1.0	0.96	11.2	121	87	0.97	0.98	
		10	1.0	0.88	13.2	95	64	0.85	0.86	
		15	1.0	0.91	14.4	87	56	0.85	0.81	
		20	1.0	0.97	17.7	70	40	0.82	0.72	
		25	1.0	0.83	21.5	60	29	0.71	0.65	
5	MIBC	20	1.0	0.90	13.2	96	64	0.78	0.86	
		30	1.0	0.90	13.3	95	64	0.75	0.86	
		45	1.0	0.91	13.6	93	61	0.80	0.84	
		60	1.0	0.91	15.3	81	50	0.73	0.78	
		75	1.0	0.96	18.0	71	40	0.67	0.72	

† DOW: Dowfroth 250C (polypropylene glycol methyl ether)
TEB: Tri ethoxy butane
MIBC: Methylisobutylcarbinol (methylamyl alcohol)

†† liquid density = 1 g/cm^3
liquid viscosity = 0.01 g/cm-s

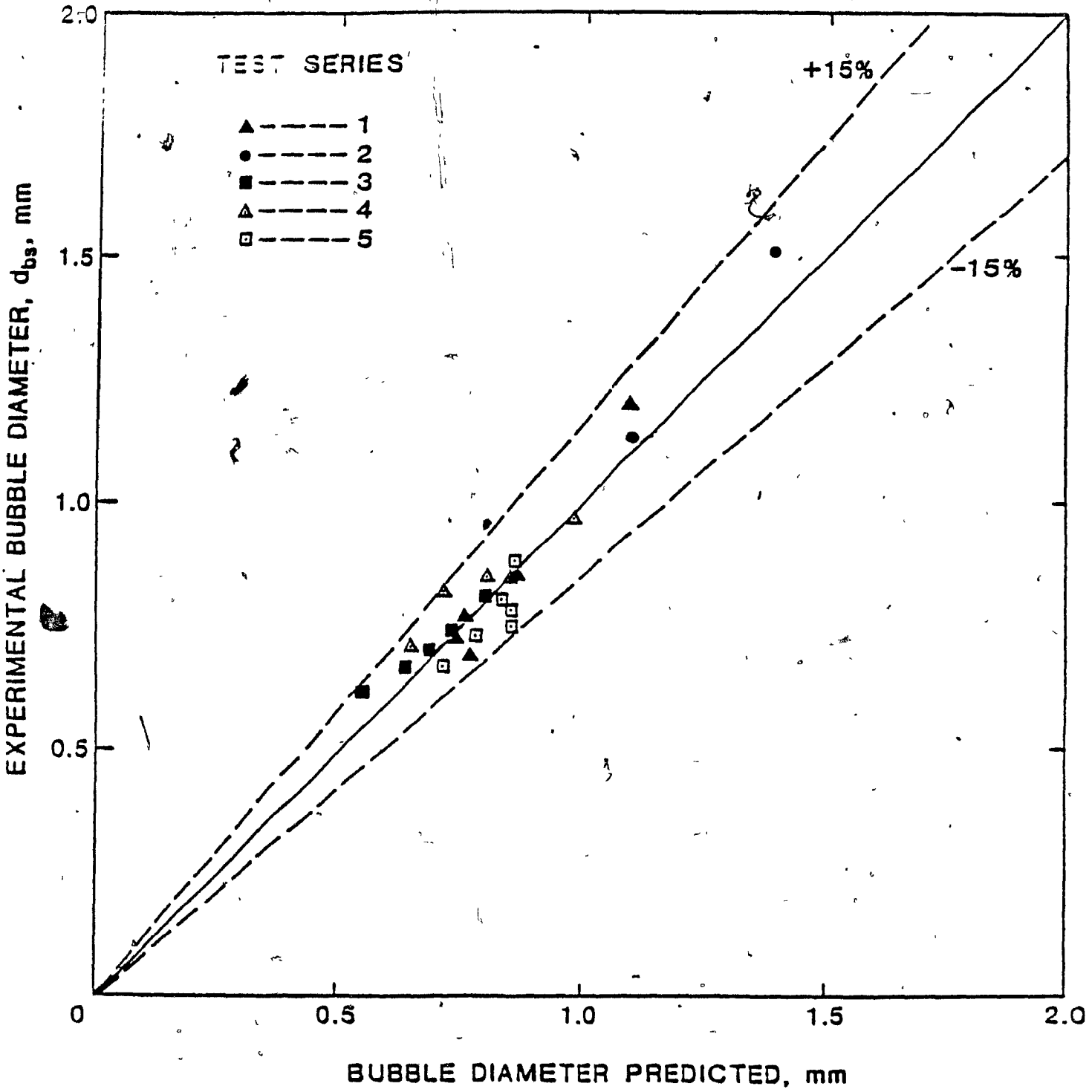

Fig.6—5 Comparison of measured (Sauter mean) with predicted bubble size by the developed method in flotation columns

TABLE 6-2

TEST CONDITIONS AND RESULTS

V_g (cm/s)	ε_g (%)	db (μm)	SD (μm)	db* (μm)
0.0333	4	240	70	143
0.0333	4	210	85	143
0.2333	6	490	120	402
0.2333	8	380	105	334
0.2333	8	310	90	334
0.5	11	490	120	486
0.5	14	415	125	421
0.5	15	375	125	407
1.167	18	610	200	714
1.167	22	600	210	639
1.167	22	540	170	629

Notes: SD: Standard Deviation
Liquid Rate V_l=0
Liquid Density = 1 g/cm^3
db : measured bubble size
db* : calculated bubble size

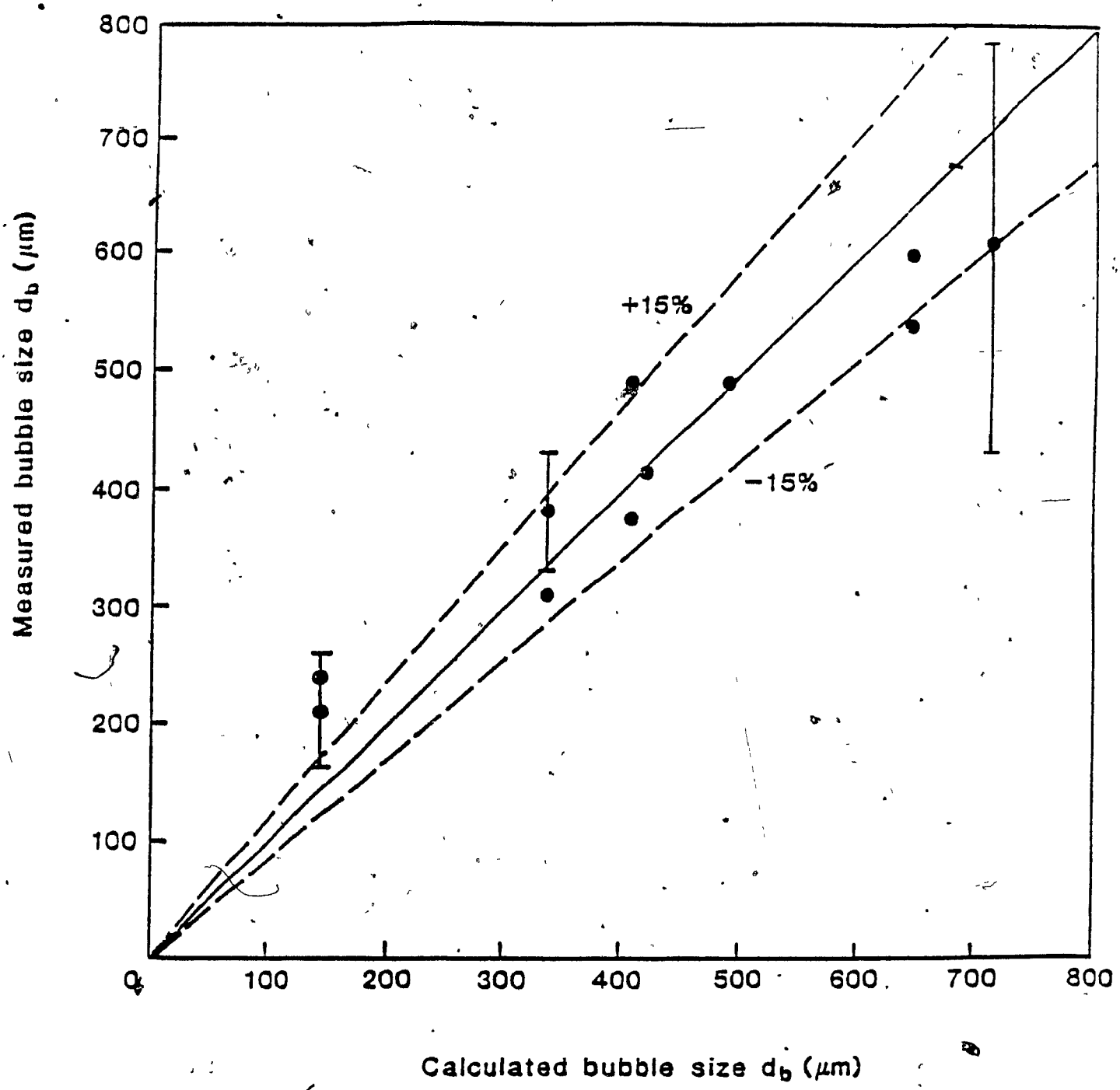

Fig6-6 Comparison between Calculated and Measured Bubble Size in Mechanical Flotation Cells

CHAPTER 7

RESULTS: EFFECTS OF OPERATING VARIABLES ON GAS HOLDUP AND BUBBLE SIZE

7-1 Gas Holdup and the Effect of Gas Flowrate and Frother Addition

Fig.7-1 and Fig.7-2 show clearly that in flotation columns gas holdup is proportional to superficial gas velocity. That is, from Eq.[4-13] β is equal to 1. It is noted in Fig.7-2, for the same chemical conditions and the same sparger, gas holdup in the smaller column is larger than in the larger column. The effect of column dimension on gas holdup is due to the difference in the parameter, Rs, the column cross-sectional area to sparger surface area ratio. This implies that for the larger column, a larger sparger size may be required to achieve a similar gas holdup. The effect of frother concentration on gas holdup can be found in Fig.7-3. In Fig.7-3. gas holdup is plotted as a function of frother concentration. Gas holdup increases with frother to a certain concentration above which the gas holdup is constant (maximum).

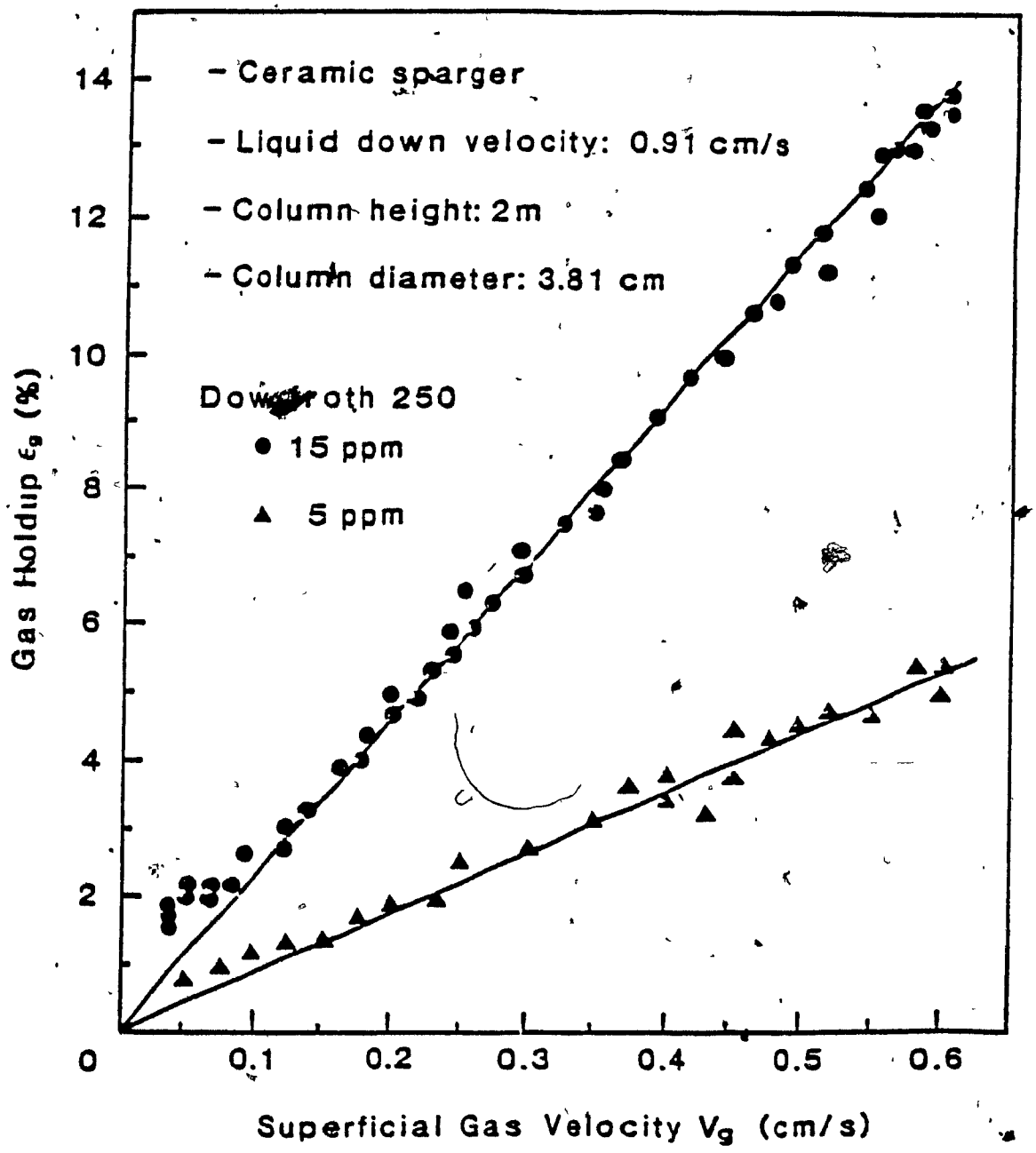

Fig. 7–1 Gas Holdup vs. Superficial Gas Velocity

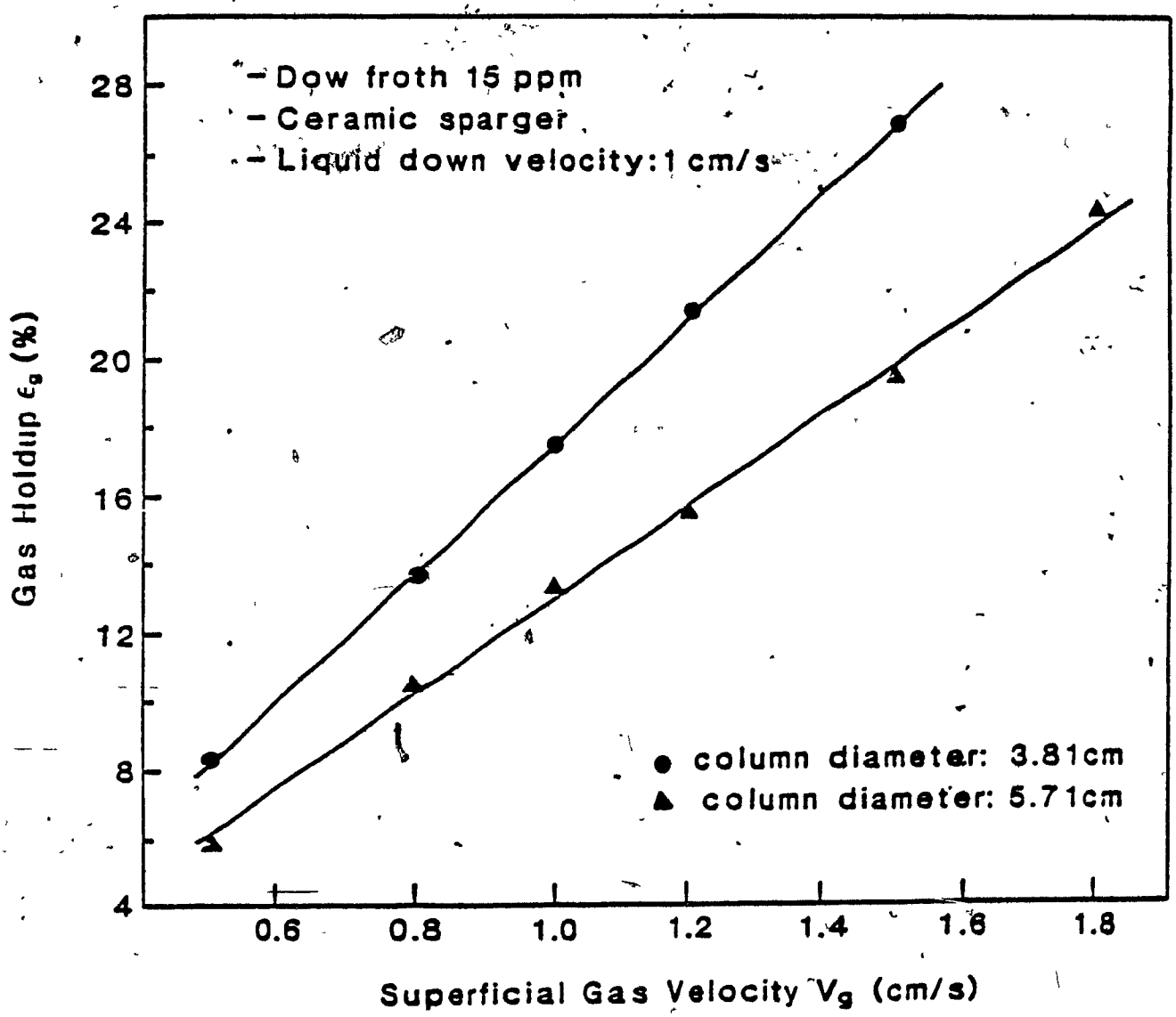

Fig.7–2 Gas Holdup vs. Superficial Gas Velocity

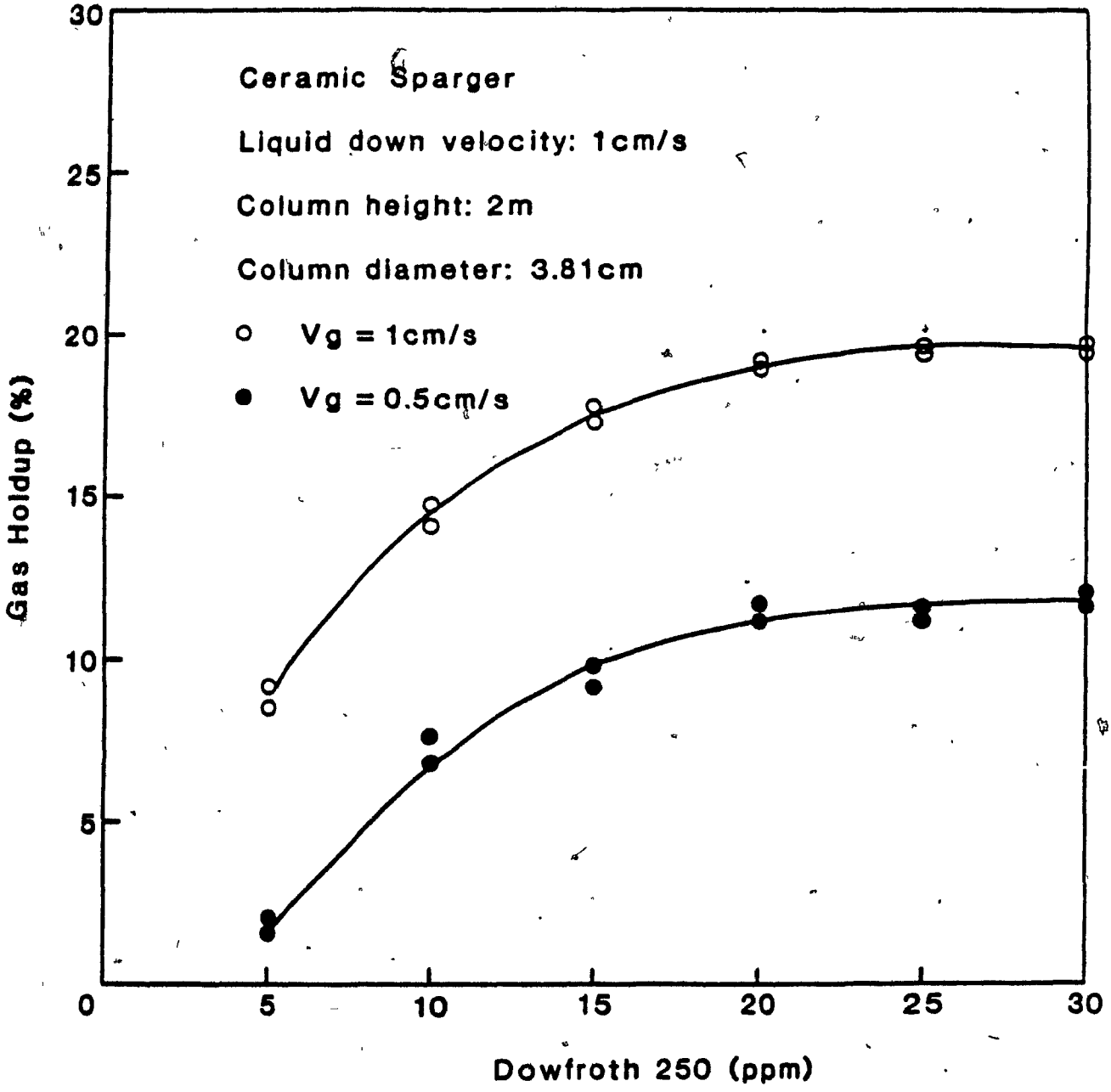

Fig.7-3 Gas Holdup vs. Frother Concentration

7-2 Bubble Formation and the Impact of Gas Flowrate and Frother Addition

As shown in Fig.7-4, at very low gas velocity (0-0.6 cm/s), bubble size increases with gas velocity, although the total change in bubble size is less than 0.1 mm. It should be noted that there exists a relatively large error in the measurement of gas holdup when gas holdup is small (<5%). This is refered by the error bar on db in Fig.7-5. It was observed that at very low gas flowrate, the gas only goes through the larger holes on the top of the sparger. (There is a limitation for the lowest gas flowrate. If gas flowrate is less than 0.03 cm/s, no gas discharges in this case). Once gas flowrate increases, the smaller orifices begin to work. An effort was made to measure the pressure drop inside the sparger, it was found to be very small (less than 2 psi).

Fig.7-5 shows the photography taken of the collection zone in the column, revealing the shape, size and density of gas bubbles with and without frother addition. The frother addition is an important factor affecting bubble size and shape. It can be noted in Fig.7-5a that the interface of froth/slurry is readily identified when frother is added.

Fig.7-6 shows that in the same chemical environment using the same superficial gas velocity and the same sparger, the bubble size is smaller in the small column than in the large column (corresponding to the gas holdup being larger in the small column than in the large column, see Fig.7-2). The

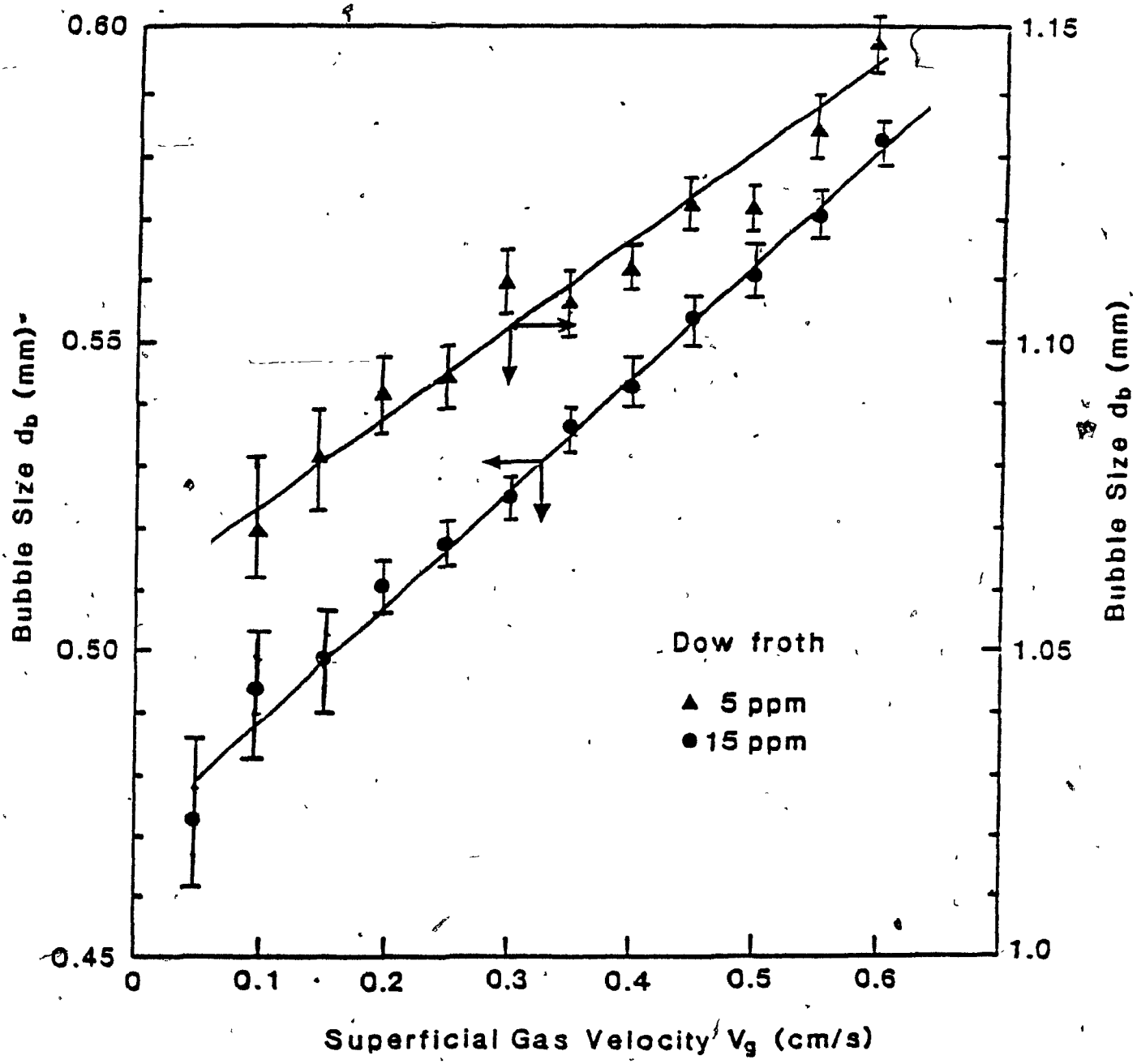

Fig.7—4 Bubble Size va. Superficial Gas Velocity
(bubble size is estimated from Masliyah's equation)

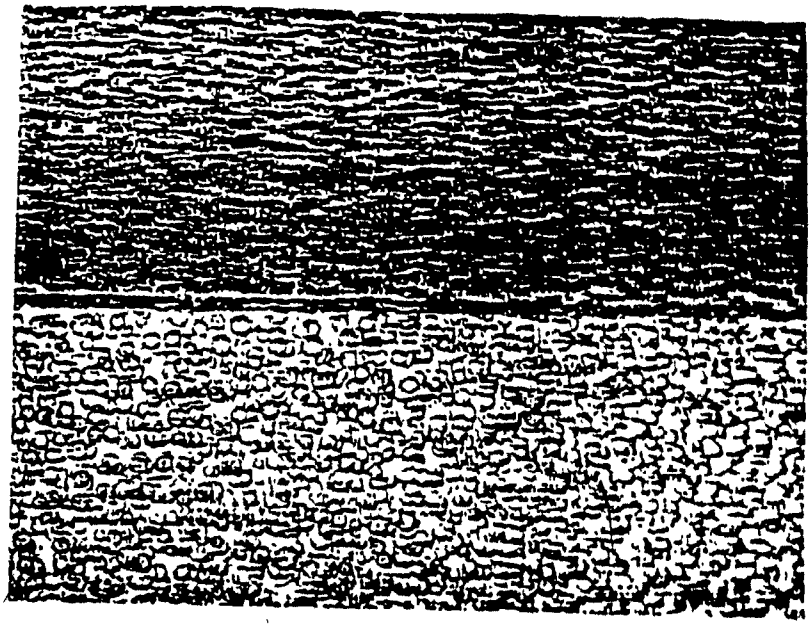

(a) With Frother Addition: Dowfroth 15 ppm

(b) Without Frother Addition

Fig.7- 5 Photographies Showing the Effect of Frother Addition on Bubble Size

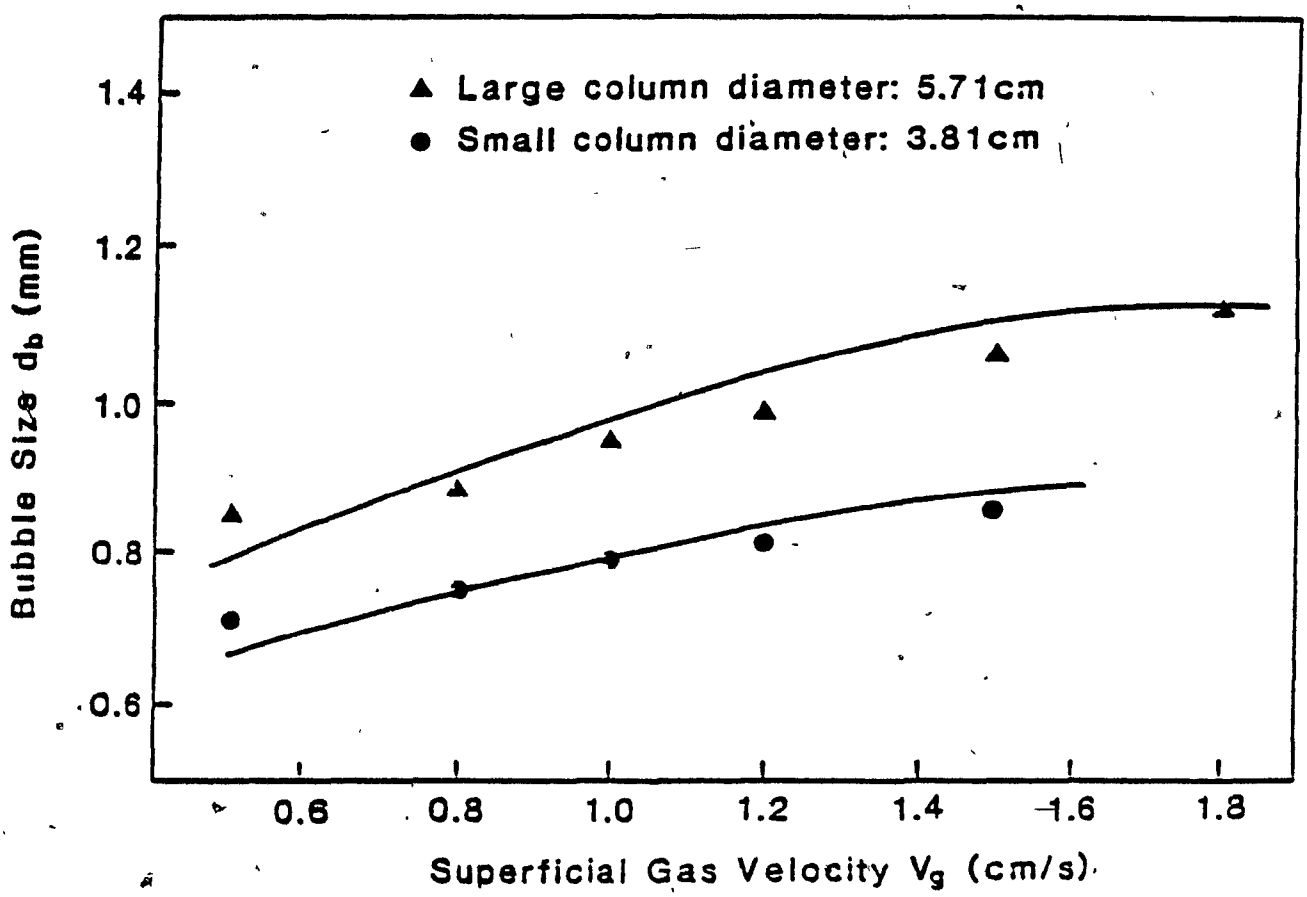

Fig. 7-6 Bubble Size vs. Superficial Gas Velocity

reason for this is that as the column cross-section increases, the volumetric flowrate of gas also increases if the same superficial gas velocity is to be maintained. As a result, the gas flowrate per unit area of sparger increases, which produces larger bubbles. By plotting bubble size vs. Rs.Vg (gas flowrate per unit area of sparger) as shown in Fig.7-7, the relation between bubble size and gas rate is independent of the column dimension. This implies that Eq.[4-15] does take into account sparger size.

7-3 The Influence of Gas Sparger Types on Gas Holdup and Bubble Size: Preliminary Findings

The bubble size without frother addition for the four type of spargers is presented in Fig.7-8. Cusual inspection suggests that the bubbles produced by the rubber sparger are the largest and by the filter cloth are the smallest. Fig.7-9 is the bubble size distribution for the four type of spargers without frother addition. The maximum difference in size between the largest and smallest bubbles is up to 3 mm. In other words, the distribution of bubble size is very wide. The bubble size distribution with frother addition for steel sparger is shown in Fig.7-10. In general the distribution is very narrow after frother is added. The range in bubble size becomes less pronounced after frother is added. An average bubble size (diameter) now becomes a useful parameter.

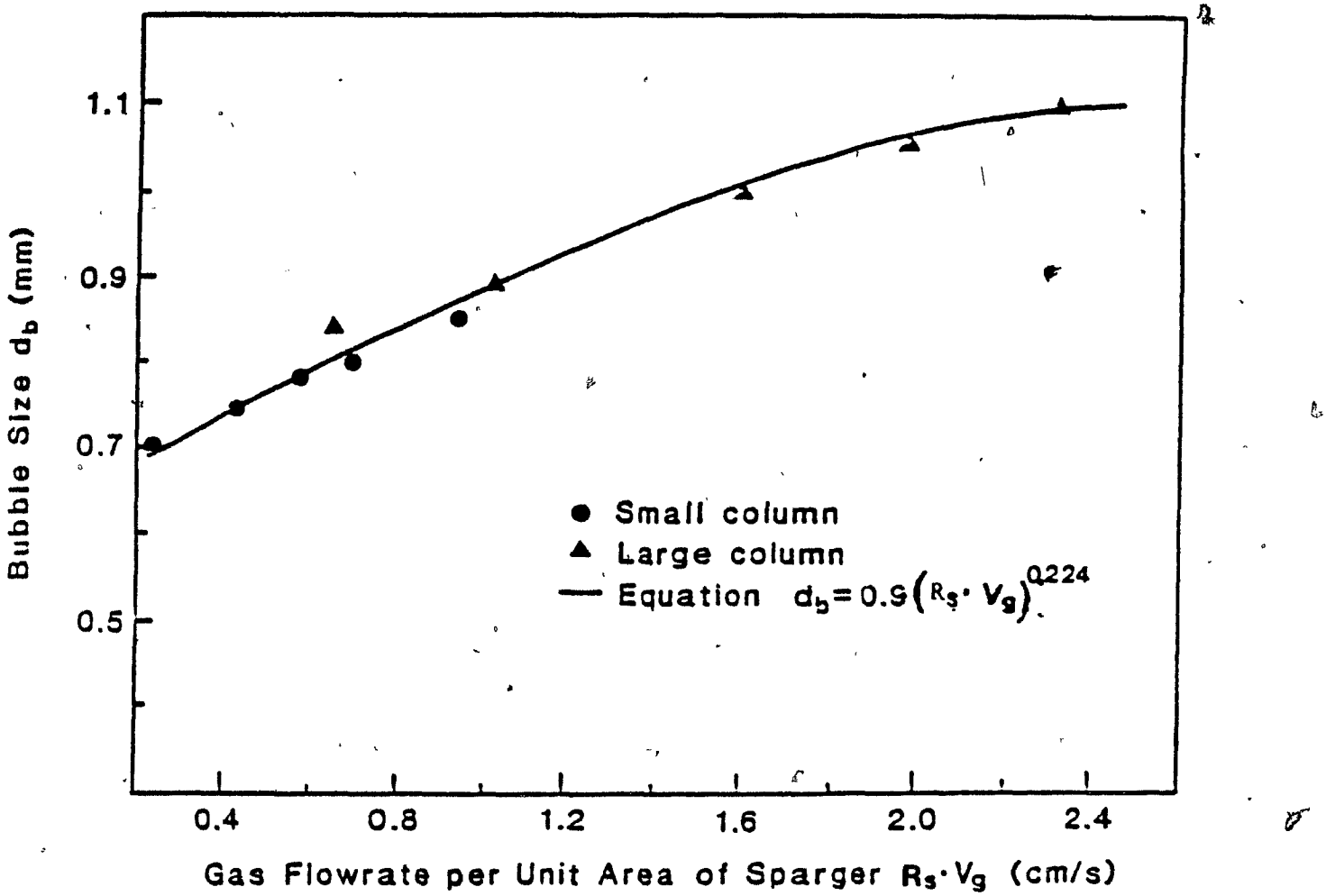

Fig.7–7 Bubble Size vs. Gas Flowrate per unit Area of Sparger Rs.Vg

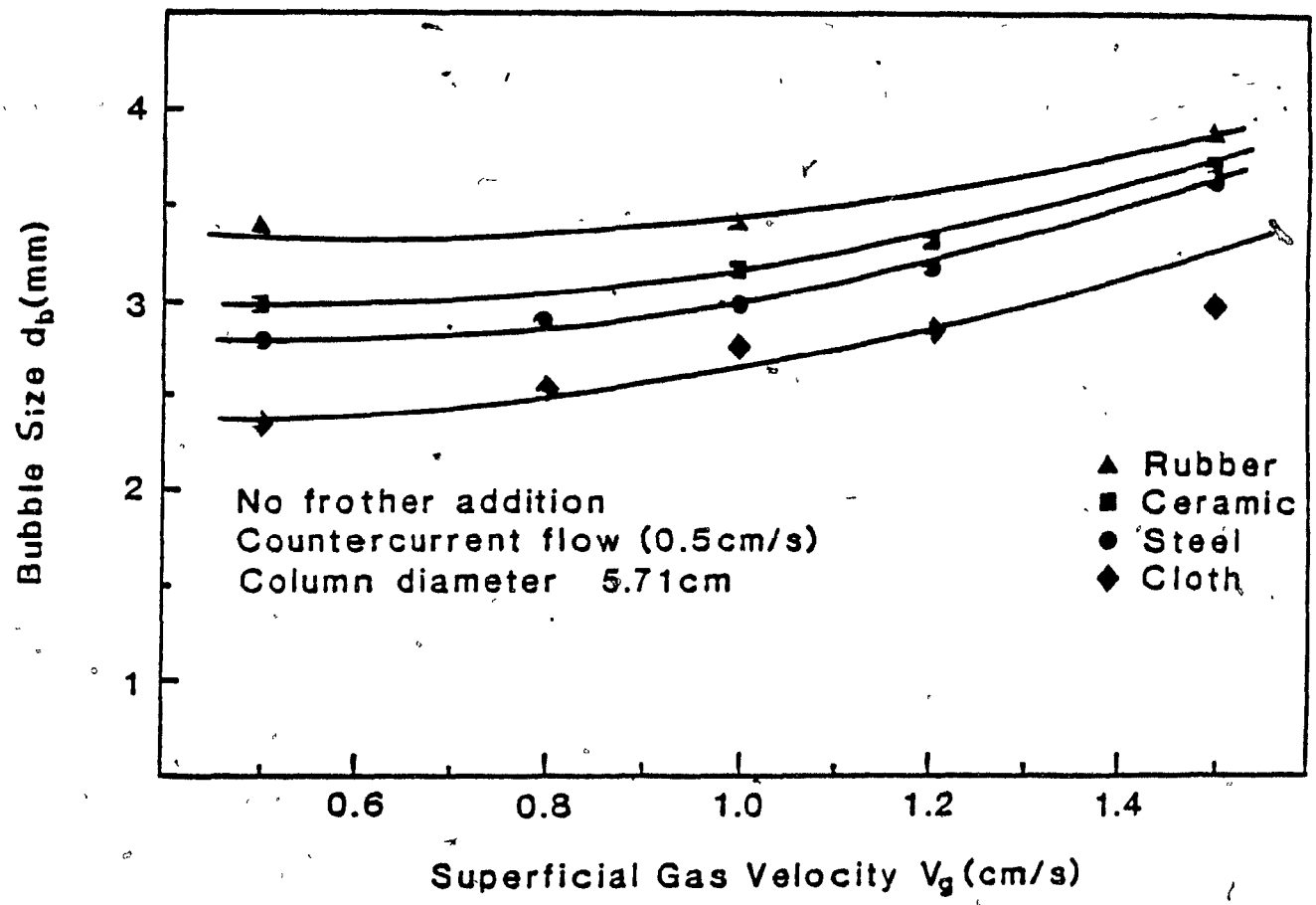

Fig. 7-8 Bubble Size vs. Superficial Gas Velocity (bubble size is photographically measured)

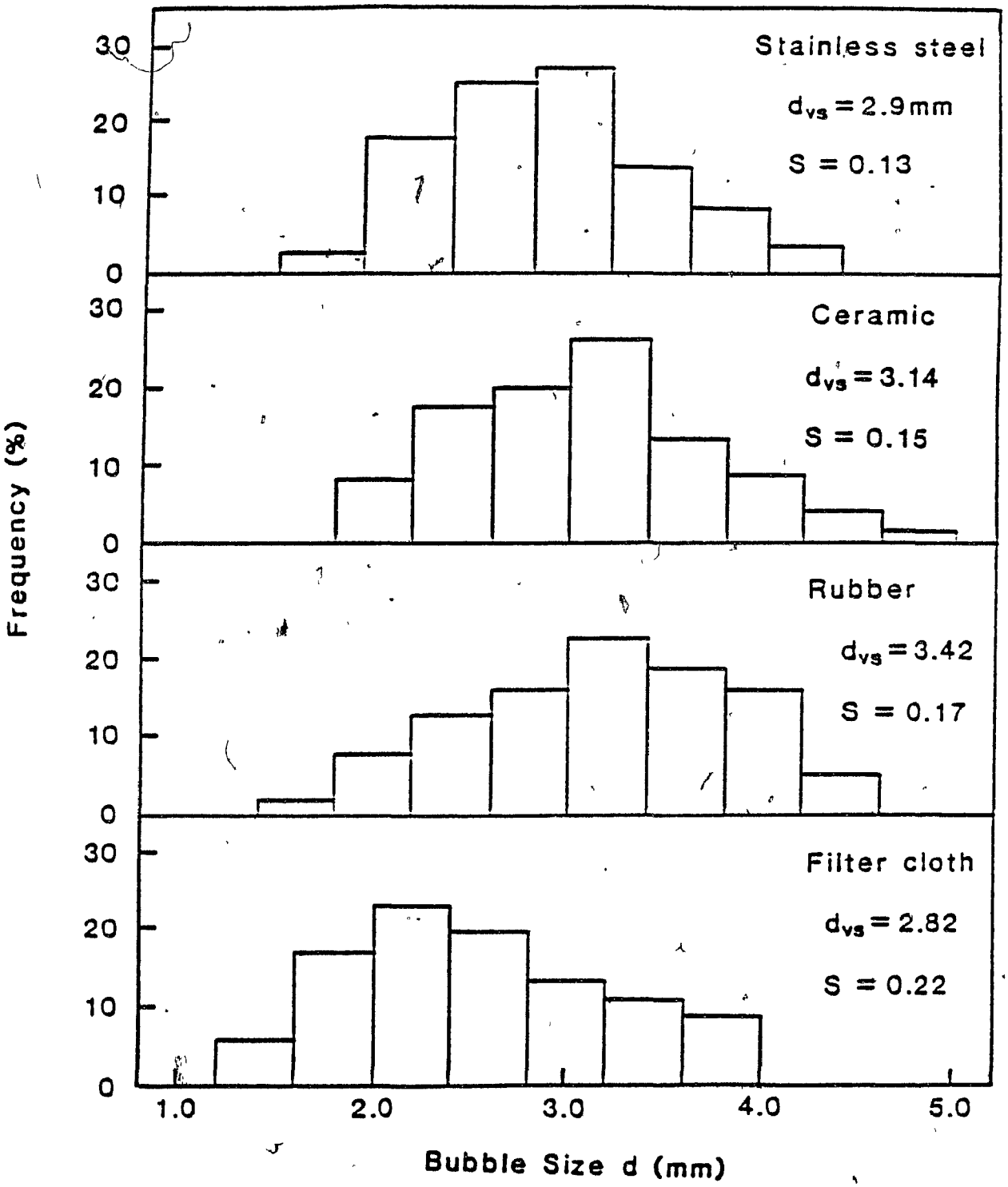

Fig.7–9 Bubble Size Distribution for Four Type of Spargers Used in This Work without frother

Vg = 1.0 cm/s

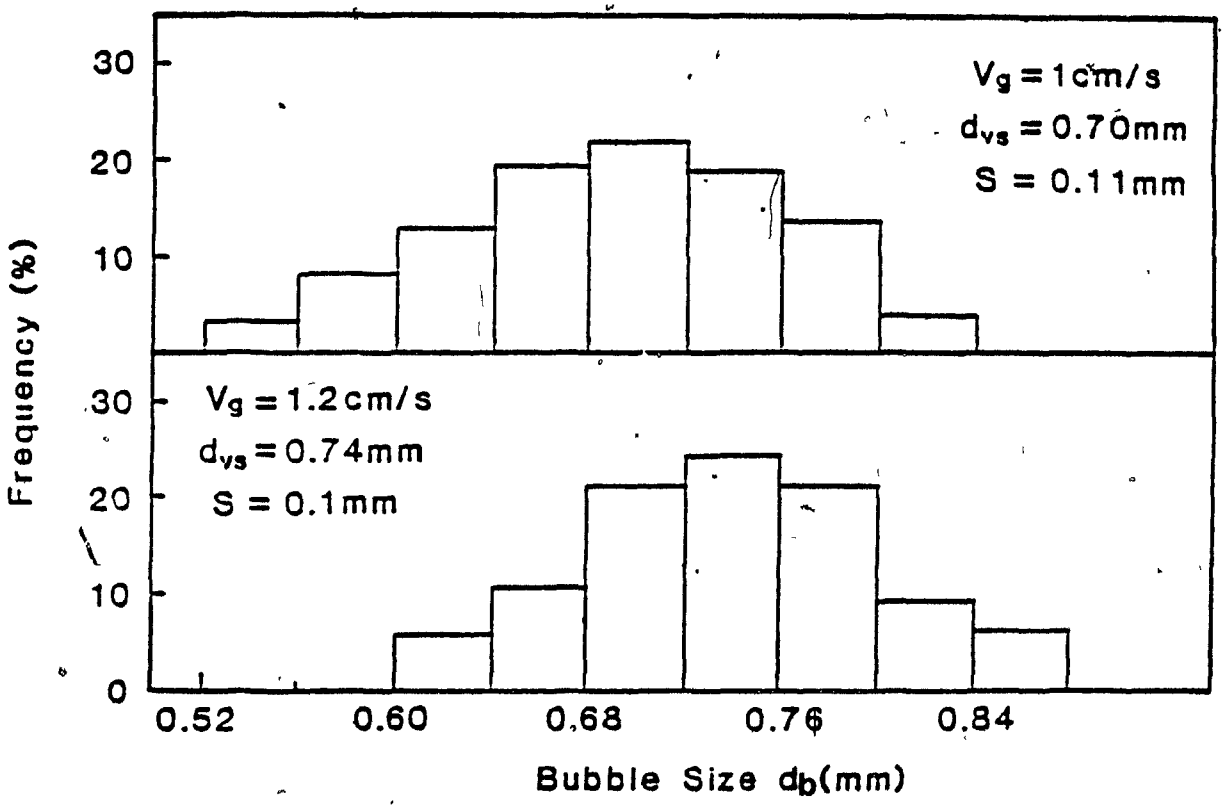

Fig.7–10 Bubble Size Distribution for Stainless Steel Sparger with Frother Addition

Fig.7-11 is a plot of gas holdup as a function of superficial gas velocity for the four type of spargers under the same conditions. Fig.7-12 is bubble size vs. superficial gas velocity based on Fig.7-11. The curves are nearly parallel, implying that the n value for each sparger is about the same. By plotting bubble size vs. gas flowrate per unit area of sparger, Fig.7-13 is obtained. It is seen from this figure that the correlation between bubble size and gas rate can be approximately generalised by Eq.[4-15]. From this preliminary study, it can be concluded that the major effect of the sparger on gas holdup and bubble size is the sparger surface area, rather than sparger material.

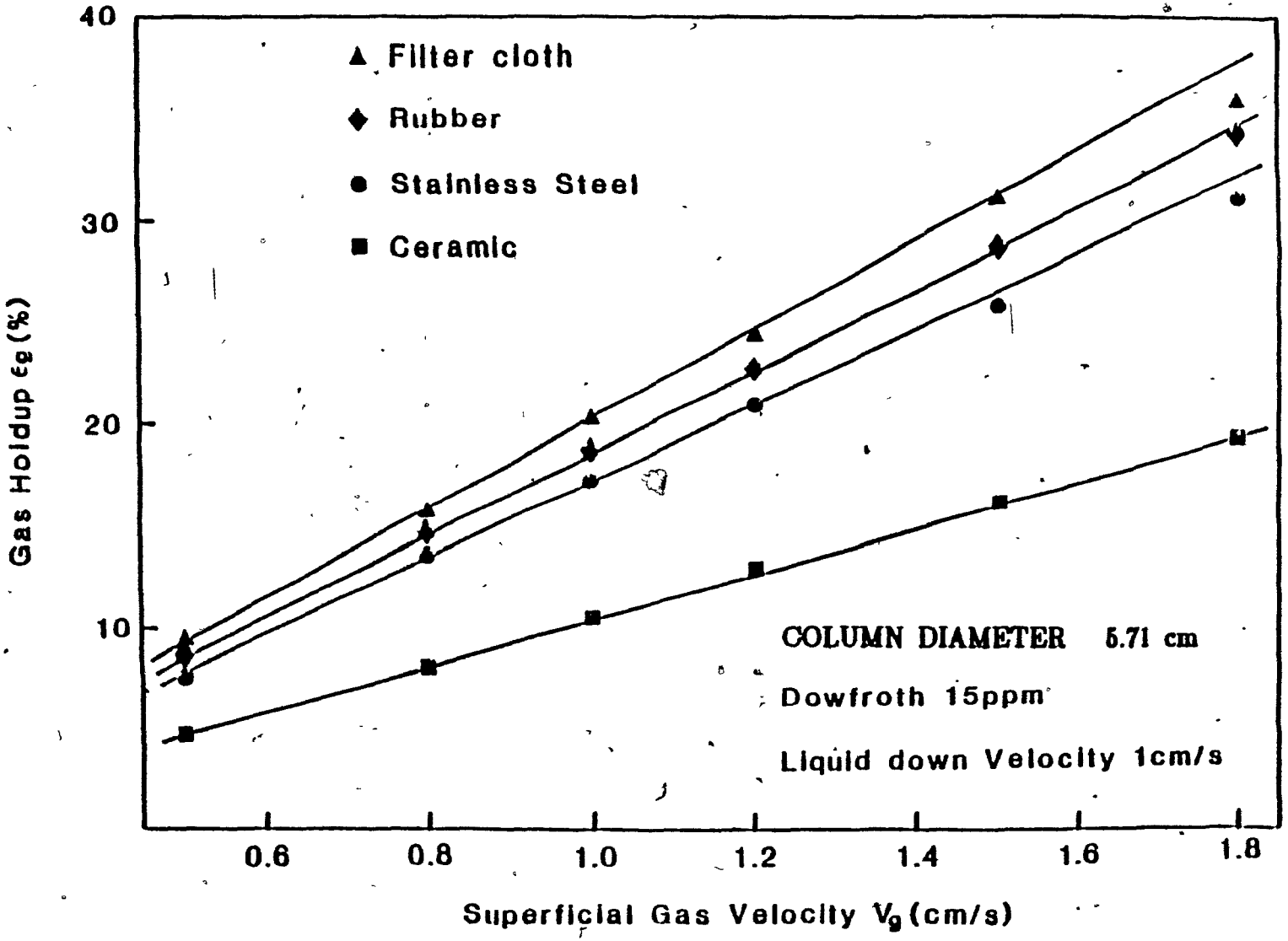

Fig. 7–11 Gas Holdup vs. Superficial Gas Velocity for Four Type of Spargers Used in This Work

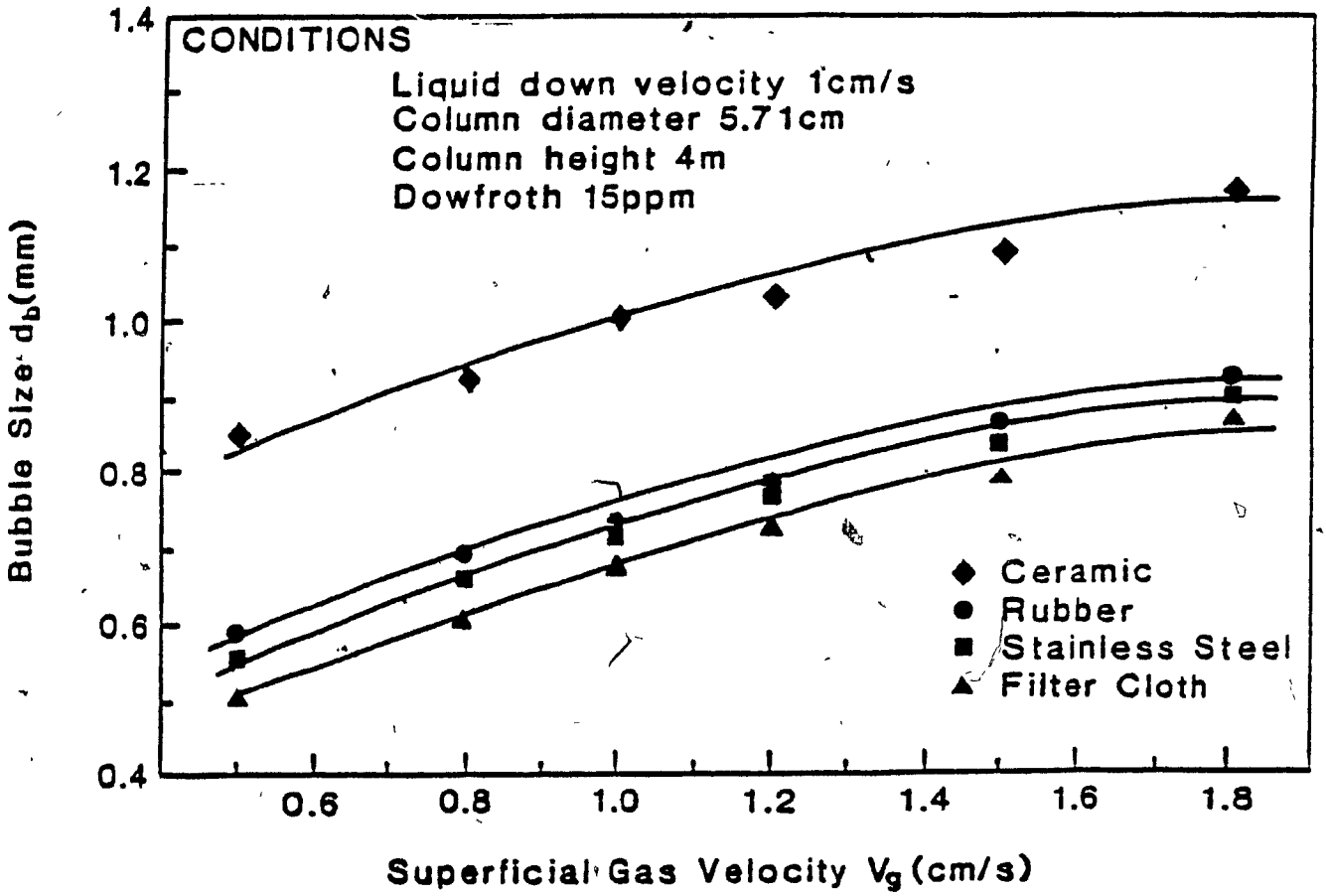

Fig.7–12 Bubble Size vs. Superficial Gas Velocity

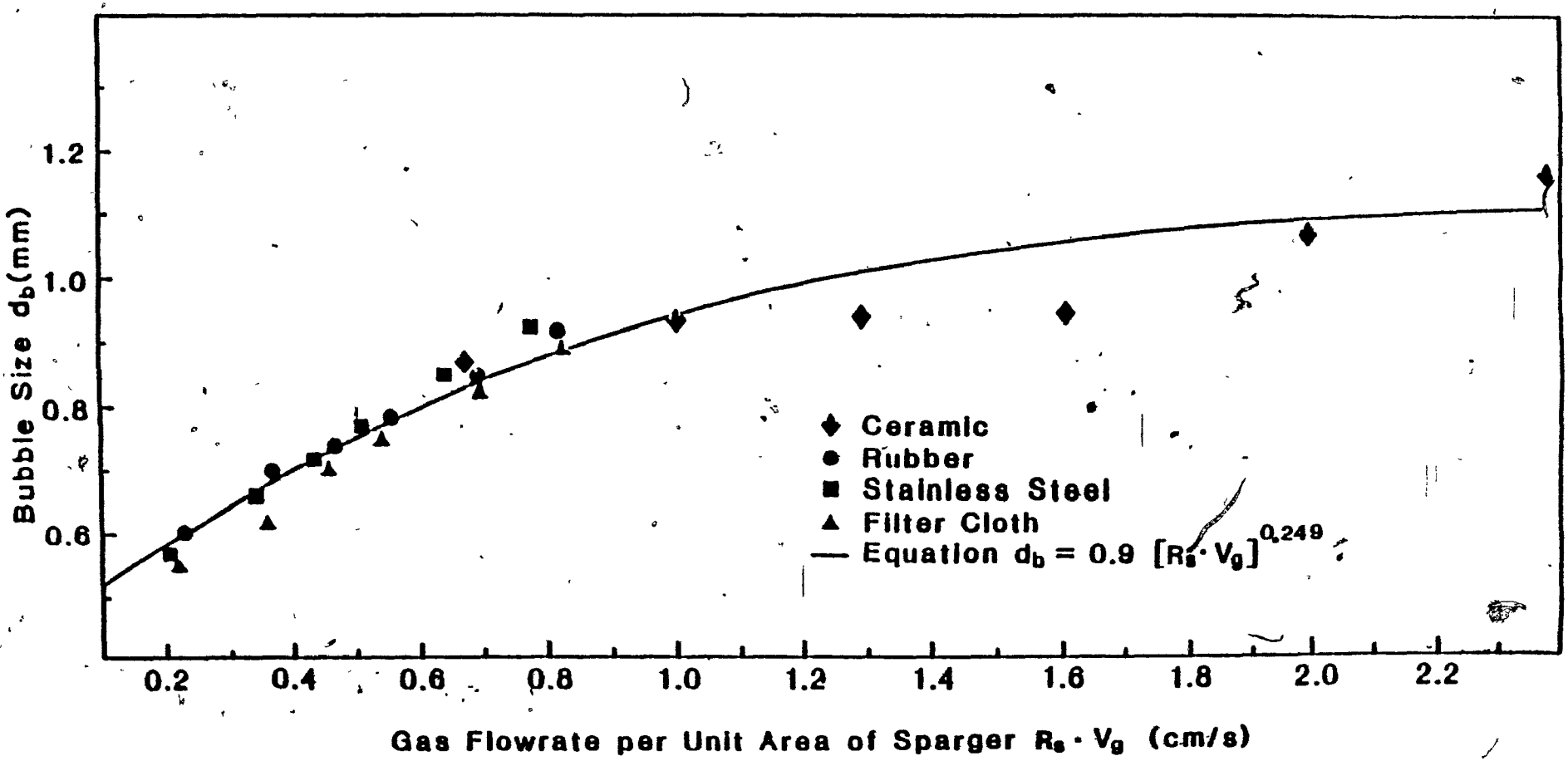

Fig. 7-13 Bubble Size vs. Gas Flowrate per Unit Area of Sparger Rs.Vg

CHAPTER 8

RESULTS: TESTING THE EFFECT OF SPARGER SIZE A SCALE-UP MODEL

From the work presented in chapter 7, it was found that sparger size is one of the important parameters affecting gas holdup and bubble size. This is important for selecting sparger size, i.e. scaling-up of spargers.

8-1 Laboratory Studies

8-1-1 Minimum Gas Flowrate, Gas Maldistribution and Bubble Coalescence

When gas flowrate reaches zero, gas holdup should be zero. However, from observation a minimum superficial gas velocity exists below which no gas emerges from the sparger (i.e. gas holdup is zero). There is a difference in this minimum flowrate depending whether the gas rate is being increased or decreased. This hysteresis is illustrated in Fig.8-1. It is noted that a decrease of sparger surface area will slightly increase this velocity.

Gas maldistribution was observed for the spargers used in this work, particularly for the home-made filter cloth spargers. Gas maldistribution may be evidenced by jetting occuring at some orifices while other orifices remain inactive. It is important to avoid gas maldistribution since

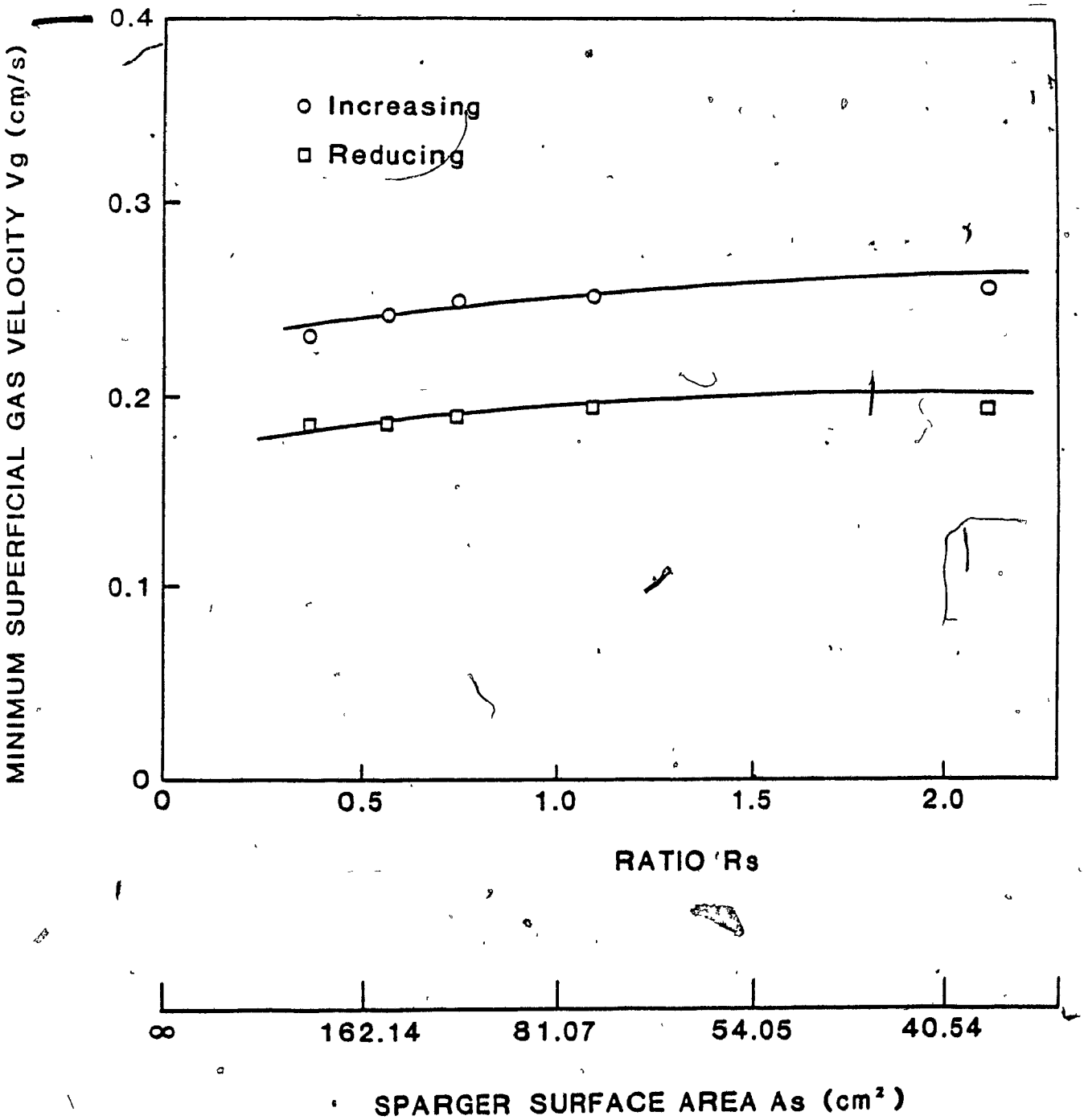

Fig. 8-1 Minimum superficial gas velocity: the effect of sparger surface area

it affects the generation of uniform bubbles and very serious gas maldistribution leads to poor column performance. Gas maldistribution can be avoided to some extent by using spargers which have a uniform orifice distribution and uniform orifice size. Gas maldistribution was eliminated by careful adjustment (avoiding any sudden change) of gas flowrate in this work.

Fig.8-2 shows one effect of gas maldistribution on gas holdup for the home-made filter cloth sparger. When gas maldistribution occurs, gas holdup no longer extrapolates to zero with decreasing gas rate.

Bubble coalescence associated with sparger design may occur when several individual spargers are used. In the present work, for sparger #2 and #3, serious bubble coalescence was found and was eliminated to some extent by using baffles between each sparger (Fig.5-2). When bubble swarms from two or more individual spargers meet, bubble coalescence may occur. This would explain the increased bubble size and reduced gas holdup with the unbaffled spargers in Fig.8-3. Most work presented here is for a single sparger.

8-1-2 Ceramic Sparger Series (Tests No.1 to No.7)

Gas holdup vs. superficial gas velocity is plotted in Fig.8-4. It is seen from this figure as Rs increases, the Gas holdup reduces. When Rs>1.42, in this case, the relation between gas holdup and superficial gas velocity deviates from a straight line. Bubble size as a function of superficial gas

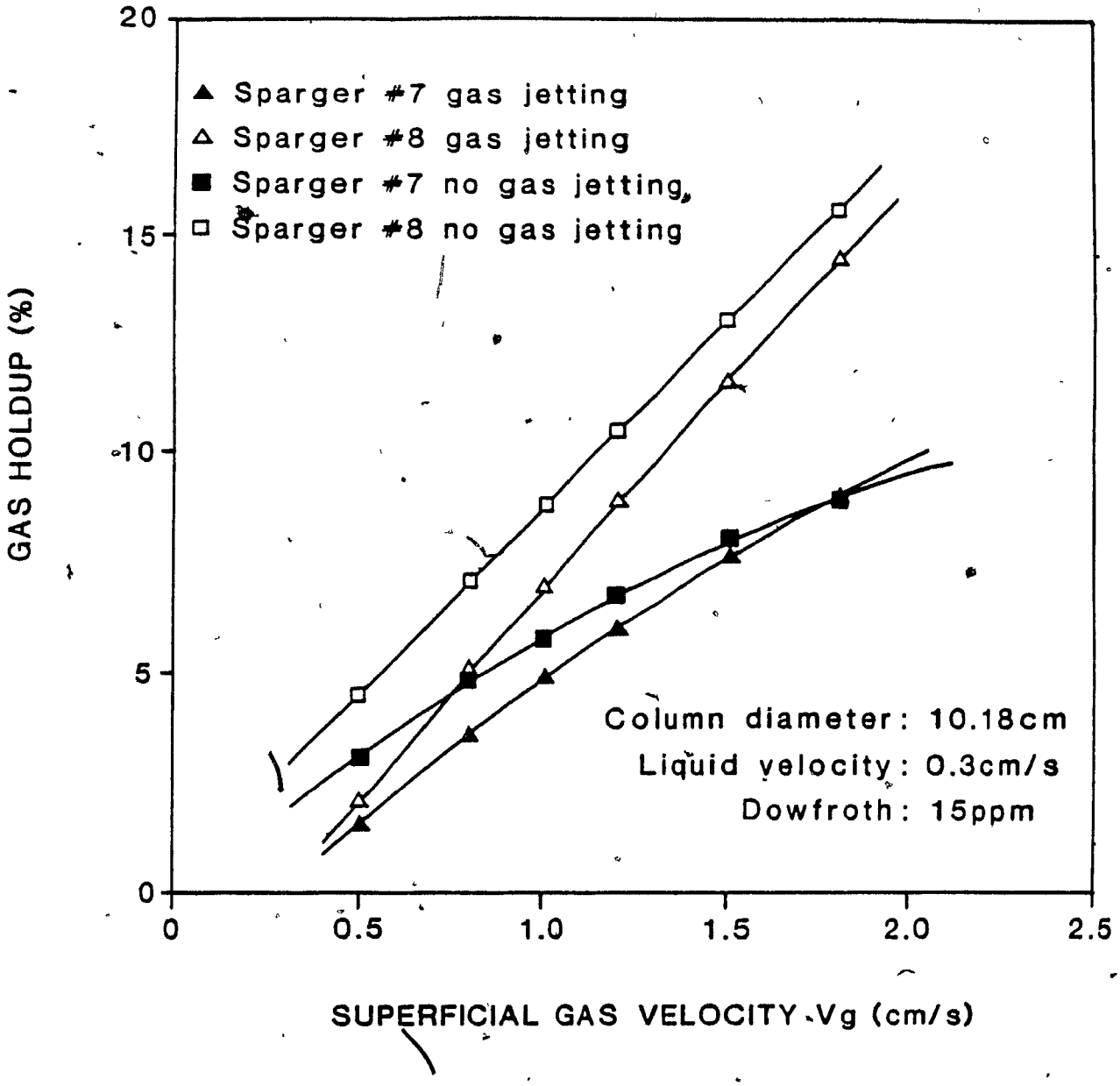

Fig. 8-2 The effect of gas maldistribution on gas holdup.

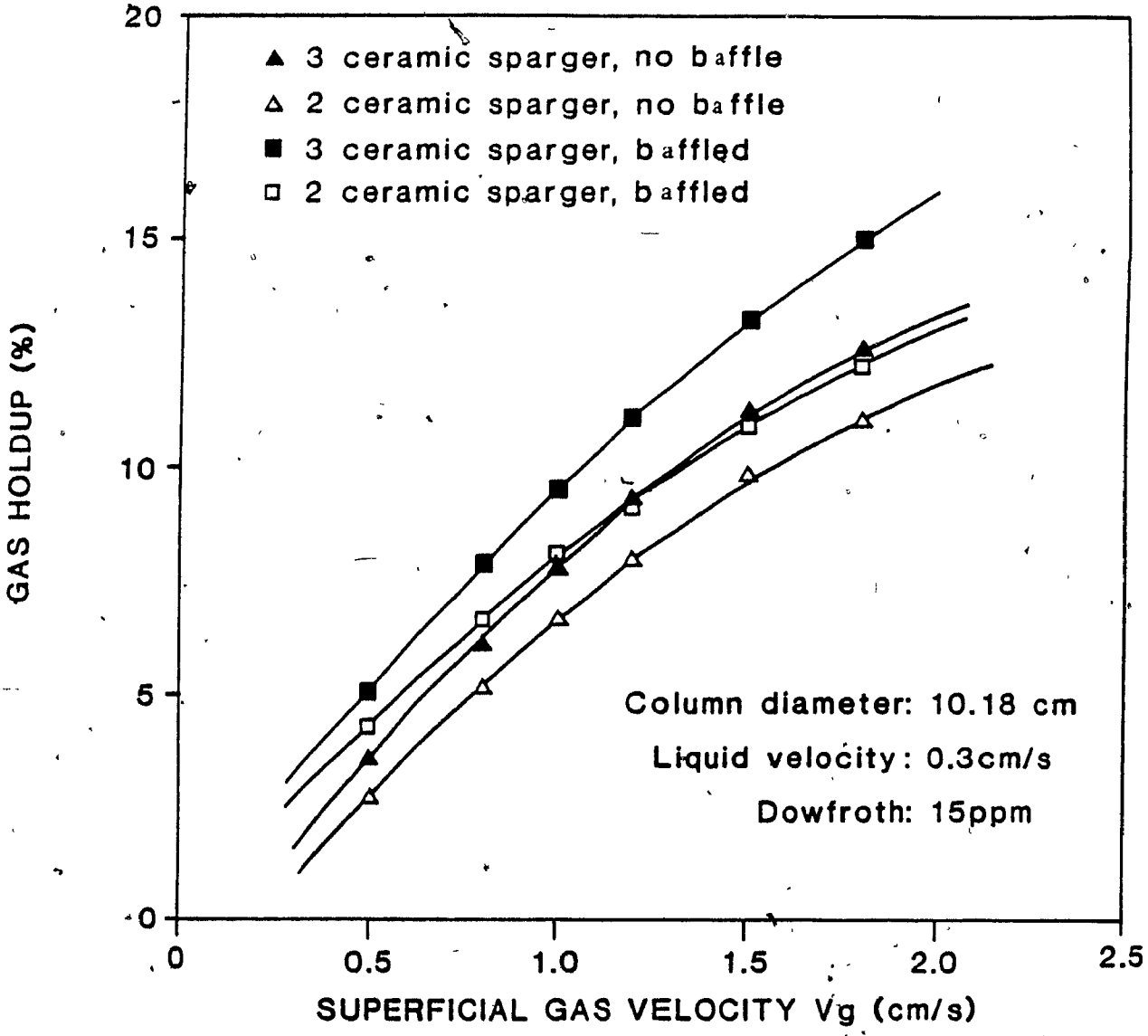

Fig. 8-3 The effect of bubble coalescence on gas holdup.

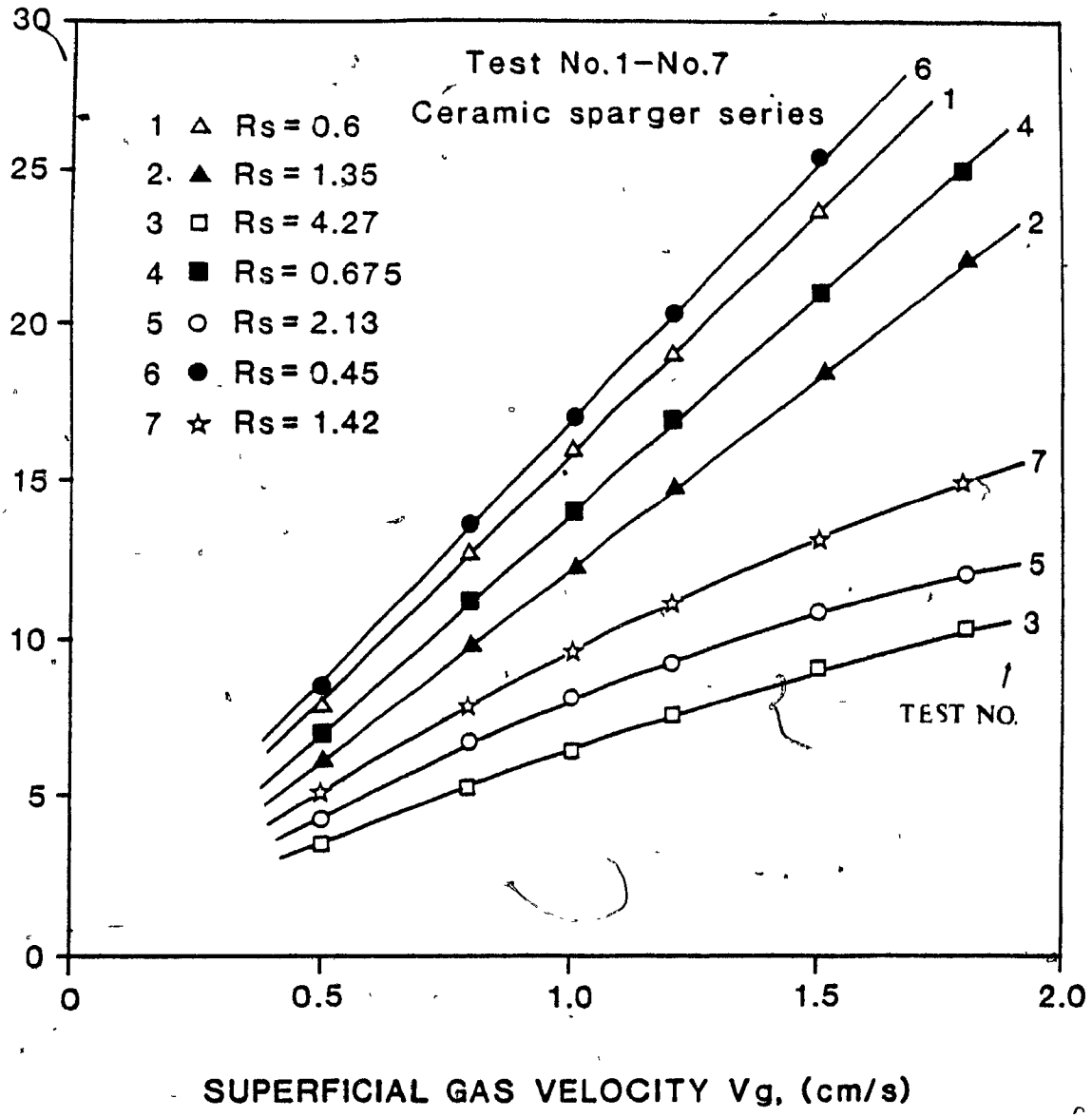

Fig. 8-4 Gas holdup vs superficial gas velocity for ceramic sparger series.

velocity is shown in Fig.8-5 based on the data in Fig.8-4. It is clear that as the sparger surface area decreases (or Rs increases) bubble size increases. If bubble size (excluding those curves, 3,5 and 7 in Fig.8-5) is replotted as a function of [Rs.Vg] as shown in Fig.8-6, all the data represents a new curve which follows Eq.[4-15] with n=0.18. If all bubble sizes are included, n will be 0.32

8-1-3 Steel Sparger Series (Tests No.8-No.13)

Gas holdup as a function of superficial gas velocity for the steel sparger series is plotted in Fig.8-7. In this case, when Rs>1.28, the relation between gas holdup and superficial gas velocity is changed from a straight line to a curve. Bubble size as a function of gas flowrate per unit area of sparger is plotted in Fig.8-8 (excluding those curves, 9, 11 and 13 in Fig.8-7). The regression of the data in Fig.8-9 represents a new curve which follows Eq.[4-15] with n=0.2 . If curves 9, 11 and 13 are included, n will be 0.37.

8-1-4 Cloth Sparger Series (Tests No.14-No.20)

Fig.8-9 presents gas holdup as a function of superficial gas velocity. In this case, little deviation from the straight line between gas holdup and superficial gas velocity occurs when Rs>1. Bubble size as a function of gas flowrate per unit area of sparger is plotted in Fig.8-10. Fig.8-10 does not include the bubble size calculated from curve 15 in Fig.8-9. Constant n in this case is 0.28 when excluding curve 15, and

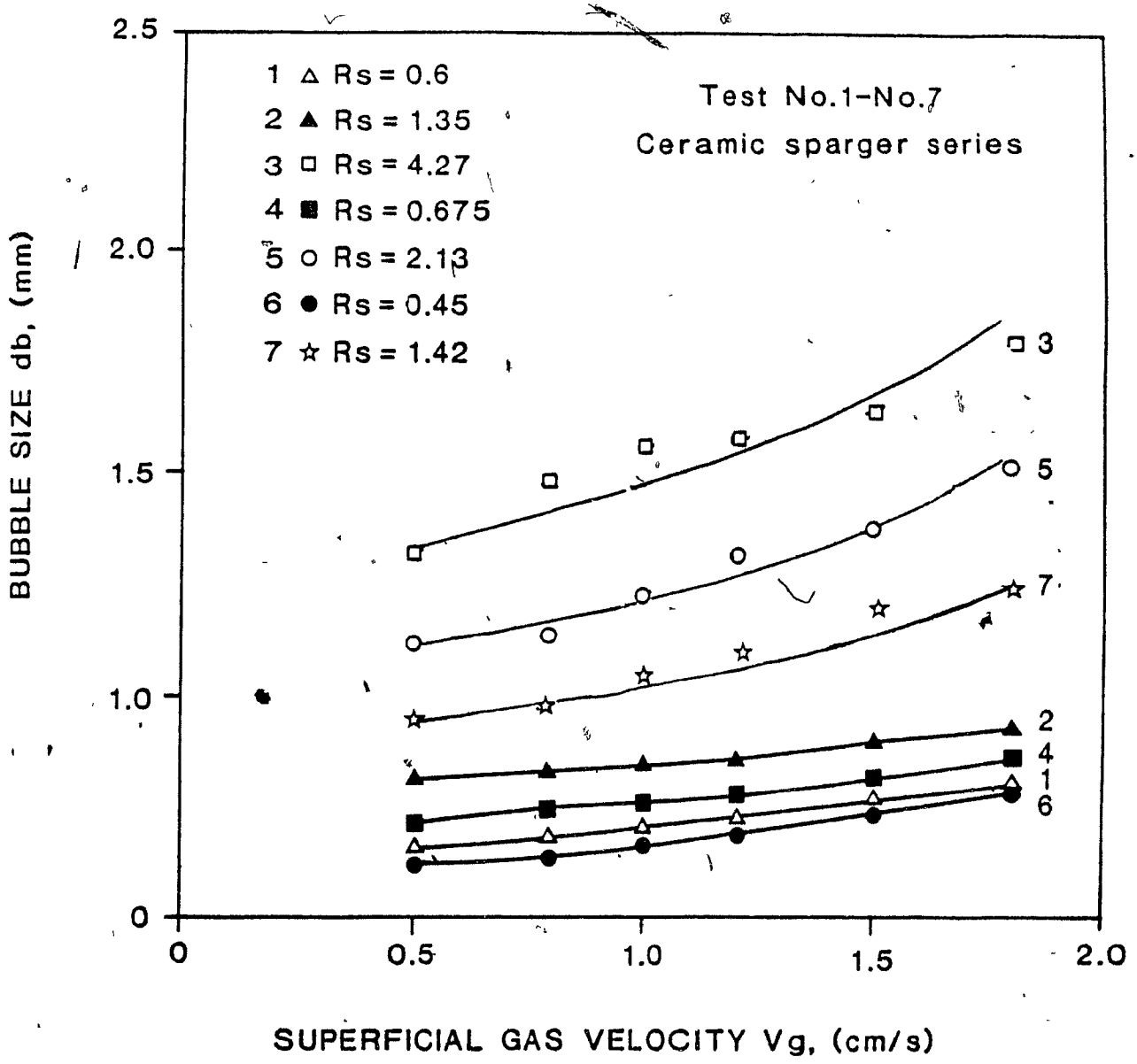

Fig. 8-5 Bubble size vs superficial gas velocity.

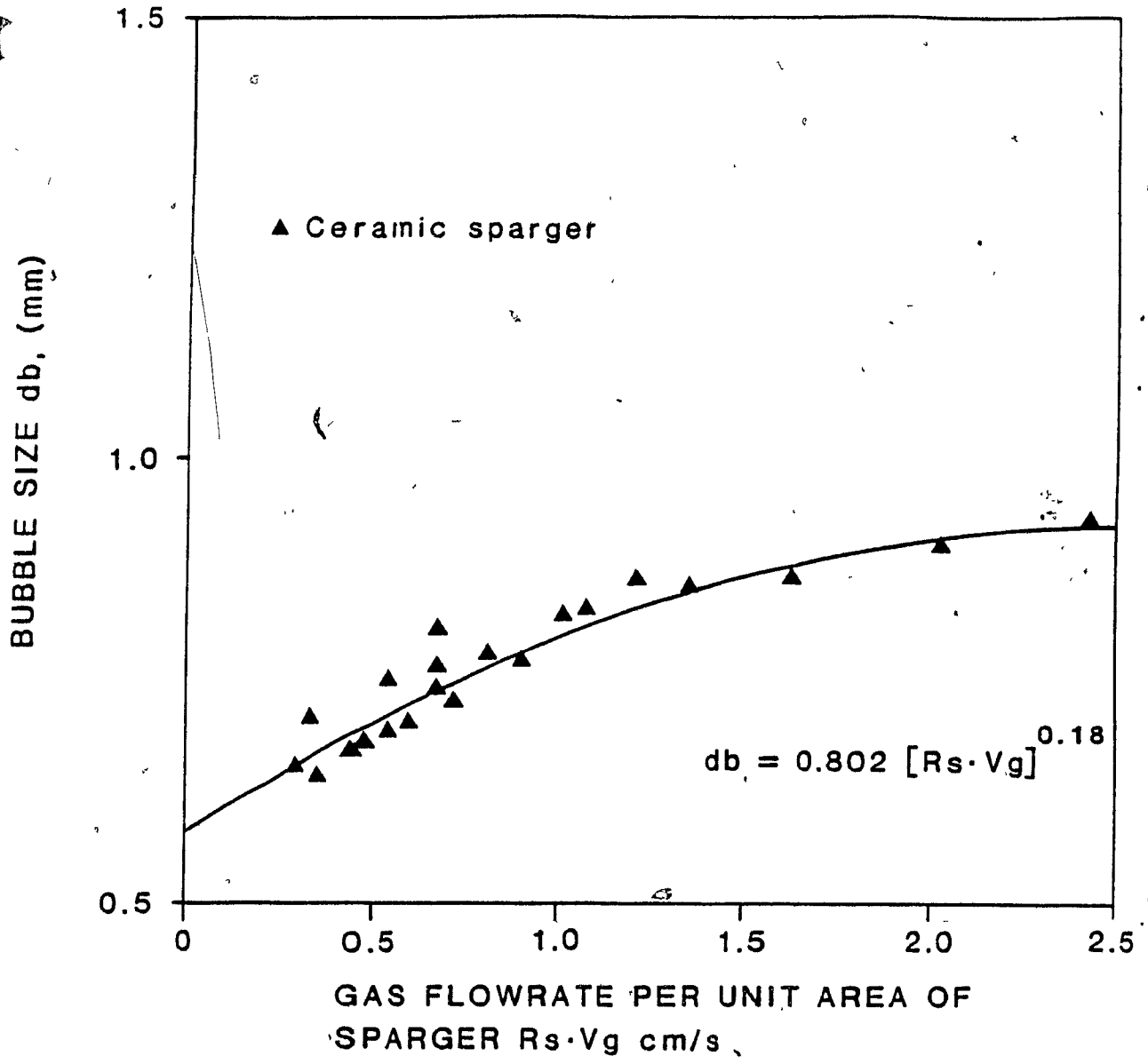

Fig. 8-6 Bubble size vs gas flowrate per unit area of sparger for ceramic sparger.

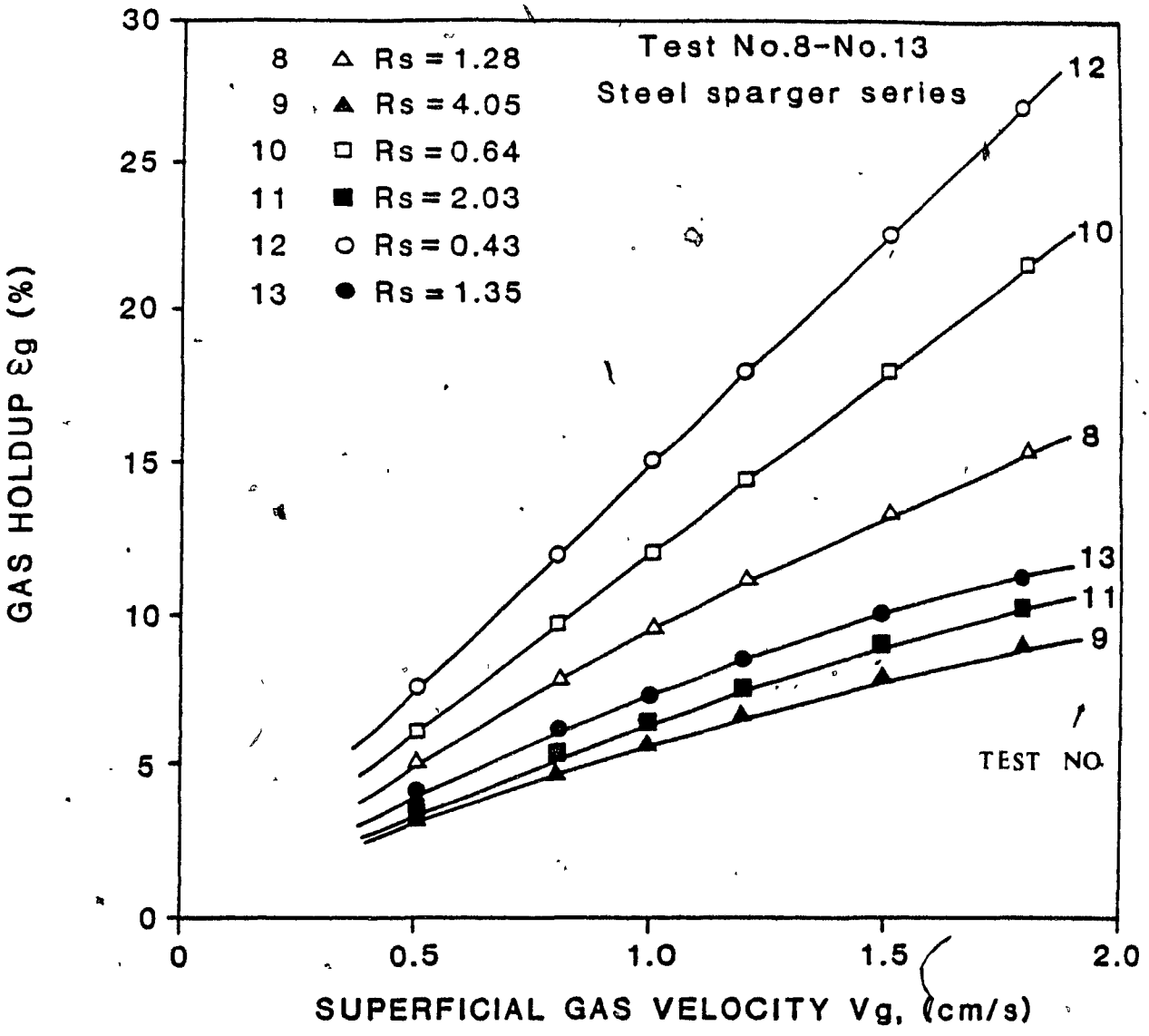

Fig. 8-7 Gas holdup vs superficial gas velocity for steel sparger series

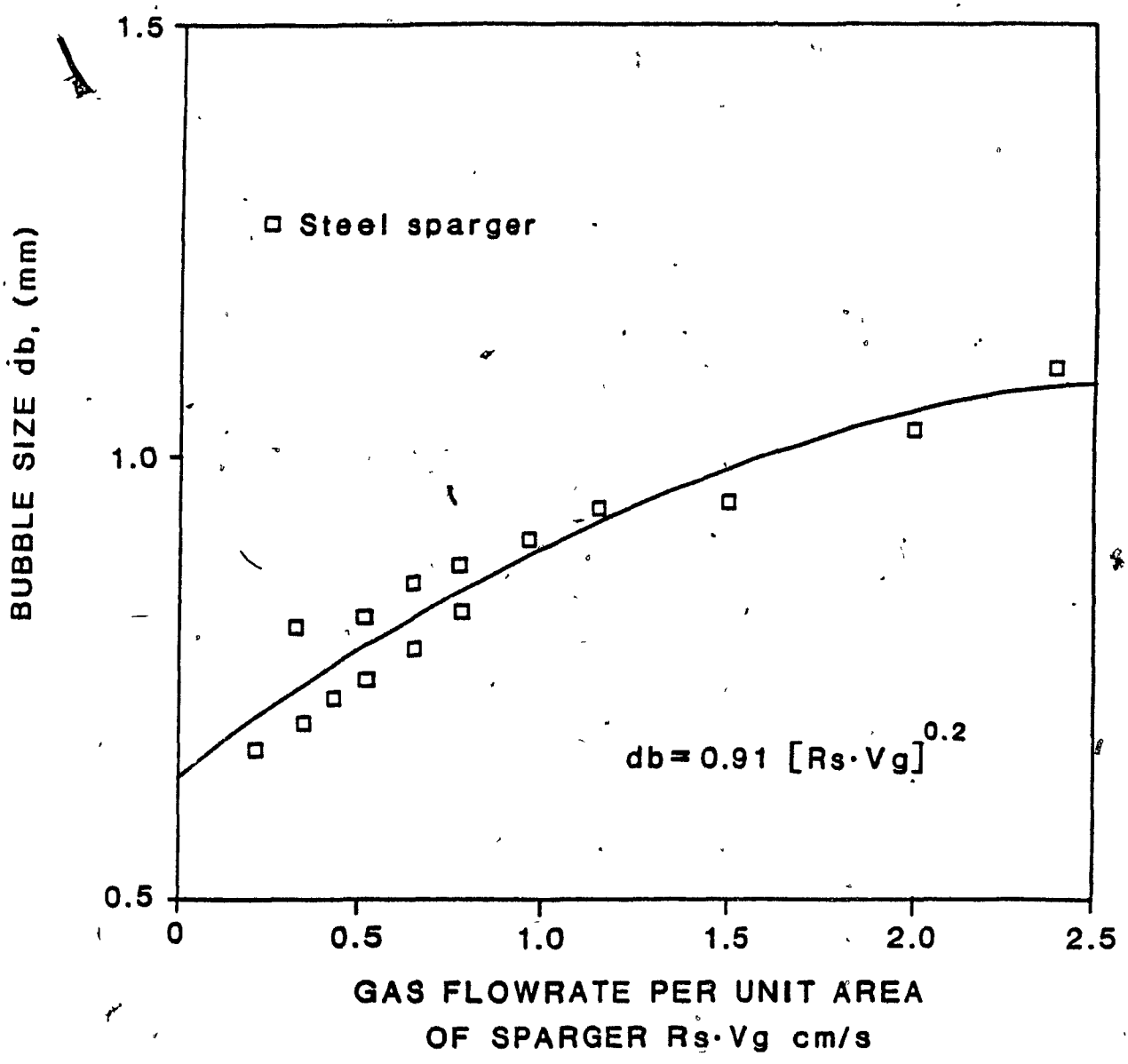

Fig 8-8 Bubble size vs gas flowrate per unit area of sparger for steel sparger series.

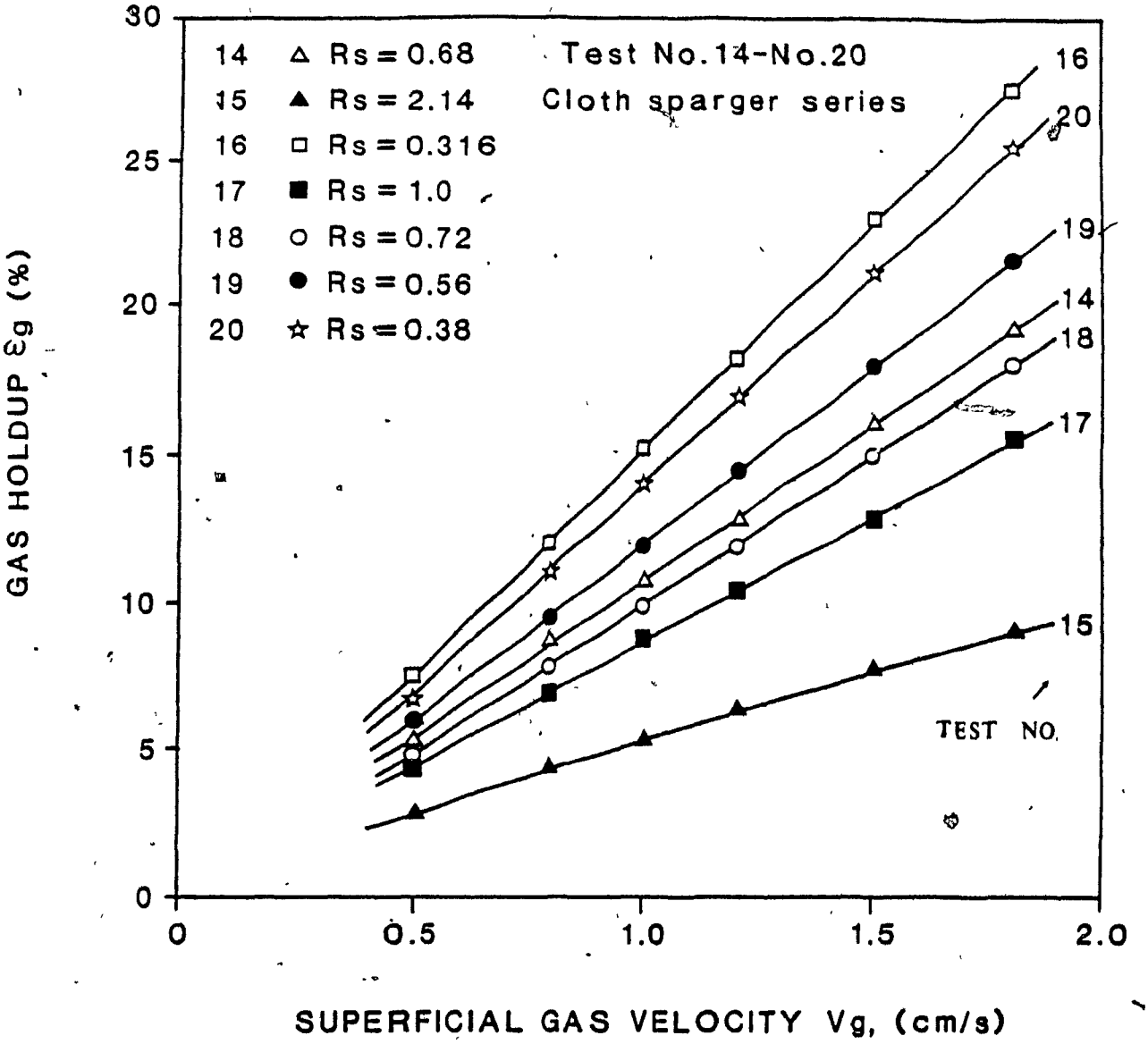

Fig. 8-9 : Gas holdup vs superficial gas velocity for cloth sparger series

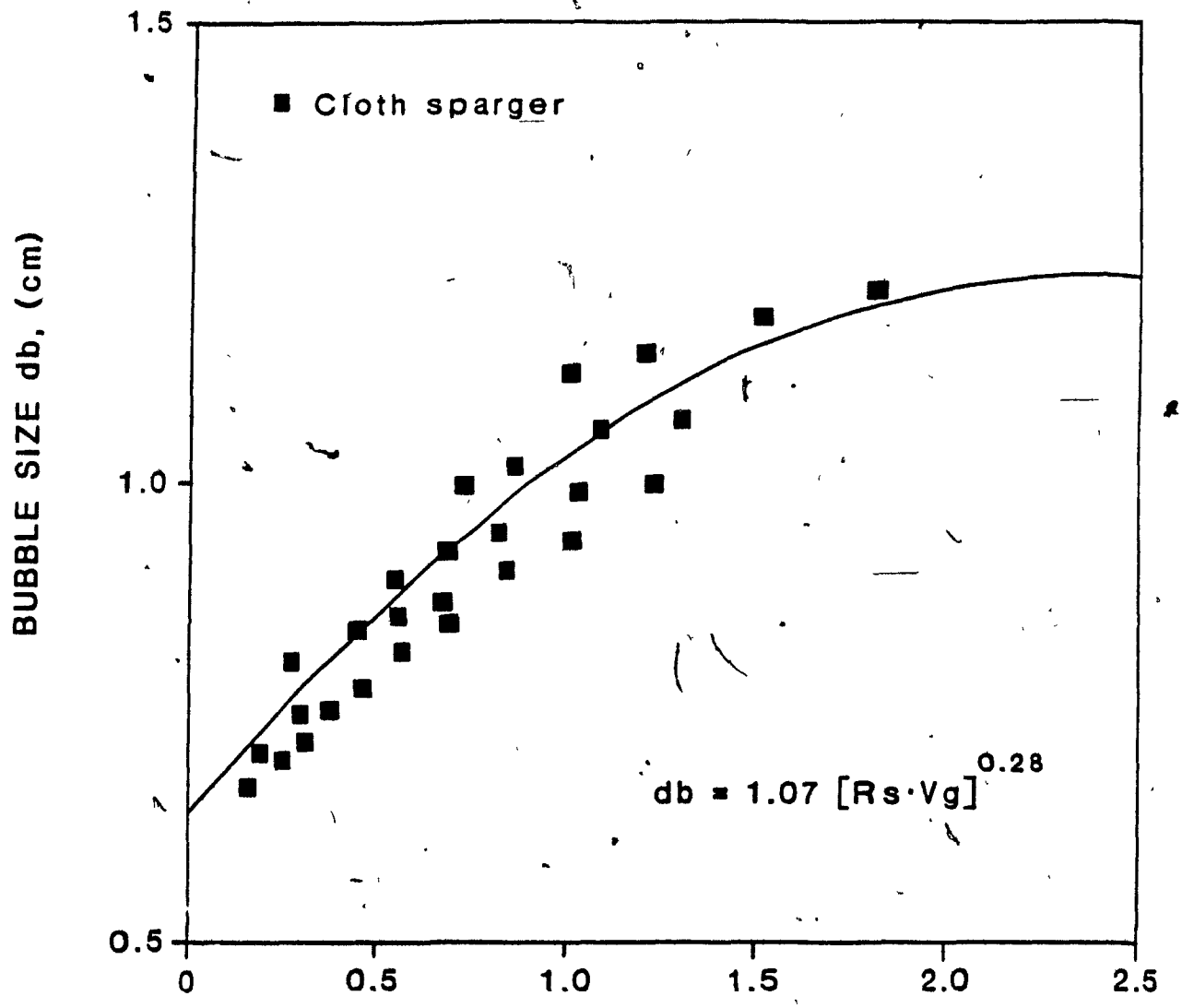

Fig. 8-10 : Bubble size vs gas flowrate per unit area of sparger for cloth sparger.

0.365 when including all the data.

8-2 Pilot Unit Tests

Some plant test work was performed at Brunswick Mining and Smelting, the stream tested mainly contained sphalerite and pyrite. The objective of the flotation is to separate ZnS from FeS2. The reagent conditioning was the same as in the plant operation. To avoid the problem of carrying capacity limitation [25], the feed was diluted to 10% by weight. Fig.8-11 plots mass fraction to concentrate vs. superficial gas velocity for two different sparger sizes. Fig.8-12 plots recovery of zinc and iron vs. superficial gas velocity. Recovery was 5% higher after doubling the sparger size in this case.

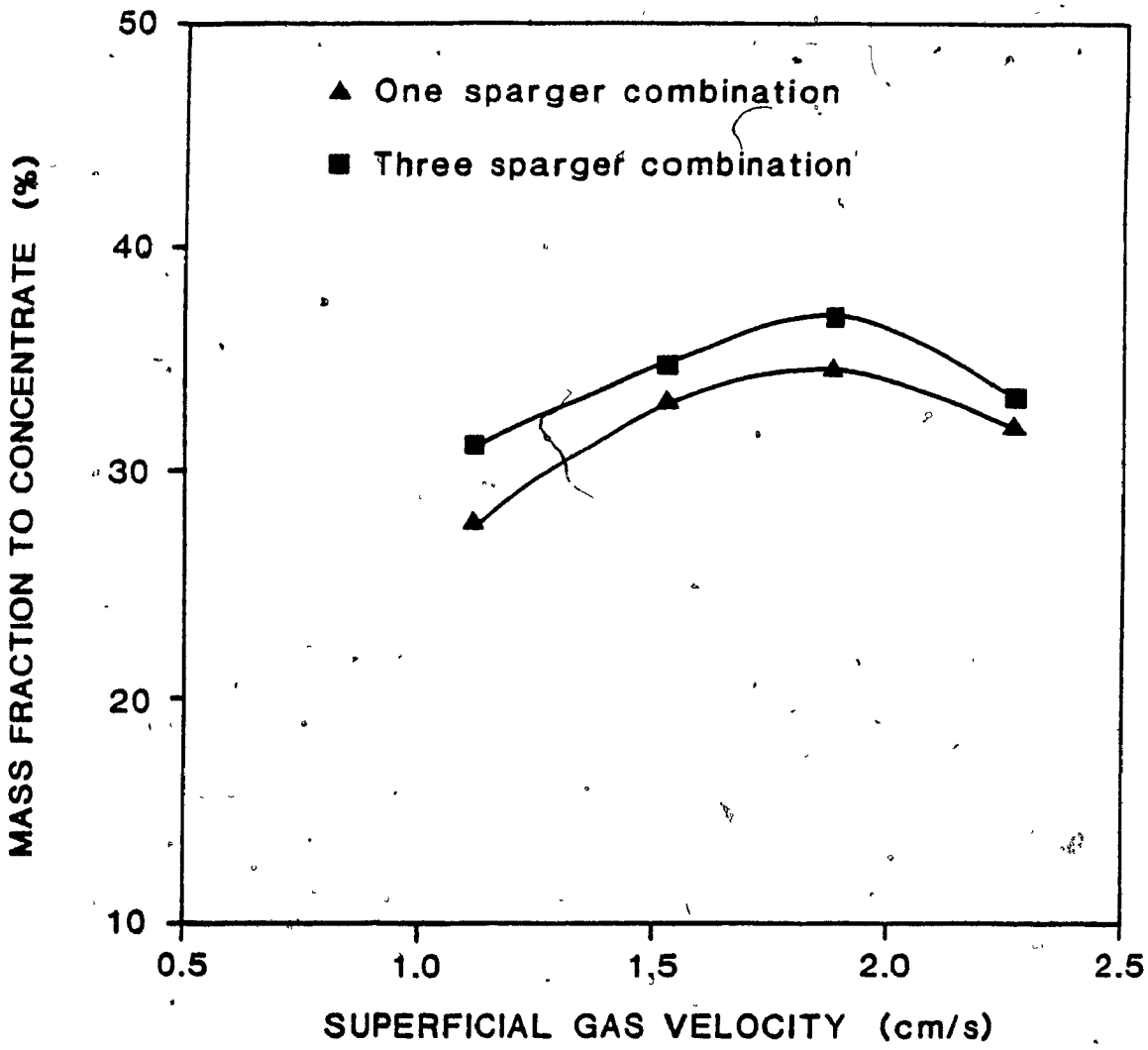

Fig. 8–11 : Mass recovery vs superficial gas velocity.

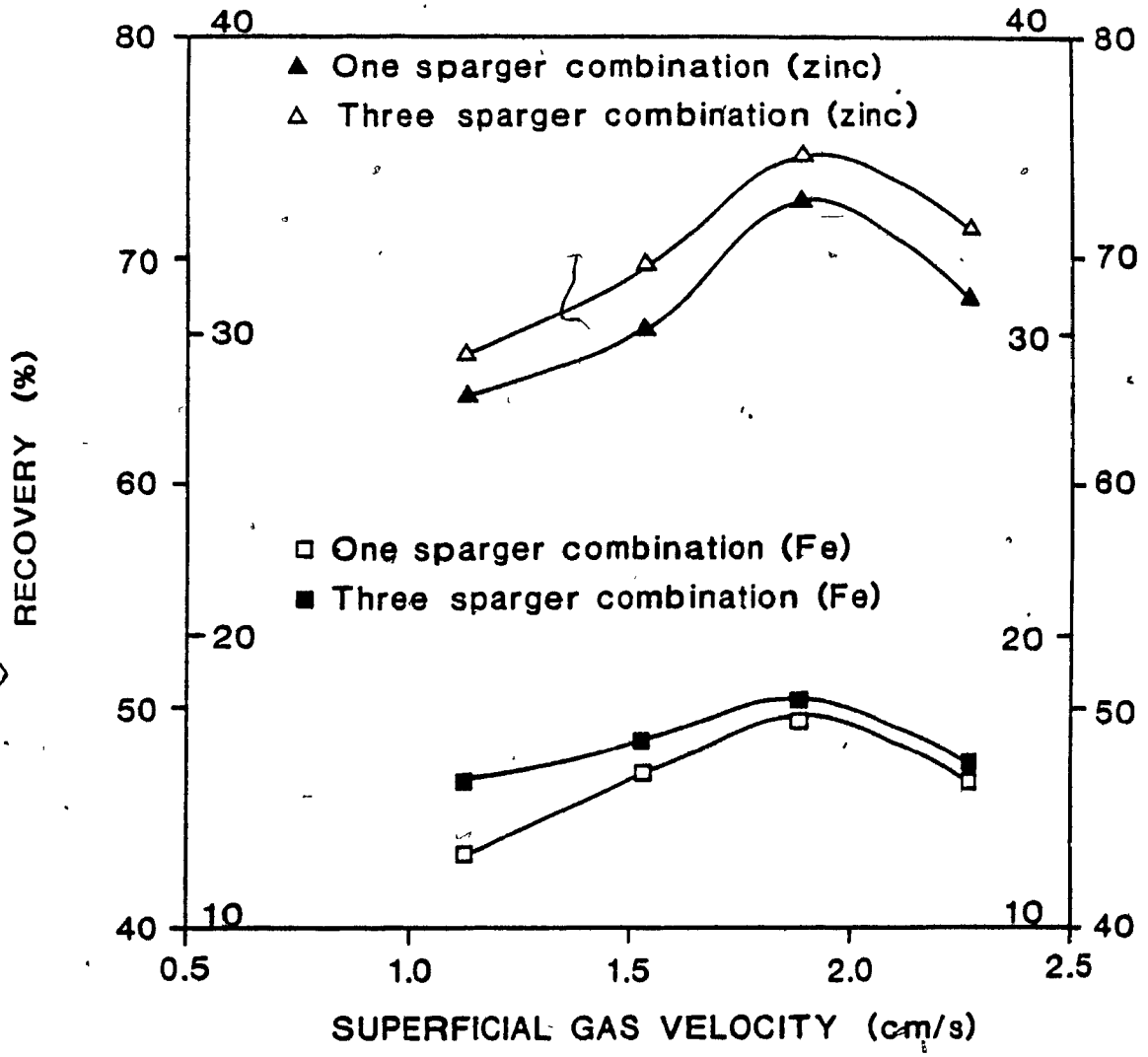

Fig. 8-12 : Concentrate recovery vs superficial gas velocity.

CHAPTER 9

DISCUSSION

9-1 Bubble Size Estimation Technique

The technique of bubble size estimation developed in this work is a direct adaptation of the particle hindered settling equation of Masliyah which gives the method a fundamental basis. Its development has been made possible by repetitive substitutions of db using a numerical approach and gives the direct prediction of bubble size. Fig.6-5 and Fig.6-6 show that the predicted bubble size is within 10 to 15% of the measured size, which is about the limit of experimental error. This accuracy is adequate for most purposes.

In principle, there is no lower bound to applicability of the method (a practical limit with the present photogaphic measurement of db is approximately 0.2 mm). The upper bound is db approximately 2 mm. Above 2 mm bubbles are no longer spherical and rise along more tortuous paths [33]. The possible application of the method in mechanical cells is very encouraging, although the work by Kaya et al [38] shows a more complex situation exists in agitated cells than in flotation columns. Mechanical agitation tends to give a non-uniform axial distribution of gas holdup [37-39], and recirculation of

gas bubbles by the impeller action may cause an increase in gas holdup without affecting bubble size. It is not possible at the time to claim general applicability of the approach to mechanically agitated vessls. Nevertherless, the success shown in Fig.6-6 should encourage further evaluation to the estimation technique in mechanical flotation machines.

9-2 Effects of Operating Variables on Gas Holdup and Bubble Size

The bubble formation process in a flotation column is very complex, and no one single model can fully predict bubble size. The work presented in chapter 7 shows that the major variables which influence gas holdup and bubble size are frother addition, gas flowrate and sparger surface area. The following two factors in order are the most important for bubble size control:

(1) frother addition

(2) gas flowrate per unit area of sparger

The effect of various types of frother on gas holdup and bubble size has not been fully explored. For Dowfroth 250C, gas holdup increases as frother concentration increases to the point where maximum gas holdup is reached.

The effect of gas flowrate on gas holdup is strong and there exists a linear relation between gas holdup and superficial gas rate for relatively low gas flowrate in flotation columns provided Rs<1.5 (or. Rs.Vg<4.5). When gas flowrate is too high, the flow regime is changed from bubbly flow into churn turbulent flow which is not desirable in column flotation.

The effect of sparger size on gas holdup is complex. In general, the increase of Rs (the decrease of sparger size) decreases gas holdup as shown in Fig.8-4, 8-7 and 8-9. The parameter α of Eq.[4-13] is plotted as a function of Rs in Fig.9-1. It is noted from this figure that for the three type of spargers tested, α decreases as Rs increases. That is, α is inversely proportional to Rs. No simple correlation is obtained but the trend is clear.

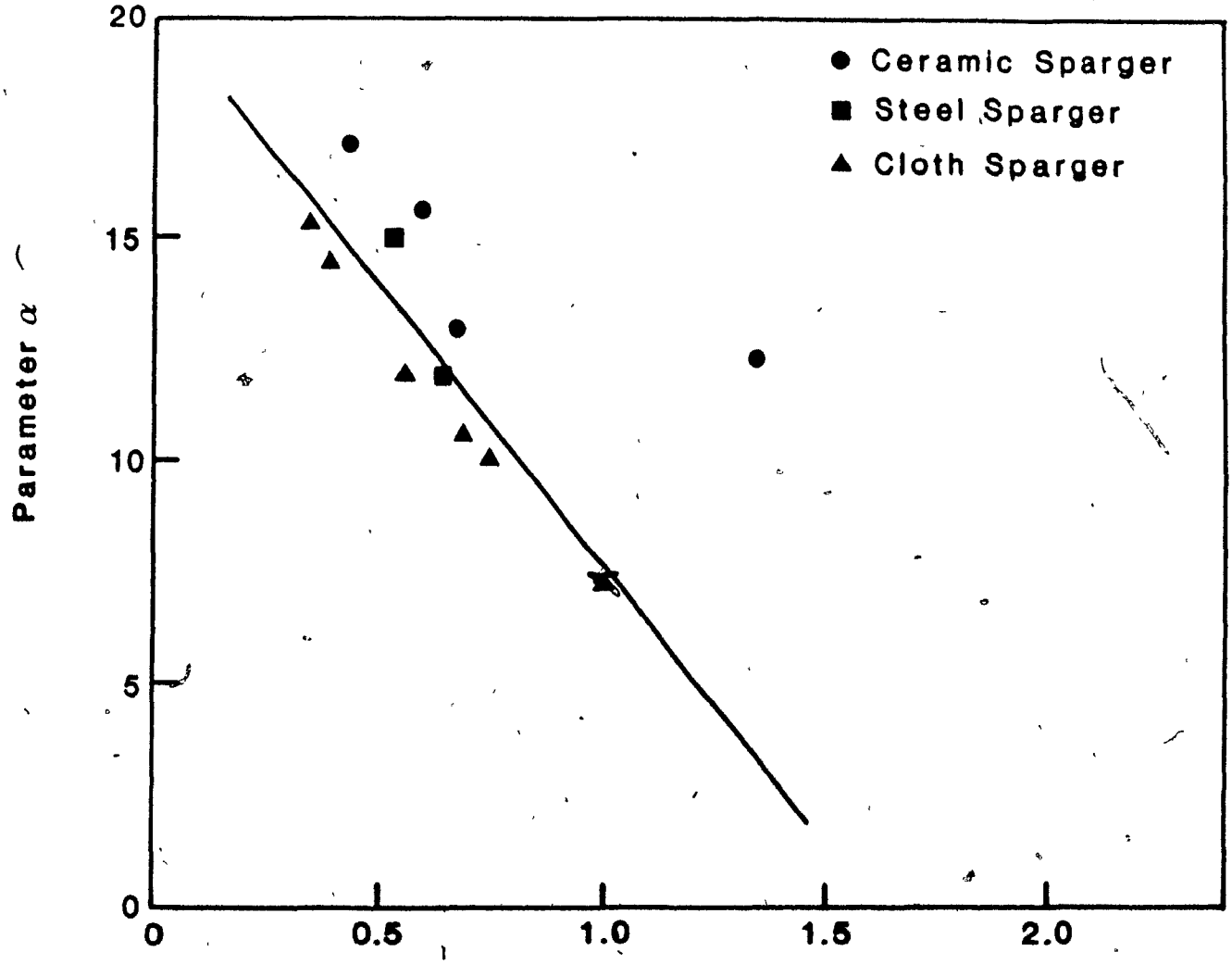

Fig.9-1 The Relationship between Parameter α and Surface Area Ratio Rs

9-3 Sparger Scale-up

The sparger scale-up model presented in chapter 4 is semi-theoretical since it was based on the observed fact that db is proportional to [Rs.Vg] . The importance of the method correctly scaling-up the sparger is illustrated by Eq.[2-9]. For scale-up of flotation columns, it is essential to maintain similar flotation rate constants. To achieve this, it is required to keep constant Vg and db. Vg can be easily controlled by setting a constant gas flowrate. Bubble size is first controlled by frother addition and secondly by ensuring the same gas rate per unit area of sparger. Sparger scale-up is therefore in direct proportion with scale-up of column cross-sectional area.

The data presented in chapter 8 includes two parts. The first was to demonstrate the importance of avoiding gas maldistribution and bubble coalescence since both result in breakdown of bubbly flow. It is seen that from Fig.8-2 and Fig.8-3 once gas maldistribution and bubble coalescence occur, gas holdup decreases and bubble size increases.

Second part was to test the sparger scale-up model. For each series of tests, the effect of sparger size on bubble size can be well described by the model. Fig.9-2 is a plot of log[db] vs. log[Rs.Vg] for the ceramic sparger. The slope of the regression line is the value of n. The other two curves presents the 90% confidence limits of the regression line: n is in the range: $0.05<n<0.3$.

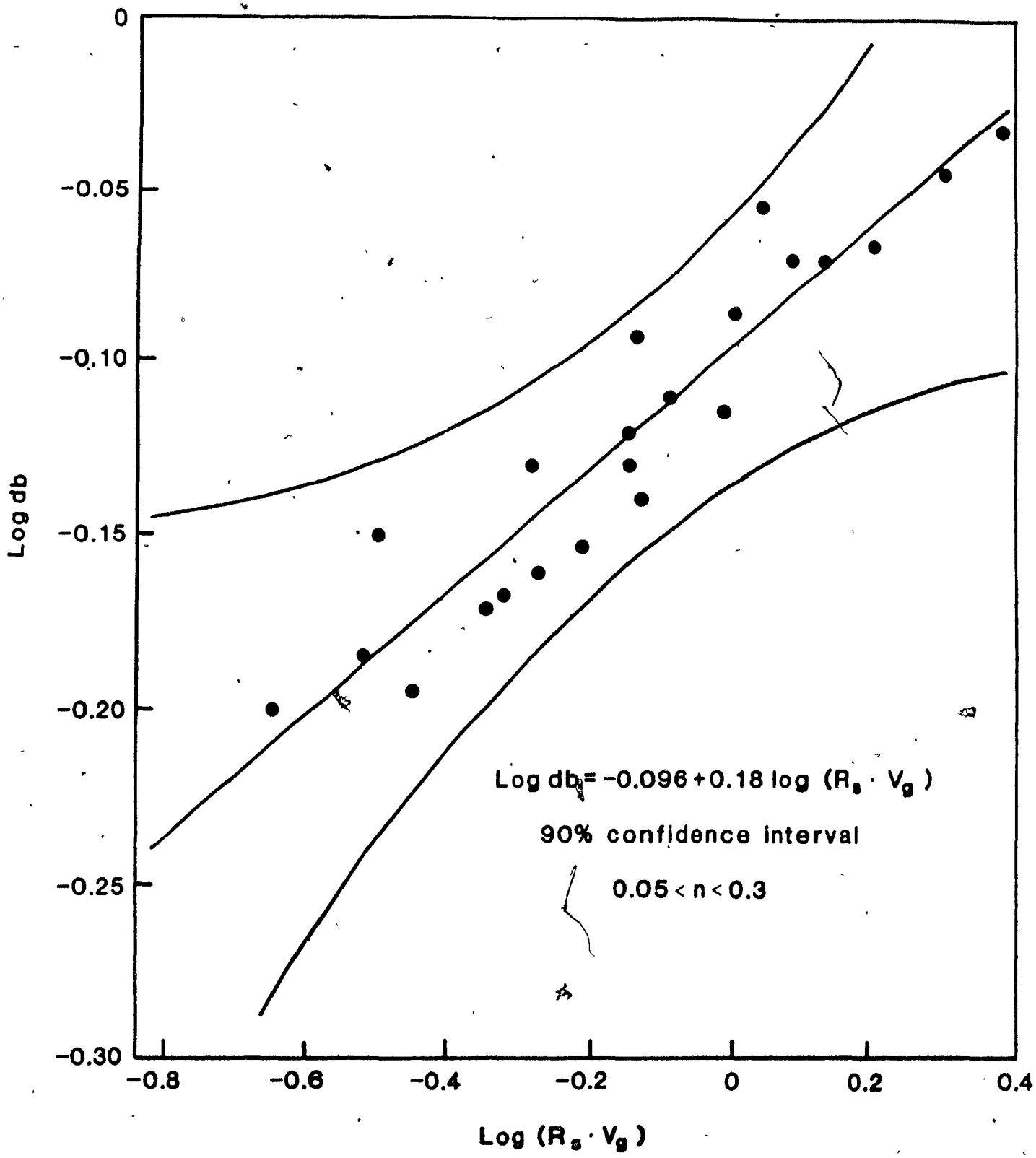

Fig.9—2 Log[db] vs. Log[Rs.Vg], the regression line and 90% confidence interval limits for ceramic sparger

Similar analysis for steel sparger shows n is in the following range: $0.05<n<0.35$ and for filter cloth sparger, $0.05<n<0.4$, as shown in Fig.9-3. Thus, the difference in n value between each type of sparger is not statistically significant.

The results from chapter 7 for the four type of spargers used in the two columns show n=0.25, and the results from chapter 8 suggest an average n=0.24 for the three types of spargers used in the three columns. This suggest the following equation is generally adequate:

$$db = C\ [\ Rs \cdot Vg\ ]^{0.25} \qquad [9\text{-}1]$$

The other possible explanation for the difference in the value of n may be due to the initial bubble size of each sparger. Initial bubble size is the bubble size at the minimum gas flowrate (gas holdup is zero). It is not possible to confirm this experimentally because of the difficulties in measuring this bubble size.

At the end of chapter 8, some plant test results were presented to demonstrate the effect of sparger size on the metallurgical performance of flotation columns. It is expected this effect can be more pronounced in industrial columns.

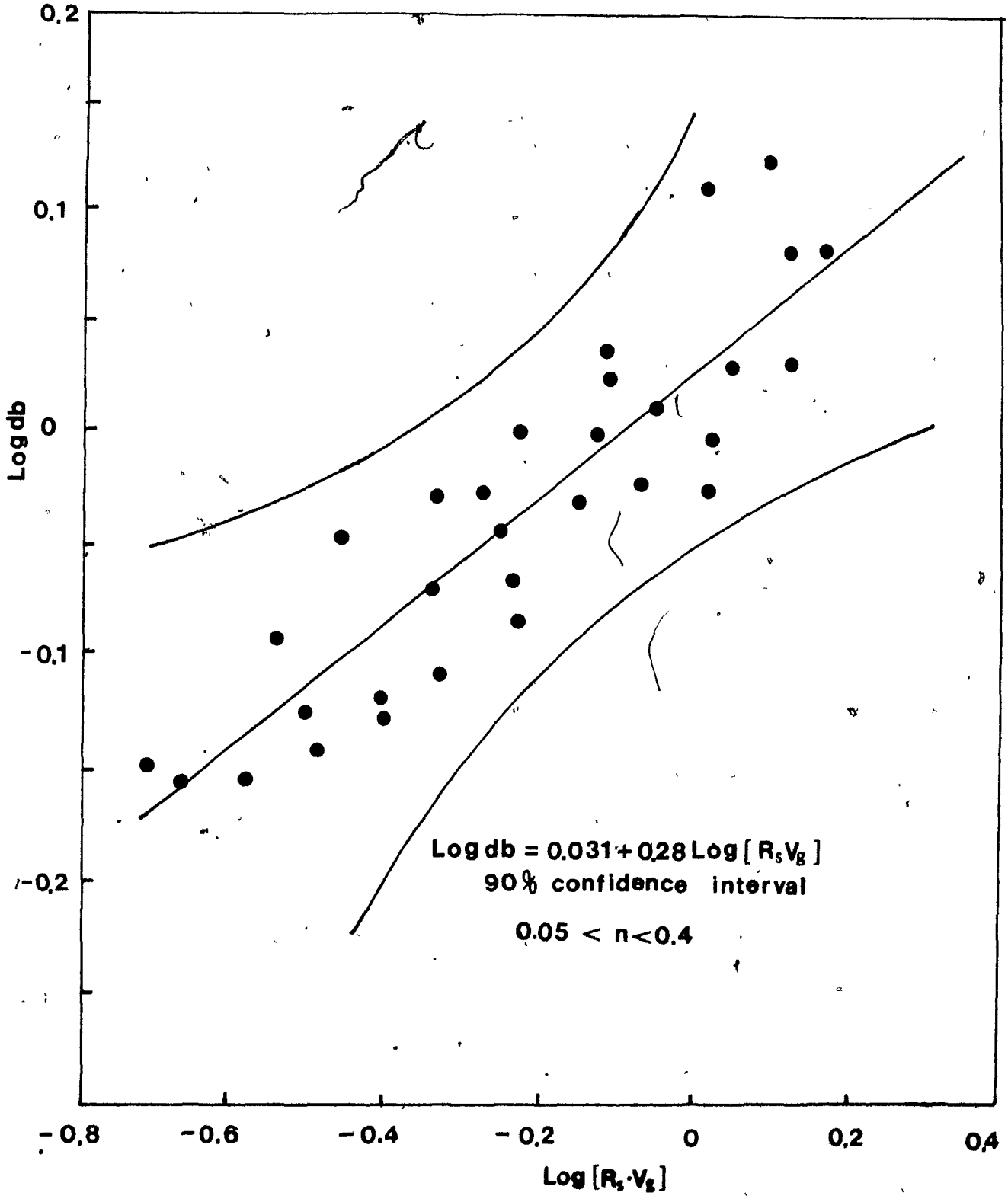

Fig.9—3 Log[db] vs. Log[Rs.Vg], the regression line and 90% confidence interval limits for filter cloth sparger

CHAPTER 10

CONCLUSIONS AND SUGGERSTIONS FOR FUTURE WORK

10-1 Summary of Conclusions

10-1-1 Bubble Size Estimation Technique

Generally speaking, in three-phase flow, i.e. gas-liquid-solid, it is extremely difficult to measure the size of the discontuous phase such as gas bubbles. The technique developed in this thesis provides an excellent means to estimate bubble size in flotation columns. The technique adopts Masliyah's particle hindered settling equation and gives a direct prediction of bubble size. It is easy to use since what is necessary for the computation of bubble size can be simply and precisely measured. The application of this approach has proved to be very accurate in flotation columns (which do not have agitation) and the use in mechanical flotation cells (which have agitation) is also very encouraging.

10-1-2 Effects of Operating Variables on Gas Holdup and Bubble Size

Bubble formation by a sparger is a suprisingly complex process. There are a large number of models developed for this process, but none of them can exactly predict bubble size. The reason is because all of them are based on a sequence of events from photographic observations and depend on some form of force balance including many assumption. There are two major factors affecting gas holdup and bubble size: frother addition and gas flowrate per unit area of sparger.

10-1-3 Sparger Scale-up Model

The sparger scale-up model developed in this work provides an effective tool for the scale-up of spargers and explains the effect of sparger size on bubble size. Based on this model, Rs has to be kept constant to have a similar bubble size for the scale-up of a flotation column, and in general, $0.5<Rs<1$.

10-2 Suggestions for Future Work

10-2-1 Bubble Size Estimation Technique

The bubble size estimation technique has been successfully used in flotation columns. The potential

application in mechanical flotation machines is worth some attention.

10-2-2 Sparger Design and Scale-up

For sparger design and scale-up in an industrial flotation column, the arrangement of individual spargers must be investigated, particularly given the preliminary findings that combining ceramic spargers caused coalescence. It has to be pointed out that the life time of a sparger in practice may become a design criterion and has to be taken into account.

10-2-3 Wash Water Distributor Design

For the effective washing of flotation froth, which ensures the elimination of entrainment of fine hydrophilic particles, it is important to design wash water distributor properly. The temperature profile in the froth bed of a flotation column provides an effective method to explore the design of wash water distributors [51].

10-2-4 Numerical Analysis of Flow Mechanism in a Flotation Column

Numerical analysis provides a powerful tool with which to study the flow mechanism and mass transfer in many processes.

processes such as bubble reactors and heat exchangers is possible. The possibility applying numerical analysis in flotation columns is quite exciting since this approach makes use of the fundamental principles and boundary conditions which govern the process and takes advantage of direct numerical calculation.

REFERENCES

1 Ahmed N., and G.S. Jameson; "The effect of bubble size on the rate of flotation of fine particles", Int. J. Miner. Process., vol.14, pp.195-215, 1985

2 Alfons Mersmann; "Design and scale-up of bubble and spray columns", Ger. Chem. Engng. pp.1-11, 1978

3 Amelunxen R.L., and M.A. Redfren; "The mmechanics of operation of column flotation machines", 17th Annual CMP Meeting, CIM Ottawa, Jan. 1985

4 Anon; "The flotation column", Canadian Mining J. vol.84, pp.55-56, 1963

5 Arun Kumar and Stanley Hartland; "Prediction of drop size produced by a multiorifice distributor", Trans ICheME, vol.60, pp.35-39, 1982

6 Bensley, C.N., T. Roberts and S.K. Nicol; "Column operation for the treatment of fine coal", 3rd Australian Coal Preparation Conference, pp.87-103, 1985

7 Bhaga, D., Master's Thesis, McGill University, Montreal Canada, 1970

8 Bogdanov, O.S., M.F. Emelyanov, I.I. Maximov and L.A. Otrozhdennov; "Influence of Some Factors on Fine Particle Flotation", In 'FINE PARTICLE PROCESSING', P.Somasundaran (ed.), AIME, New York, vol.1, pp.706-719, 1980

9 Boutin P. and D.A. Wheeler; "Column Flotation Development Using a 18-inch pilot unit", Canadian Mining J. vol.88, pp.94-101, 1967

10 Boutin P. and R. Tremblay, Canadian Patents No. 680576 and 680654

11 Bhavaju, S.M., T.W.F. Russel and H.W. Blanch; "The design of gas sparged device for viscous liquid systems", AIChE J. vol.24, pp.254, 1978

12 Cienski T. and V.L. Coffin; "Column operation at Mines Gaspe molybdenum circuit", 13th CMP Meeting, CIM, paper No.18, Ottawa, Jan. 1981

13 Clift, R., Grace J.R. and Weber M.E. "Bubbles, Drops and Particles", chpt.12, pp.321-347, ACADEMIC PRESS,New York, 1978

14 Clingan, B.V. and D.R. McGiregor; "Column flotation Experience at Magma Copper Company with related experience of other mineral processors", presented at the SME Annual Meeting, Denver, Feb, 1987

15 Coffin V.L. and J. Miszczak; "Colum flotation a Mines Gaspe" 14th IMPC, paper IV.21, Toronto, 1982

16 Concha, F, and E.R. Almendra; "Settling velocity of particulate system: I. settling velocity of individual spherical particles", Int. J. Mineral Process. vol.5, pp.435-365, 1979

17 Dobby G.S. ; "A Fundamental Flotation Model and Flotation Column Scale-up" Ph.D Thesis, McGill University, Montreal, Canada, August, 1984

18 Dobby, G.S., R. Amelunxen and J.A. Finch; "Column flotation - some experience and model developemnt", IFAC Symposium on Automation for Mineral Resource Development, Brisbane, Australia, pp.259-263, 1985

19 Dobby G.S. and J.A. Finch; "Mixing Characteristics of Industrial flotation columns", Chem. Engng. Sci. vol.40 No.7, pp.1061-1068, 1985

20 Dobby G.S. and J.A. Finch; "Flotation column Scale-up and Modelling", CIM bulletin, vol.79, No.889, pp.89-96, 1986

21 Dobby G.S. and J.A. Finch; "Particle size dependence derived from fundamental model of capture process", Int. J. of Mineral Process. in press, 1986

22 Dobby G.S. and J.A. Finch; "Particle collection in columns -- gas rate and bubble size effects" Canadian Metall. Quarterly, vol.25, pp.9-13, 1986

23 Dobby G.S. and J.A. Finch; " A model of particle sliding time for flotation sized bubbles". J. of collide and interface Sci. vol.109, No.2, pp.493-498, 1986

24 Dobby G.S., J.B. Yianatos and J.A. Finch; Submitted to Can. J. of Chem. Engng., 1986

25 Espinosa-Gomez R., J.B. Yianatos and J.A. Finch, "Carrying capacity limitations in flotation columns"; to be presented at first international symp. on column flotation, AIME, Phoenix, Arizona, Jan.26-29, 1988

26 Espinosa-Gomez, R.; "Recovery of pyrochlore from slimes discarded at Niobec by column flotation", Ph.D Thesis,

McGill University, Montreal, June, 1987

27 Flint L.R. and W.J. Howarth, "Discussion on theoretical analysis of a countercurrent flotation column"; Trans. SME/AIME, vol.250, pp.32-38, 1971

28 Flint I.M., P. MacPhail and G.S. Dobby; "Aerosol frother addition in column flotation", 25th Annual Conference of Metallurgist, CIM, Toronto, paper No.28, Aug. 1986

29 Field, R.W., and Dvidson, J.F.; "Axial dispersion in columns", Trans. ICheME, vol.58, 1980

30 Foot D.G., J.D. Mckay and J.L. Huiatt; "Column flotation of chromite and fluorite ores", Canadian Met. Quarterly, vol.25, No.1, pp.15-21, 1986

31 Fuerstenau, D.W., "Fine particle flotation", vol.1, chpt.35, Ed. P. Somasundaran, New York, 1980

32 Guy, C., P.J. Carreau and J. Paris; "Mixing characteristics and gas holdup of a bubble column", Canadian J. of Chem. Engng., vol.64, Feb. 1986

33 Harris C.C., N. Arbiter and M.J. Musa; "Mixing and gangue dispersion in flotation machine pulps", Inter J. of Mineral Process. No.10, pp.45-60, 1983

34 Harper, J.F.; Adv. Appl. Mech., vol.12 No.59, 1972

35 Jameson G.J.; "Physics and hydrodynamics of Bubbles", In " THE SCIENTIFIC BASIS OF FLOTATION", K.J. Ives (ed) pp.53-77, 1984

36 Jameson G.J., S. Nam and M. Moo Young; "Physical factors affecting recovery rates in flotation", Minerals Sci. engng. Vol.9, No.3, July, 1977

37 Kaya, M. and A.R. Laplante; "Factors influencing design, hydrodynamics, mixing, residence time distribution, scale-up and sizing of flotation machines", presentation at Mineral Processing System Seminar , McGill University, April, 1986

38 Kaya, M.; Master's Thesis, McGill University, Aug. 1985

39 Kaya, M. and A.R. Laplante; "Estimation of gas holdup and bubble size in a laboratory cell", to be presented at 26th Annual Conference of Metallurgists, CIM, Winnipeg, Aug. 1987

40 Kelkar, B.C. et al; "Effect of addition of alcohols on

gas holdup and backmixing in bubble coulmns", AIChE J. vol.29, No.3 pp.361-369

41 King R.P.; In "PRINCIPLE OF FLOTATION", South Africa Inst. of Min. and Met. King R.P. (ed.), pp.215-225, 1983

42 Laplante A.R., J.M. Toguri and H.W. Smith; "The effect of air flowrate on the kinetics of flotation", Int. J. of Miner. Process. 11:203-234, 1983

43 Leja J.; "Surface chemistry of Froth flotation", Plenum Press, New York, chpt.9, 1982

44 Levenspiel, O., "Chemical reaction engineering", Wiley, 2th edition, pp.286-287, 1972

45 Lynch A.J., N.W. Johnson, E.V. Manlapig and C.G. Throne; "Mineral and coal flotation circuits: their simulation and control" , Elsevier Scientific Publishing Company, New York, 1981

46 Lynch, A.J., N.W. Johnson, D.J. McKee and G.C. Throne; "The behaviour of minerals in chalcopyrite flotation processes with reference to simulation and control", J. of South Africa Min. and MEt., pp.349-356, 1974

47 Luttrel, G.H., G.T. Adel and R.H. Yoon; "A population balance model of column flotation developed from first principles', 25th Annual Conference of Metallurgists, CIM, Toronto, paper 28, Aug. 1986

48 Mathieu, G.I,; "Comparison of flotation column with conventional flotation machines for concentration of a molybdenum ore", CIM Bull. pp.41-45, May, 1972

49 Mauro, F.L. and M.R. Grundi; "The application of flotation columns at Lornex Mining Coorporation Ltd.", 9th District Six Meeting, CIM, paper No.2, Kamloops, British Columbia, Oct. 1984

50 Moon, K.S. and L.L. Sirois; "Column flotation", 15th Annual CMP Meeting, CIM, paper No.18, Ottawa, Jan. 1983

51 Moys, M.H. and J.A. Finch; "Developments in the control of flotation columns", Int. J. Min. Processing, in press 1987

52 Masliyah, J.H.; "Hindered settling in a multi-species system", Chem. Engng. Sci., vol.34, pp.1166-1168, 1987

53 Mckay, J.D., D.G. Foot and M.B. Shirts; "Parameters affecting column flotation of fluorite", presentation

at the SME Annual Meeting, Denver, Colorado, Feb. 1987

54 Narasimhan, K.S., S.B. Rao and G.S. Chowdhurry; "Column flotation improves graphite recovery", E&MJ vol.173, No.4, pp.84-85,1972

55 Perry, R.H. and D.W. Green; "Perry's Chemical Engieering Handbook", 6th edition, McGraw-Hill, section 5, pp.65, 1984

56 Richardson, J.F. and N.W. Zaki; "Sedimentation and fluidisation: part I", Trans. Tnst. Chem. Engrs., vol.32, pp.32-35, 1954

57 Rice R.G., A.D. Oliver, J.P. Newman and R.J. Wille; "Reducing dispersion using baffles in column flotation", Powder Tech. vol.10, pp.201-210, 1974

58 Rice, R.G., M.I. Tupperainen and R.M. Hedge; "Dispersion and holdup in bubble columns, comparison of rigid and flexible spargers", Canadian J. of Chem. Engng. vol.59, Dec. 1981

59 Rice, R.G. and S.W. Howell; "Elastic and flow mechanics for membrance spargers", AIChE J. vol.32, No.8, Aug. 1986

60 Sastry, K.V.S. and D.W. Fuerstenau; "Theoretical analysis of a countercurrent flotation column", Trans. SME/AIME, vol.247, pp.46-52, 1970

61 Shah, Y.T. et al; "Design parameters estimations for bubble column reactors", AIChE J. vol.28 No.3, pp.353-363, 1982

62 Shah, Y.T., G.J. Stiegel and M.M. Sharma; SIChE J. vol.24(3), pp.369, 1978

63 Szatkowski M. and W.L. Freyberger; "Kinetics of flotation with fine bubbles", Trans. Instn. Min. Met. (sect. c) vol.94, June, 1985

64 Szatkowski M. and W.L. Freyberger; "Model describing mechanism of the flotation process", Trans. Instn. Min. Met. (sect. c) vol.94, Sept. 1985

65 Szatkowski M.; "Effects of ais usage on flotation of coal", Mineral and MEtallurgical Processing, vol.4, No.1 pp.37-39, 1987

66 Trahar W.J., "A rational interpretation of the role of particles size in flotation", Int. J. fo Min. Proc. No.8, pp.289-327, 1981

67 Unno, H. and I. Inove; "Size reduction of bubbles by orifice mixer", Chem. Engng. Sci. vol.35, pp.1571-1579 1978

68 Udo Oels, Joachim Lucke, Rainer Buchholz and Karl Schugerl; "Influence of gas distributor type and composition of liquid on the behaviour of a bubble column biaoreactor", Ger. Chem. Engng. pp.1135-129, 1978

69 van Kevelen, D.W. and P.J. Hoftijzer; "Studies of gas-bubble formation", Chem. Engng. Processing, vol.46, No.1, pp.29, 1976

70 Wheeler D.A.; "Column flotation", presented at the professional development seminar, McGill University, March, 1983

71 Wheeler, D.A.; Engng. and Mining J., vol.167, pp.98-193, 1966

72 Wheeler, D.A. ; "Column Flotation - the original column", 87th Annual General Meeting, CIM, Vancouver, Aug. 1985

73 Warren, L. "Determination of the contributions of the true flotation and entainment in batch flotation tests", Int. J. of Min. Proc., 14. pp.33-44, 1985

74 Wallis, G.B., "One Dimensional Two-phase flow", McGraw-Hill, N. Y., Chpt.9, 1969

75 Wheeler, D.A. ; Short course on flotation column at McGill University, April, 1986

76 Xu Changlian; "Kinetic models for batch and continuous flotation column", XVI IMPC. Cannes, Tome III,pp.16-26, 1985

77 Xu M.Q. and J.A. Finch; "Carrying Capacity: gas rate and bubble size effects", paper submitted to Int. J. of Min. Procc., 1987

78 Xu M.Q.; "Process control in column flotation", project proposal, McGill University, Dec. 1985

79 Yu Shaning; "Particle collection in a flotation column", Master's Thesis, Montreal, April, 1987

80 Yianatos, J.B. "Column flotation froths", Ph.D Thesis Montreal, March, 1987

81 Yianatos J.B., A.R. Laplante and J.A. Finch; "Estimation of local holdup in the bubbling and froth zones of a gas-liquid column", Chem. Engng. Sci. vol.40, No.10, pp.1965-1968, 1985

82 Yianatos J.B., J.A. Finch and A.R. Laplante; " Cleaning action in cloumn flotation froths", Trans. I.M.M., in press, 1987

83 Yianatos J.B., J.A. Finch and A.R. Laplante; "Holdup profiles and bubble size distribution of column flotation frroths", Canadian MEt. Quarterly, vol..25, No.1, pp.23-29, 1986

84 Yianatos J.B., J.A. Finch and A.R. Laplante: "Apparent hindered settling in a gas-liquid-solid countercurrent column", Int. J. of Min. Procc. vol.18 No.3/4, pp.155-165, 1986

85 Yianatos J.B., J.A. Finch and A.R. Laplante; "Selectivity in column flotation froths", submitted to Int. J. of Min. Proc. Jan. 1987

86 Yianatos, J.B., R.G. Espinosa and J.A. Finch; "Column flotation manual", short course on flotation column at McGill University, May, 1986

87 Yianatos, J.B., R.G. Espinosa, J.A. Finch, G.S. Dobby and A.R. Laplante; "Effect of column height on flotation column performance", 116th Annual AIME-SME Annual Meeting. Denver, Feb. 1987

88 Yianatos, J.B., J.A. Finch, G.S. Dobby and M.Q. Xu; "Bubble size estimation in a bubble swarm", J. of Coll. and Interf. Sci., paper in review, 1987

APPENDIX A

Complementary information for Fig.2-12 and Fig.2-13

In order to analyse bias and ratio control loops and find out which one is better, it is assumed that a column, the dimension of which is 0.9X0.9X10 m^3, will be tested.

bias = 0.2 m^3/min at Gaspe

ratio = 1.2 at Gibraltar

Qc = 2 m^3/min

Table A-1 shows the calculation of retention time

Table A-1

mine	at Gaspe		at Gibraltar	
Qf m^3/min	τ min	Qw m^3/min	τ min	Qw m^3/min
1.0	6.75	2.2	6.75	2.2
1.1	6.23	2.2	6.14	2.22
1.2	5.79	2.2	5.63	2.24
1.3	5.40	2.2	5.19	2.26
1.4	5.06	2.2	4.82	2.28
1.5	4.76	2.2	4.50	2.30

APPENDIX B

Some experimental data selected

Table B-1 [Fig.6-2]

Vg cm/s	V_l cm/s	ε_g %	Vg cm/s	V_l cm/s	ε_g %
0.5	0.377	9.20	0.8	0.377	13.4
	0.65	9.78		0.65	14.8
	0.825	10.8		0.825	15.8
	1.00	11.8		1.00	17.0
	1.092	13.0		1.092	18.0
	1.17	13.8		1.17	18.8
	1.26	14.5		1.26	20.0
1.0	0.377	16.4	1.2	0.377	19.4
	0.65	17.8		0.65	20.5
	0.825	19.0		0.825	22.0
	1.00	20.2		1.00	23.4
	1.092	21.2		1.092	24.5
	1.17	22.0		1.17	25.6
	1.26	23.0		1.26	28.0
1.5	0.377	23.7	1.8	0.377	28.0
	0.65	25.5		0.65	30.5
	0.825	26.5		0.825	32.0
	1.00	28.0		1.00	33.5
	1.092	29.2		1.092	34.0
	1.17	30.6		1.17	24.5
	1.26	33.0		1.26	35.6

Table B-2 [Fig.6-4]

Photographic measurement of bubble size

Dowfroth : 15 ppm

sparger : steel

column diameter: 5.71 cm

liquid velocity: 1.0 cm/s

Vg cm/s	N	dbs cm	s* cm	dvs cm	s** cm
0.5	400	0.62	0.10	0.62	0.08
0.8	384	0.67	0.10	0.65	0.07
1.0	386	0.70	0.11	0.69	0.08
1.2	339	0.74	0.10	0.74	0.07
1.5	368	0.81	0.11	0.80	0.08
1.8	359	0.88	0.11	0.88	0.08

N : number of bubbles counted

dbs : Sauter mean diameter

dvs : volumetric mean diameter

s* : standard deviation of dbs

s** : standard deviation of dvs

APPENDIX C

Computer program for the estimation of bubble size by the developed method

```
100  REM  THE SECANT METHOD FOR THE ESTIMATION OF BUBBLE SIZE
110  REM  THE ESTIMATION IS BASED ON MASOLYIAH SETTLING EQUATION
120  REM  WRITTEN BY SHEN GONG AND MODIFIED BY MANQIU, APR.2.1987
130  CALL  - 936: VTAB (8)
140  PRINT  TAB( 5);"*****************************"
150  PRINT  TAB( 5);"**      BUBBLE  SIZE       **"
160  PRINT  TAB( 5);"**   ESTIMATION PROGRAM    **"
170  PRINT  TAB( 5);"*****************************"
180  PRINT : PRINT
190  PRINT  TAB( 8);"WRITTEN BY MANQIU XU"
200  PRINT  TAB( 19);"GONG SHEN"
210  PRINT  TAB( 19);"APR.2.1987"
220  VTAB (23): HTAB (10): INPUT "ENTER Y TO CONTINUE ?";Y$
230  IF Y$ <  > "Y" GOTO 130
240  HOME
250  VTAB (5): HTAB (4): INPUT "(1) SUP GAS RATE (CM/S):";VG
260  VTAB (7): HTAB (4): INPUT "(2) SUP LIQ RATE (CM/S):";VL
270  VTAB (9): HTAB (4): INPUT "(3) GAS   HOLDUP    (%) :";EG
280  VTAB (23): HTAB (12): INPUT "ARE INPUT DATA CORRECT ?";Y$
290  IF Y$ <  > "Y" GOTO 250
300 EG = EG / 100
310  HOME
320  VTAB (5): HTAB (7): PRINT "DB IS BUBBLE SIZE (MM)"
330  VTAB (7): HTAB (3): INPUT "(1)ENTER FIRST  GUESS OF DB (MM) :";X1
340  VTAB (9): HTAB (3): INPUT "(2)ENTER SECOND GUESS OF DB (MM) :";X2
350  VTAB (13): HTAB (12): INPUT "ARE INPUT DATA CORRECT ?";Y$
360  IF Y$ <  > "Y" GOTO 330
370  HOME
380 G = 980
390 UL = 0.01
400 PL = 1
410  PRINT
420 I = 1
430 X = X1
440  GOSUB 750
450 F1 = F
460 X = X2
470  GOSUB 750
480 F2 = F
490 XN = (X1 * F2 - X2 * F1) / (F2 - F1)
500 X = XN
510  GOSUB 750
```

```
520 F3 = F
530 FD =  ABS (F3)
540  IF FD < 1.0E - 6 THEN  GOTO 620
550  IF I > 60 THEN  GOTO 730
560 X1 = X2
570 X2 = XN
580 F1 = F2
590 F2 = F3
600 I = I + 1
610  GOTO 490
620  VTAB (9): HTAB (7): PRINT "SUP GAS RATE: VG = ";VG;"CM/S"
630  VTAB (11): HTAB (7): PRINT "SUP LIQ RATE: VL = ";VL;"CM/S"
640  VTAB (13): HTAB (7): PRINT "GAS  HOLDUP : EG = ";EG * 100;"%"
650  VTAB (15): HTAB (7): PRINT "BUBBLE SIZE : DB = "; INT (X * 10000 + 0.5) / 1000;"M
660  PRINT
670  VTAB (17): HTAB (5): PRINT "THE MAXIMUM DIFFERENCE IN SLIP"
680  VTAB (19): HTAB (5): PRINT "VELOCITY BETWEEN  MEASURED AND"
690  VTAB (21): HTAB (5): PRINT "ESTIMATED   IS  ";FD
700  VTAB (23): HTAB (3): INPUT "DO YOU WAND A HARD COPY OF THE DATA ?";D$
710  IF D$ = "Y" GOTO 1070
720  GOTO 740
730  PRINT "PLEASE CHECK INPUT DATA ."
740  END
750 VS = VG / EG + VL / (1 - EG)
760  GOSUB 800
770 BS = G * X ^ 2 * (1 - EG) ^ (M - 1) * PL / (18 * UL * (1 + 0.15 * REB ^ 0.687))
780 F = BS - VS
790  RETURN
800  REM  THE SECANT METHOD FOR M
810 M1 = 2.2
820 M2 = 0.9 * M1
830 M = M1
840  GOSUB 1000
850 T1 = FM
860 M = M2
870  GOSUB 1000
880 T2 = FM
890 MN = (M1 * T2 - M2 * T1) / (T2 - T1)
900 M = MN
910  GOSUB 1000
920 T3 = FM
930  IF  ABS (T3) < 1E - 6 THEN  GOTO 990
940 M1 = M2
950 M2 = MN
960 T1 = T2
970 T2 = T3
980  GOTO 890
990  RETURN
1000 REB = X * VS * PL * (1 - EG) / UL
1010 CRE = X * VS * PL / (UL * (1 - EG) ^ (M - 1))
1020 Z = 4.45 * CRE ^ ( - 0.1)
1030 FM = Z - M
1040  VTAB (5): HTAB (11): PRINT "DB=";X * 10
1050  VTAB (7): HTAB (11): PRINT "M =";Z
1060  RETURN
1070 D$ =  CHR$ (4): REM  CHR$(4)=CTRL-D
```

```
1071  PRINT D$;"PR#1"
1080  PRINT  TAB( 26);"DB=";X * 10
1090  PRINT
1100  PRINT  TAB( 26);"M=";Z
1110  PRINT
1120  PRINT  TAB( 22);"SUP GAS RATE : VG = ";VG;"CM/S"
1130  PRINT
1140  PRINT  TAB( 22);"SUP LIQ RATE : VG = ";VL;"CM/S
1150  PRINT
1160  PRINT  TAB( 22);"GAS   HOLDUP : EG = ";EG * 100;"%"
1170  PRINT
1180  PRINT  TAB( 22);"BUBBLE SIZE  : DB = ";  INT (X * 10000 + 0.5) / 1000;"MM"
1190  PRINT
1200  PRINT  TAB( 20);"THE MAXIMUM DIFFERENCE IN SLIP"
1210  PRINT
1220  PRINT  TAB( 20);"VELOCITY BETWEEN  MEASRED AND "
1230  PRINT
1240  PRINT  TAB( 20);"ESTIMATED   IS    ";FD
1250 D$ =  CHR$ (4): REM  CHR$(4)=CTRL-D
1251  PRINT D$;"PR#0"
1260  END
1270  PRINT  TAB( 26);"DB=";X * 10
```

APPENDIX D

Regression program for experimental data processing

```
8000  GOTO 8064
8002  PRINT
8004  FOR S = 1 TO N
8006  FOR T = S TO N
8008  IF A(T,S) >  < 0 THEN  GOTO 8016
8010  NEXT T
8012  PRINT "NO UNIQUE SOLUTION"
8014  GOTO 8062
8016  GOSUB 8036
8018 C = 1 / A(S,S)
8020  GOSUB 8048
8022  FOR T = 1 TO N
8024  IF T = S THEN  GOTO 8030
8026 C =  - A(T,S)
8028  GOSUB 8056
8030  NEXT T
8032  NEXT S
8034  GOTO 8062
8036  FOR J = 1 TO N + 1
8038 B = A(S,J)
8040 A(S,J) = A(T,J)
8042 A(T,J) = B
8044  NEXT J
8046  RETURN
8048  FOR J = 1 TO N + 1
8050 A(S,J) = C * A(S,J)
8052  NEXT J
8054  RETURN
8056  FOR J = 1 TO N + 1
8058 A(T,J) = A(T,J) + C * A(S,J)
8060  NEXT J
8062  RETURN
8064  HOME : PRINT "FUNCTION: Y=  A + A1*X1 + A2*X2 + A3*X3+ A4*X4 + ...": PRINT
8065  PRINT "INPUT NUM. OF VARABLE N"
8066  INPUT N
8068  PRINT
8070  PRINT "INPUT NUM. OF DATA M"
8072  INPUT M
8074  PRINT
8076  DIM F(N,M),A(N + 1,N + 1),B(N + 1,N + 1),W(N)
8078  PRINT "READ YOUR DATA Y...,X...": PRINT
```

```
8080  PRINT "Y:"
8082  FOR I = 0 TO N
8084  IF I = 0 THEN  GOTO 8088
8086  PRINT "X:"
8088  FOR J = 0 TO M - 1
8090  READ F(I,J)
8091  PRINT F(I,J),
8092  NEXT J
8094  PRINT : PRINT
8096  NEXT I
8098  FOR I = 0 TO N - 1
8100 U4 = 0
8102 U5 = 0
8104  FOR J = 0 TO N - 1
8106 U1 = 0
8108 U2 = 0
8110 U3 = 0
8112  FOR K = 0 TO M - 1
8114 U1 = U1 + F(I + 1,K)
8116 U2 = U2 + F(J + 1,K)
8118 U3 = U3 + F(I + 1,K) * F(J + 1,K)
8120  NEXT K
8122  IF J < I THEN  GOTO 8128
8124 A(I + 1,J + 1) = U3 - (U1 * U2) / M
8126 A(J + 1,I + 1) = A(I + 1,J + 1)
8128  NEXT J
8130  FOR K = 0 TO M - 1
8132 U4 = U4 + F(I + 1,K) * F(0,K)
8134 U5 = U5 + F(0,K)
8136  NEXT K
8138 A(I + 1,N + 1) = U4 - (U5 * U1) / M
8140  NEXT I
8142  FOR I = 1 TO N
8144  FOR J = 1 TO N + 1
8146 B(I,J) = A(I,J)
8148  NEXT J
8150  NEXT I
8152  GOSUB 8002
8154  FOR I = 0 TO N
8156 W(I) = 0
8158  FOR K = 0 TO M - 1
8160 W(I) = W(I) + F(I,K)
8162  NEXT K
8164 W(I) = W(I) / M
8166  NEXT I
8168 L = 0
8170  FOR I = 1 TO N
8172 L = L + W(I) * A(I,N + 1)
8174  NEXT I
8176 B0 = W(0) - L
8178  PRINT "Y=";B0;
8180  FOR I = 1 TO N
8182  PRINT " + ";A(I,N + 1);" X";I;
8184  NEXT I
8186  PRINT
8188 U = 0
8190  FOR I = 1 TO N
```

```
8192 U = U + A(I,N + 1) * B(I,N + 1)
8194  NEXT I
8196 U1 = 0
8198 U2 = 0
8200  FOR K = 0 TO M - 1
8202 U1 = U1 + F(0,K) * F(0,K)
8204  NEXT K
8206 Q = U1 - (U5 * U5) / M - U
8208 S =  SQR (Q / (M - N - 1))
8210 R =  SQR (1 - Q / (U1 - (U5 * U5) / M))
8212 F1 = (M - N - 1) * U / (N * Q)
8214  PRINT "U=";U
8216  PRINT "Q=";Q
8218  PRINT "F=";F1
8220  PRINT "S=";S
8222  PRINT "R=";R
8224  END
8226  DATA  25,81,36,33,70,54,20,44,1.4,41,75
8228  DATA  110,184,145,122,165,143,78,129,62,130,168
```

APPENDIX E

derivation of $F(\varepsilon_l) = (\varepsilon_l)^{m-1}$

The defination of $F(\varepsilon_l)$ is introduced by Masliyah [52], but, no general expression is given. An expression can be derived from Richardson and Zaki [56]. They developed an empirical correlation for the relative velocity between fluid and solid, Us, and the terminal velocity of a single bubble, U_T

$$Us = U_T \cdot \varepsilon_l^{m-1} \qquad [E-1]$$

since

$$U_T \propto (\rho_s - \rho_l) \qquad [E-2]$$

and, by definition

$$\rho_s - \rho_{susp} = \rho_s - \rho_s (1-\varepsilon_l) + \rho_l \varepsilon_l \qquad [E-3]$$

or,

$$\rho_s - \rho_{susp} = \varepsilon_l (\rho_s - \rho_l) \qquad [E-4]$$

then, substituting Eqs.[2], [4] in [1] yields

$$Us \propto (\rho_s - \rho_{susp}) \varepsilon_l^{m-2} \qquad [E-5]$$

Comparing Eqs.[4-9] and [5], then $F(\varepsilon_l)$ is

$$F(\varepsilon_l) = \varepsilon_l^{m-2} \qquad [E-6]$$

which is equation [4-11]

For Re < 0.2, m = 4.65. Consequently, for low Re, Masliyah used

$$F(\varepsilon_l) = \varepsilon_l^{m-1} \qquad [E-7]$$

For high Re (R_e > 500), m is again constant (m=2.39). For the bubbles of interest here (up to 2 mm) Re is intermediate, and m is a function of Re.

APPENDIX F

Gas flowmeter calibration

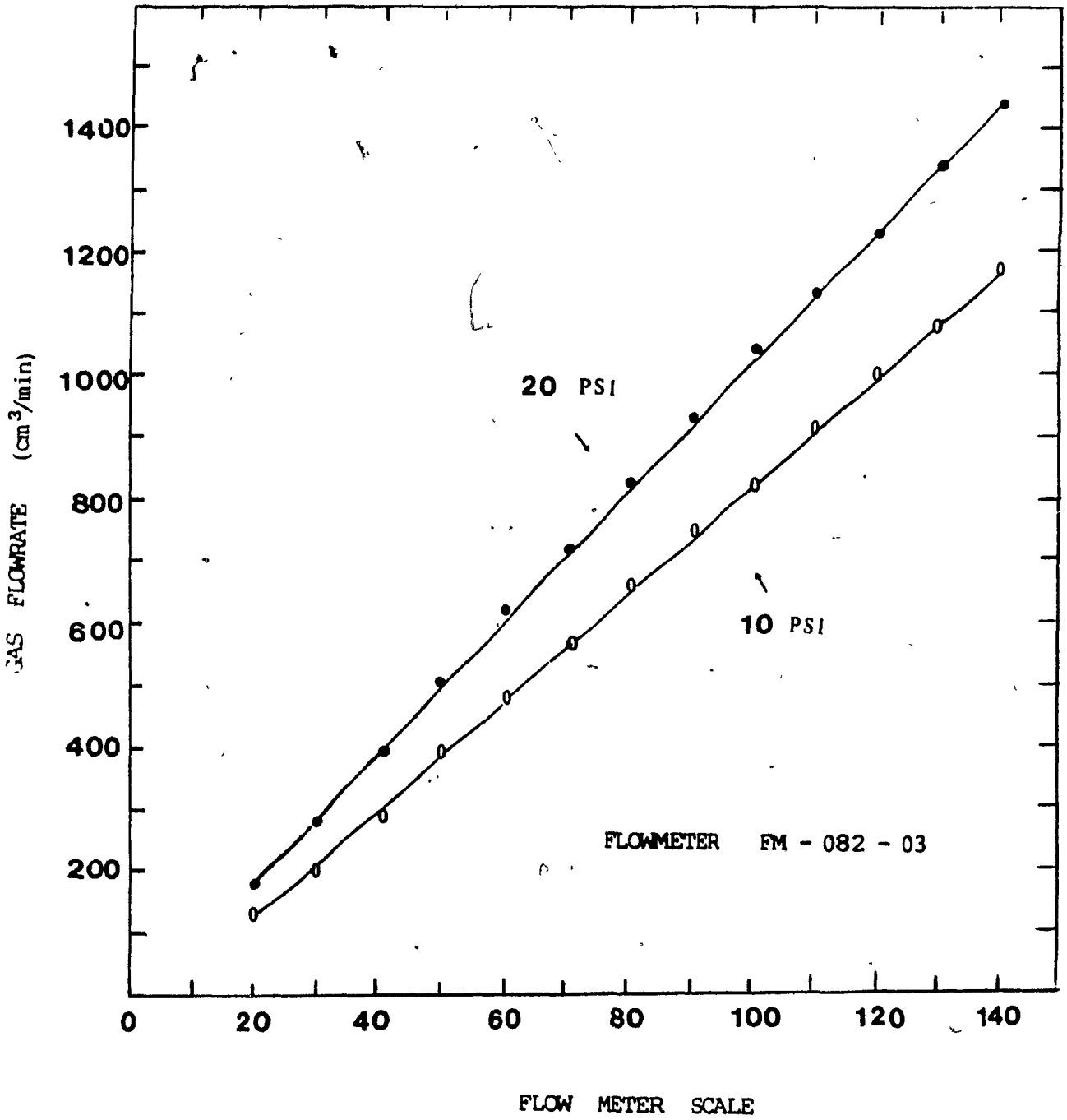

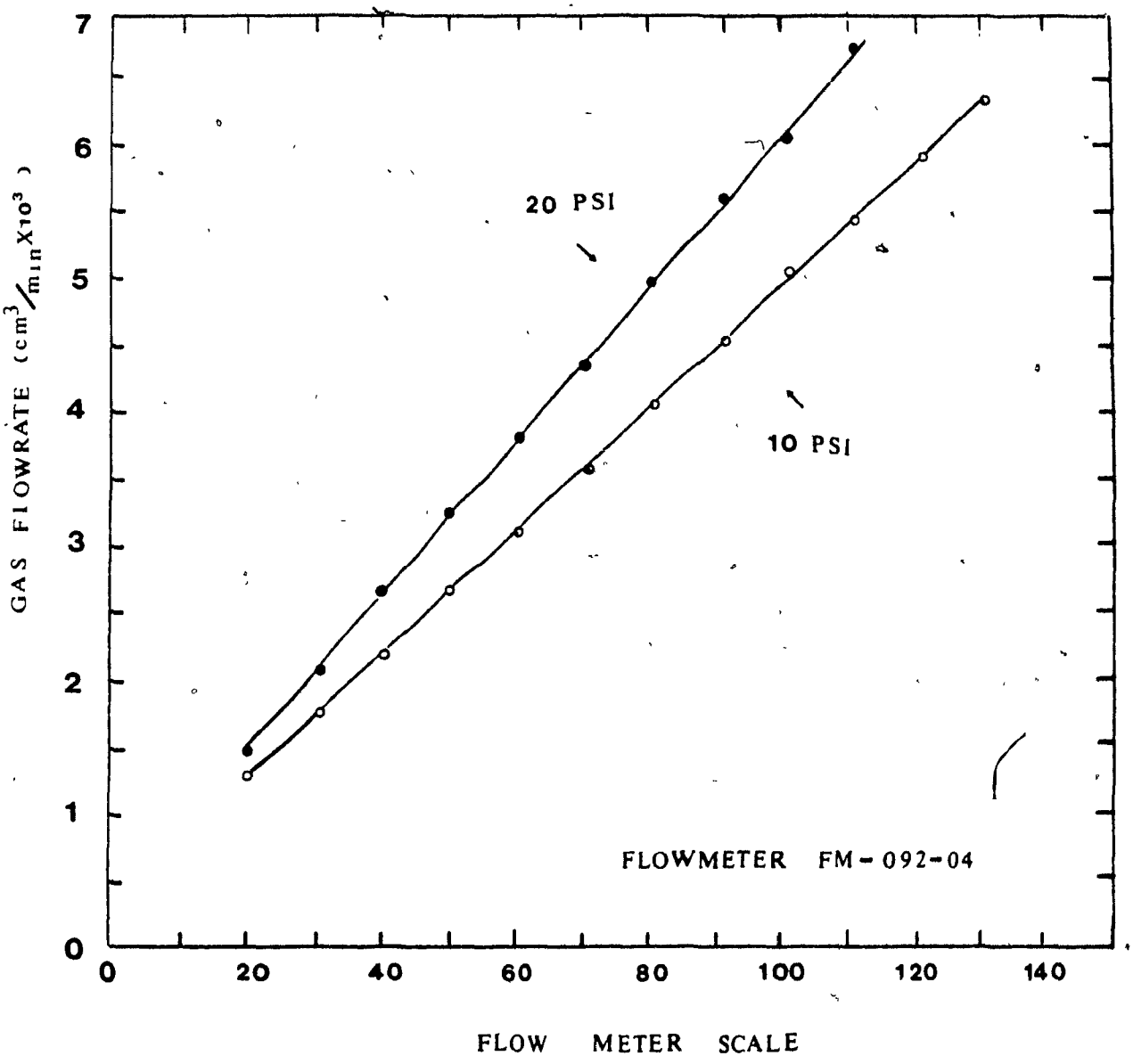
GAS FLOWRATE ($cm^3/_{min} X10^3$)
7
6
5
4
3
2
1
0
20 PSI
10 PSI
FLOWMETER FM-092-04
0
20
40
60
80
100
120
140
FLOW METER SCALE

APPENDIX G

(manustript)

CARRYING CAPACITY IN COLUMNS - GAS RATE AND BUBBLE SIZE EFFECTS

Manqiu Xu, J.A. Finch and J.B. Yianatos

Mining and Metallurgical Eng

McGill University

Montreal, H3A 2A7

Canada

ABSTRACT

The collection zone of a flotation column should be operated in the bubbly flow regime. This imposes limits in the allowed bubble size and gas rate combinations. A model of bubbly flow is used to explore these combinations. It is shown that the superficial bubble surface rate (cm^2 bubble / s / cm^2 column cross-section) is maximum in the bubble size range 1-1.6 mm. Carrying capacity is related to superficial bubble surface rate. Using a model of bubble loading it is shown that for particles less than 10 um, carrying capacity is maximum for bubbles in the range of 1-1.6 mm. For larger particles, carrying capacity increases with increasing bubble size. The loading model assumes that the bubble has sufficient retention time to reach its equlibrium, or full load. It is noted that retention time increases as bubble size decreases and this needs to be considered in testing the effect of bubble size.

INTRODUCTION

The collection zone in a flotation column should be operated in the bubbly flow regime [Dobby et al, 1985]. This requirement imposes a minimum bubble size at a given gas rate (or conversely a maximum gas rate at a given bubble size). Attempting to go below this bubble size will move the collection zone into the churn-turbulent flow regime. With increasing gas rate, the minimum bubble size increases.

This interaction between bubble size and gas rate has important consequences for column flotation. Dobby and Finch [1986a] showed it leads to an optimum bubble size to maximise the collection rate constant. In this communication, the effect on solids carrying capacity in the collection zone is analysed. The analysis is achieved by introducing and determining the maximum superficial bubble surface rate, which combined with bubble loading defines the maximum solids carrying capacity. The impact of bubble loading on the minimum bubble size is also considered.

MODEL OF BUBBLY FLOW

Description

The model constitutes two equations for U_{bs}, the relative bubble to slurry velocity (or slip velocity) in a bubble swarm, which must be satisfied simultaneously. (The model has been described in full

elsewhere) [Yianatos et al, 1987].

$$U_{bs} = \frac{J_g}{\varepsilon_g} + \frac{J_{sL}}{(1-\varepsilon_g)} \qquad (1)$$

$$U_{bs} = \frac{g\, d_b^2 (1-\varepsilon_g)^{m-1} (\rho_b - \rho_{sL})}{18\, \mu_{sL} (1+0.15 Re_{bs}^{0.687})} \qquad (2)$$

Eq.(1) is the defination of slip velocity in countercurrent flow, and Eq.(2) is an adaptation of the particle settling equation due to Masliyah [1979], and is applicable up to d_b = 2 mm. The symbols are defined in the notation.

Determination of Minimum Bubble Size

The method of solution is illustrated in Figure 1, for J_g = 1.2 cm/s and J_L = 0.5 cm/s (no solids present). The U_{bs} from Eq.(1) is plotted against ε_g. The actual U_{bs}, ε_g combination depends on d_b. The U_{bs} from Eq.(2), therefore, is plotted against ε_g for various d_b. Where the two curves intersect gives the ε_g for that d_b. (There appear to be two solutions but only the one at lower ε_g is physically realised). Thus for d_b = 1.0 mm, ε_g is about 10%, for d_b = 0.6 mm, ε_g is about 30%. There is no solution for d_b < 0.6 mm. Thus at J_g = 1.2 cm/s, J_L = 0.5 cm/s, the minimum bubble size $d_{b_{min}}$ is about 0.6 mm. Or, conversely at d_b = 0.6 mm, the maximum J_g = 1.2 cm/s.

The locus of db_{min} for various J_g and J_L calculated in this manner is shown in Figure 2. The result is comparable to that found by Dobby and Finch (1986a) from a drift-flux model of bubbly flow.

Experimental validation of the db_{min} estimate is difficult. This is due to problems in accurately determining visually the transition from bubbly to churn-turbulent flow and the inability to independently manipulate db and J_g (d_b increases as J_g increases). Figure 3 illustrates that $J_{g_{max}}$ does decrease with increasing frother dosage i.e. decreasing bubble size. Bubble size was estimated photographically at 15 ppm frother concentration to be about 1.35 mm. At J_g = 3.5 cm/s, J_L = 0.5 cm/s, ε_g = 32%, the calculated db from the model is about 1.35 mm which is quite close to the photographically measured bubble size. However, at J_g = 3.5 cm/s, J_L = 0.5 cm/s, the calculated db_{min} (as opposed to db) from the model is about 1.15 mm appearing at ε_g = 53%.

SUPERFICIAL BUBBLE SURFACE RATE

The superficial bubble surface rate, J_{g_a}, is the surface area of bubbles per unit time moving through the column per unit column cross-section. It is derived as follows:

$$Q_g = \frac{\pi}{6} db^3 N_b \qquad (3)$$

where Qg is the volumetric flowrate of gas and Nb is the number of bubbles per unit time.

Therefore, the surface area rate is

$$= Nb\ \pi\ db^2 \qquad (4)$$

which on substituting for Nb becomes

$$= \frac{6\ Qg}{db} \qquad (5)$$

Dividing by the column cross-sectional area, Ac gives

$$Jgs = \frac{6\ Qg}{db\ Ac}$$

or

$$Jgs = \frac{6\ Jg}{db} \qquad (6)$$

The maximum Jgs is

$$Jgs_{max} = \frac{6\ Jg}{db_{min}} \qquad (7)$$

Eq.(6) is plotted in Figure 4. Without respecting the restriction on db, Jgs continues to increase with decreasing db. However imposing

db_{min} , Jgs_{max} actually decreases with decreasing db.

CARRYING CAPACITY Ca

Bubble Loading

Assuming spherical particles each occupying dp^2 of spherical bubble surface [Szatkowski and Freyberger, 1985] and that the maximum loading is 50% of a monolayers [Jameson, personal communication. 1986], then the mass of particles per bubble is,

$$= \frac{\pi^2}{12} db^2 \, dp \, \rho p \qquad (4)$$

Therefore, the mass of solids per unit area of bubble is

$$= \frac{\pi}{12} dp \, \rho p$$

This multiplied by Jgs gives the mass of solids carried per unit time per unit column cross-section, or carrying capacity, Ca .

$$Ca = \frac{\pi \, Jg}{2 \, db} dp \, \rho p \qquad (8)$$

Eq.(8) will be refered to as carrying capacity constraint 1 to distinguish it from a second possible constraint considered below. The maximum in carrying capacity, Ca_{max} , occurs at db_{min} .

Bubble Density and db_{min}

Knowing the mass of particles per bubble (Eq.(8)), the mass per bubble volume can be calculated. Assuming $dp \ll db$, this is equivalent to a bubble/particle aggregate density, ρb

$$\rho b = \frac{\pi}{2} \frac{dp\ \rho p}{db} \tag{11}$$

The term ρb in Eq.(2) is normally taken as zero. As ρb increases, db_{min} increases, all other parameters being constant. The db_{min} can be solved in a siminar manner to that described in Figure 1. An illustration is given in Figure 5. The interpretation is that at ρb = 0.56 g/cm^3, db_{min} at the given conditions is 1 mm. In contrast for ρb = 0, db_{min} is about 0.6 mm (Figure 1).

By comparing Eqs.(10) and (11), it is evident that

$$Ca = \rho b\ Jg \tag{12}$$

Eq.(12) is carrying capacity constraint 2.

The term ρb is sometime used as a measure of carrying capacity since it is equivalent to the mass of solids carried per unit volume of gas.

RESULTS

Figure 6 shows the carrying capacity calculated from Eq.(10) (constraint 1) and Eq.(12) (constraint 2). Constraint 1 shows the increase in Ca with decreasing db corresponding to the increase in Jgs (Figure 4). In the absence of constraint 2, the maximum Ca_{max} would be at the intercept of constraint 1 and the vertical dashed line (at db = 1.18 mm). Allowing for constraint 2, the minimum db increases slightly which has the effect of slightly reducing the maximum Ca_{max} .

This method of determining Ca_{max} was repeated for various Jg at JL = 1 cm/s. The result is given in Figure 7. Ca_{max} is plotted as a function of db for various particle sizes. For fine particles (dp< 10 μm) the optimum db is between 1 - 1.6 mm. For coarser particles, the optimum appears to shift to larger bubbles, bubble sizes above the range covered by the model.

DISCUSSION

The model of bubbly flow used here has been verified for the 2-phase gas-water system by showing good agreement between estimated and measured bubble size [Yianatos, et al, 1987]. The model's use enables the experimentally more difficult 3-phase (gas-water-solid) system to be explored. To make the solution more tractable, it was assumed here that ρ_{SL} = 1 g/cm^3 and μ_{SL} = 0.01 poise (i.e. as if there were no solids in suspension). The effect of solids in suspension is to increase ρ_{SL} and μ_{SL} which have opposite effects on db_{min}.

The analysis reveals an optimum bubble size range for maximizing the superficial bubble surface rate. This in turn leads to an optimum range in db to maximize Ca_{max} which is slightly modified by the effect of ρ_p on db_{min}. The dependence of J_{gS} on db is an unavoidable limitation to the carrying capacity.

Translating J_{gS} to Ca involves arguable assumptions regarding loading of the bubble. No justification of the assumptions used is offered here, other than that they have been used eslewhere. Experimental verification of Ca_{max} is not feasible. It can not be proved that the bubble has reached its maximum load (e.g. 50% of a monolayer as assumed here) and it is not possible to hold bubble size at the db_{min} for the given J_g. Measurement of Ca (as opposed to Ca_{max}) for columns is becoming increasing common as the limitation it places on capacity is gaining in appreciation. Table 1 gives a set of results for Ca from Espinosa et al [1988]. The estimated Ca is in

tolerable agreenment given the measured Ca is for a column with a froth zone and the problem of estimating dp (taken as 0.3 of the d_{80} of the collected particles) and db at the top of the froth (taken as 2 times the bubble size in the collection zone [Yianatos, et al, 1986]). The model here is for the collection zone, the froth zone can be expected to place added restriction on carrying capacity Ca.

The analysis has revealed that for dp ≤ 10 μm (approximately d_{80} ≤ 30 μm) the optimum bubble size to maximise Ca_{max} is 1 - 1,6 mm. This is similar to the range found by Dobby and Finch (1986a) to maximise the collection rate constant. This bubble size is readily obtainable by the available spargers and seems to obviate the need to design sophisticated spargers with the target of producing db < 1 mm. There is, however, a possible advantage with finer bubbles not considered here. As bubble size decreases, bubble retention time in the collection zone increases. Thus the load on finer bubbles may more closely approach the maximum (equilibrium) loading. Tyurnikova and Naumaov (1981) used the argument to explained increased carrying capacity with finer bubbles. Certainly in any measurements of carrying capacity with bubble size, this kinetic factor must be considered.

CONCLUSIONS

1. A model of bubbly flow is used to determine the maximum superficial bubble surface rate as a function of bubble size. This gives an optimum bubble size of about 1 - 1.6 mm.

2. Using a model of bubble loading the analysis is extended to determine maximum carrying capacity as a function of bubble size. For particles less than 10 μm, the optimum size is 1 - 1.6 mm; for larger particles, the optimum bubble size appears to increase.

3. The bubble loading model assumes that the bubble will have sufficient retention time in the collection zone to reach its equilibrium load. Retention time increases as bubble size decreases, and this needs to be considered in experimentally testing carrying capacity vs. bubble size.

NOTATION

Ca	carrying capacity, mass of solids carried per unit time per unit column cross-sectional area, $g/s.cm^2$ or $g/min.cm^2$
Ca_{max}	maximum carrying capacity, the Ca value at the minimum bubble size allowed for the given operating conditons
db	bubble diameter, mm
db_{min}	minimum bubble size allowed for the given conditons, mm
dp	particle size, μm
d_{80}	80% passing size of a particle size distribution, μm
g	acceleration due to gravity, cm/s^2
Ji	superficial velocity of phase i, cm/s where i=g (gas), SL(slurry), L(liquid)
Jg_{max}	maximum superficial gas velocity at db_{min} , cm/s
JgS	superficial bubble surface rate, $cm^2/s/cm^2$
JgS_{max}	maximum superficial bubble surface rate at db_{min}
m	parameter in Eq.(2)
Nb	number of bubbles per second, s^{-1}
Qg	volumetric flowrate of gas, cm^3/s
RE_{bs}	bubble Reynolds number
Ubs	slip velocity between bubbles and slurry, cm/s
εg	fractional gas holdup
ρb	bubble/particle aggregate density, g/cm^3
ρi	density of phase i, g/cm^3 , where i=p (particle), SL(slurry), L(liquid)
$\mu SL, \mu L$	slurry, liquid viscosity, poise

REFERENCES

Dobby, G.S., Amelunxen, R. and Finch, J.A. (1985); "Column Flotation: some plant experience and model development", IFAC Symp. Brisbane, July, 1985

Dobby, G.S. and Finch, J.A. (1986a); "Particle Collection in Columns: -- gas rate and bubble size effects", Can. Metall. Quart. vol.25, No.1, pp9-13

Dobby, G.S. and Finch, J.A. (1986b); "Flotation Column Scale-up and Modelling", C.I.M. Bull. vol.79, No.889, pp89-96

Espinosa-Gomez, R., Yianatos, J.B. and Finch, J.A.; (1988) "Carrying Capacity Limitations in Flotation Columns",To be presented First Int. Symp. on Column, AIME, Phoenix.

Masliyah, J.H. (1979); "Hindered Settling in a Multi-species System", Chem. Eng. Sci., vol.34, pp1166-1168

Szatkowski, M. and Freyberger, W.L. (1985); "Kinetics of Flotation with Fine Bubbles", Trans IMM (section C) vol.84, pp61-70

Yianatos, J.B., Finch, J.A. and Laplante A.R. (1986), "Holdup Profile and Bubble Size Distribution of Flotation Column Froths", Can. Met. Quart. vol.25, No.1, pp23-29

Yianatos, J.B. et al, (1987), "Bubble Size Estimation in a Bubble Swarm", J. Coll. Interf. Sci., paper in review.

Tyurnikova, V.I. and Naumov, M.E.,"Improving the Effectiveness of Flotation", Technicopy Ltd., English Edition,1982, Chap.5, pp203-219

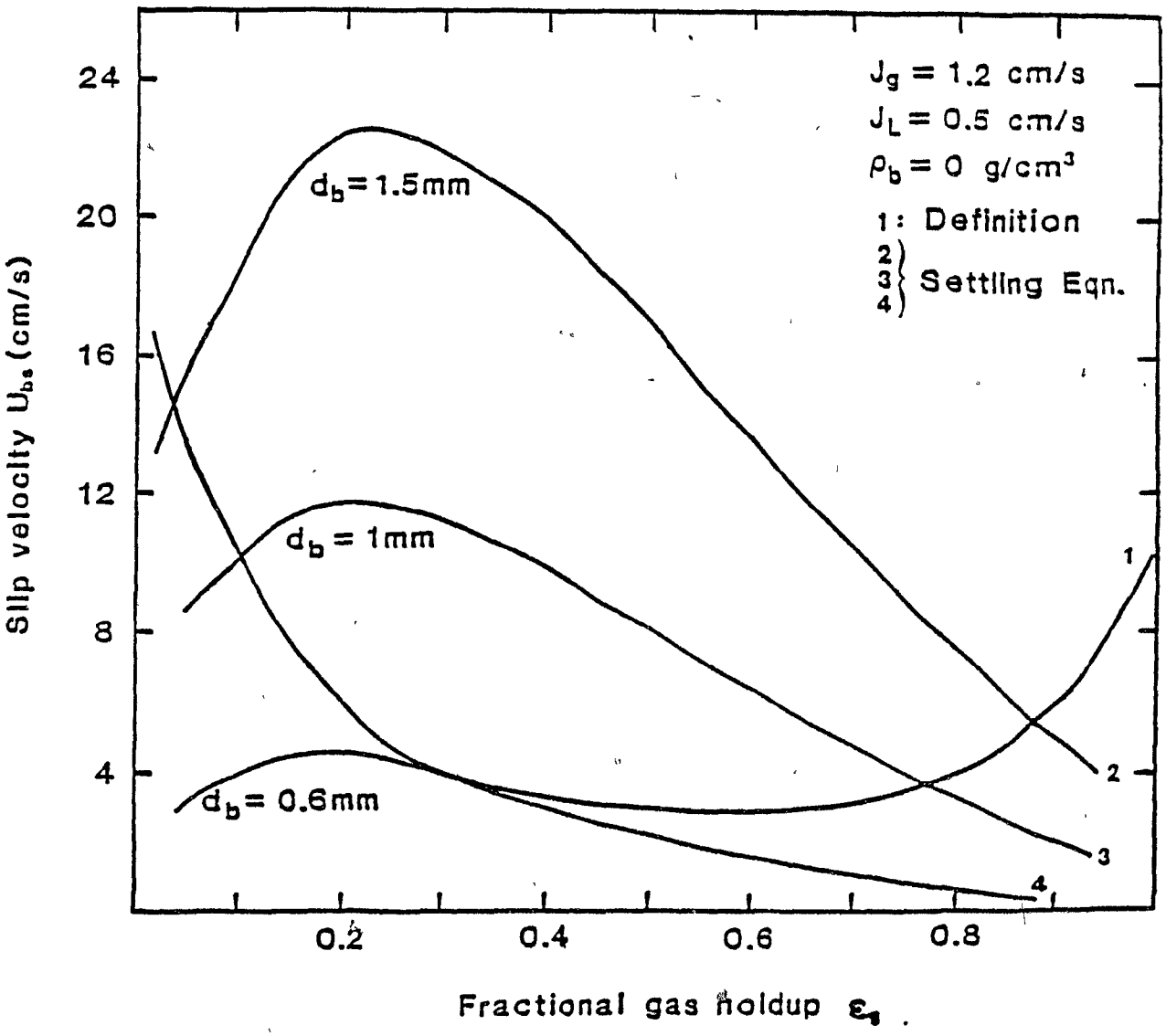

Figure 1 Ubs [from the definition Eq.(1) and the settling Eq. Eq.(2) vs gas holdup for various db. The solution is where curves intercept. There is no solution for db < 0.6 mm

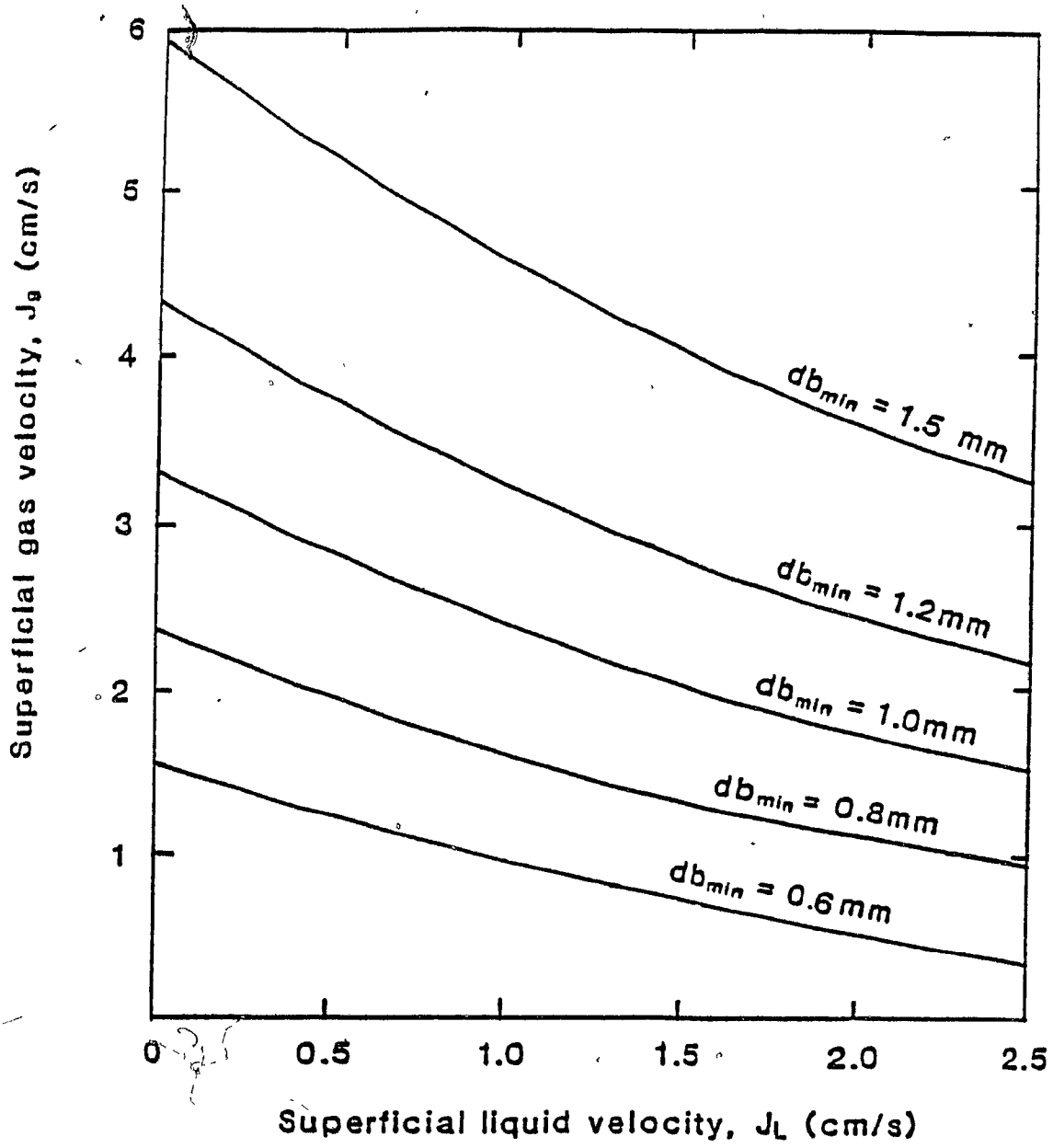

Figure 2 Locus of dbmin for Jg, J_L combinations. This is for countercurrent flow, J_L positive downwards. Alternatively the figure gives Jgmax for given db, J_L combinations.

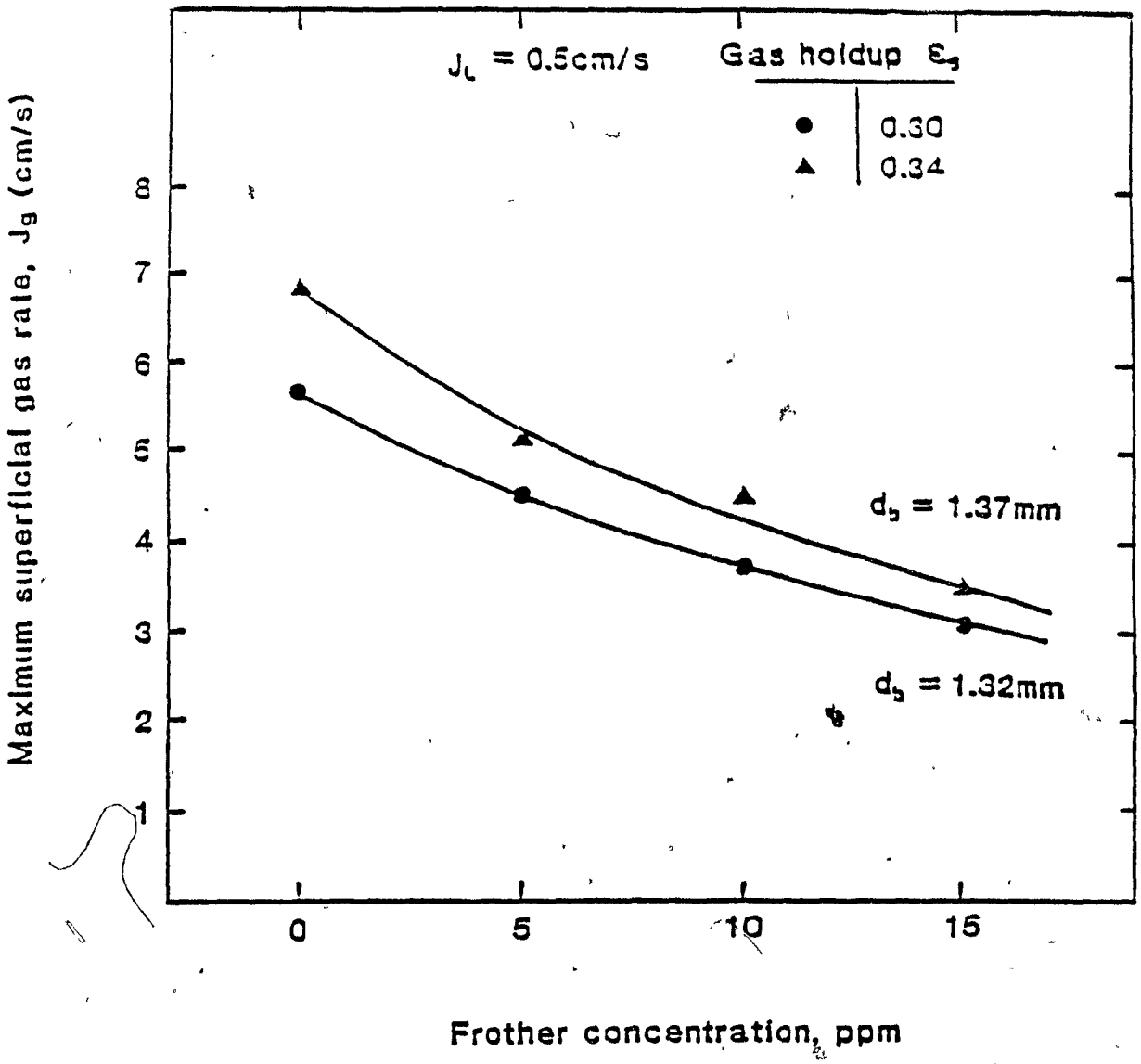

Figure 3 Measured decrease in Jgmax with increased frother (Dowfrother 250C) dosage [two gas holdup values are shown which straddle the transition from bubbly flow to churn–turbulent flow]

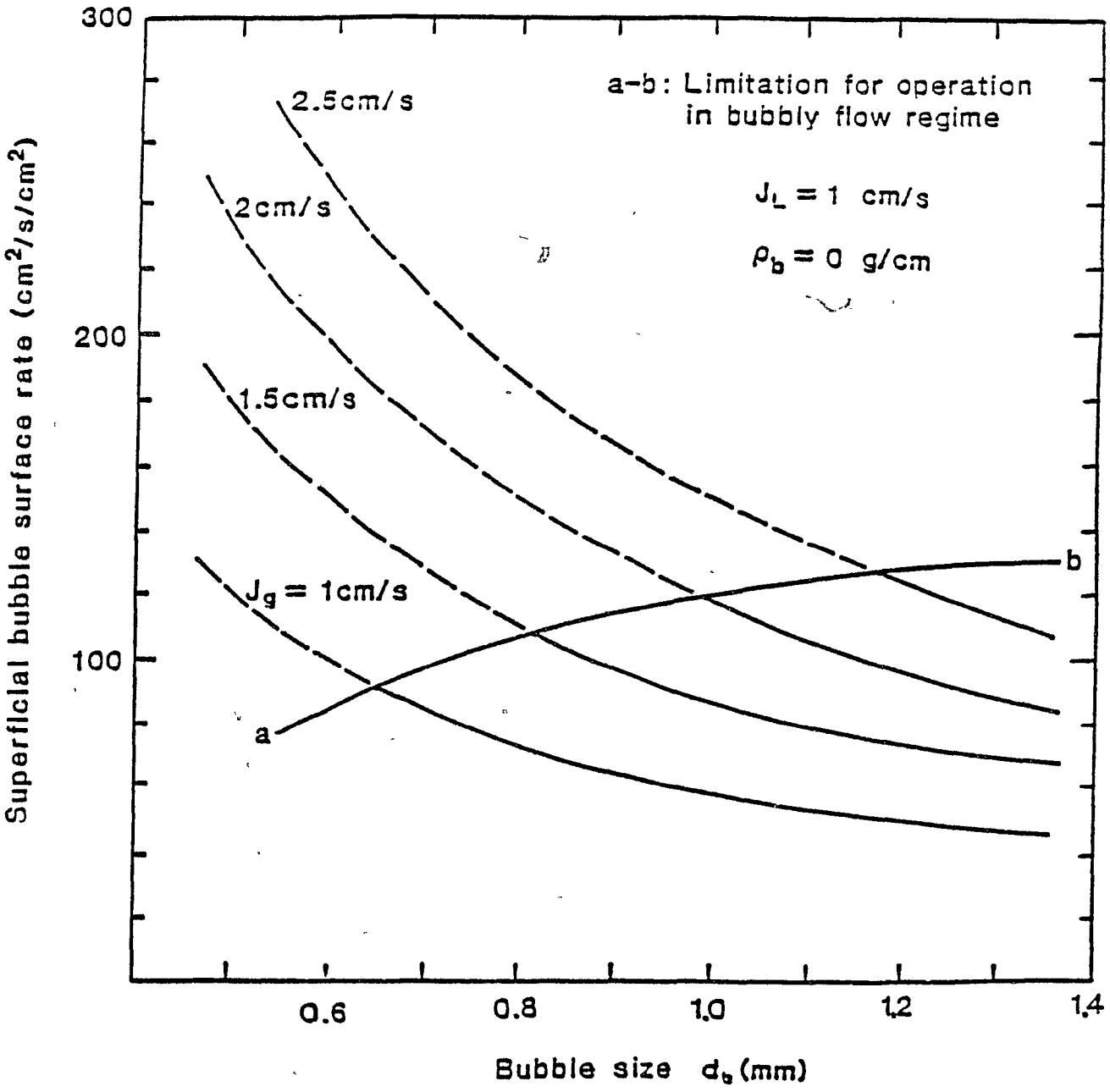

Figure 4 Superficial bubble surface rate vs db

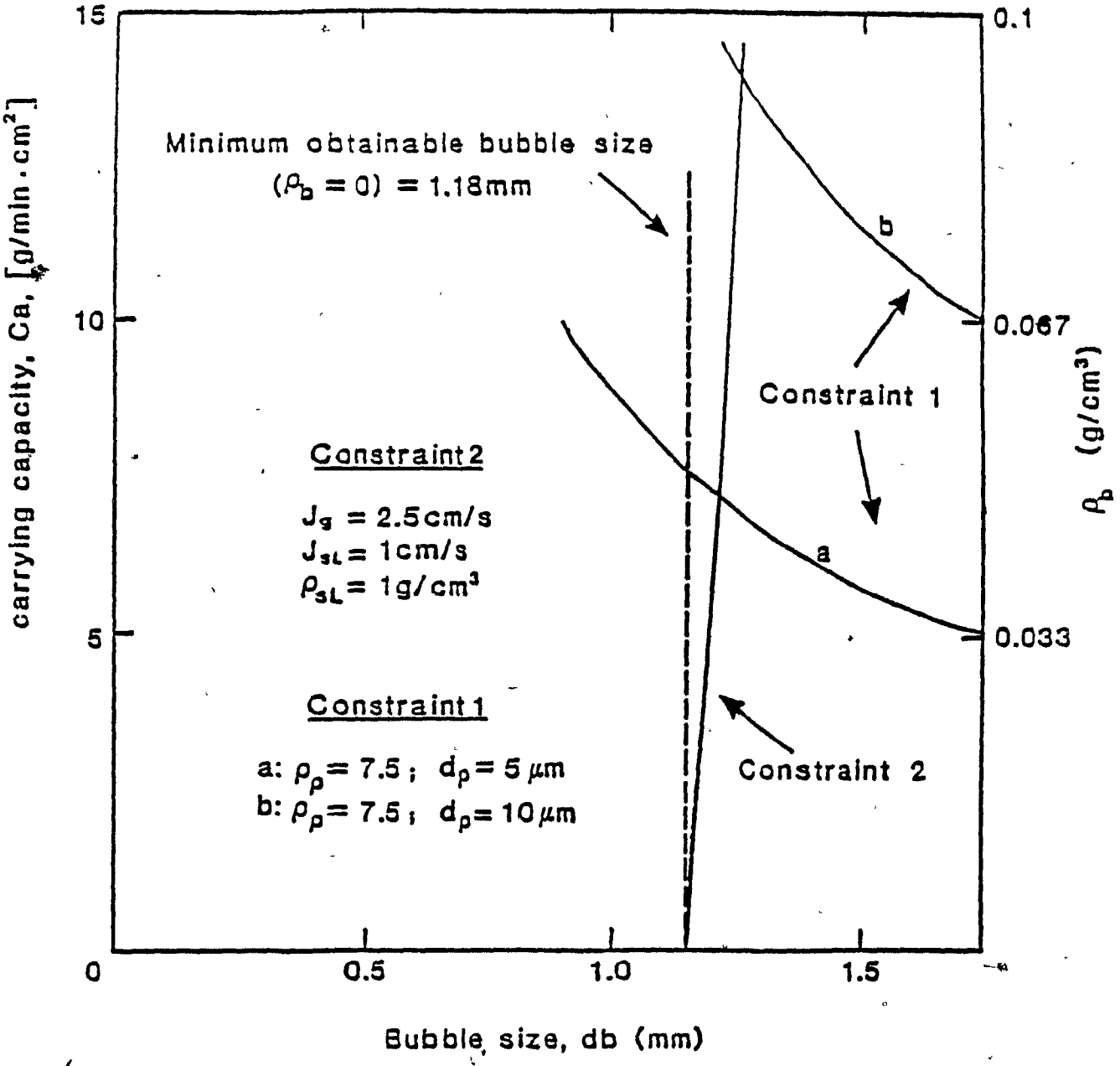

Figure 6 Carrying capacity vs db. Maximum carrying capacity (for given conditions) occurs at the intercept of constraint 1 and constraint 2

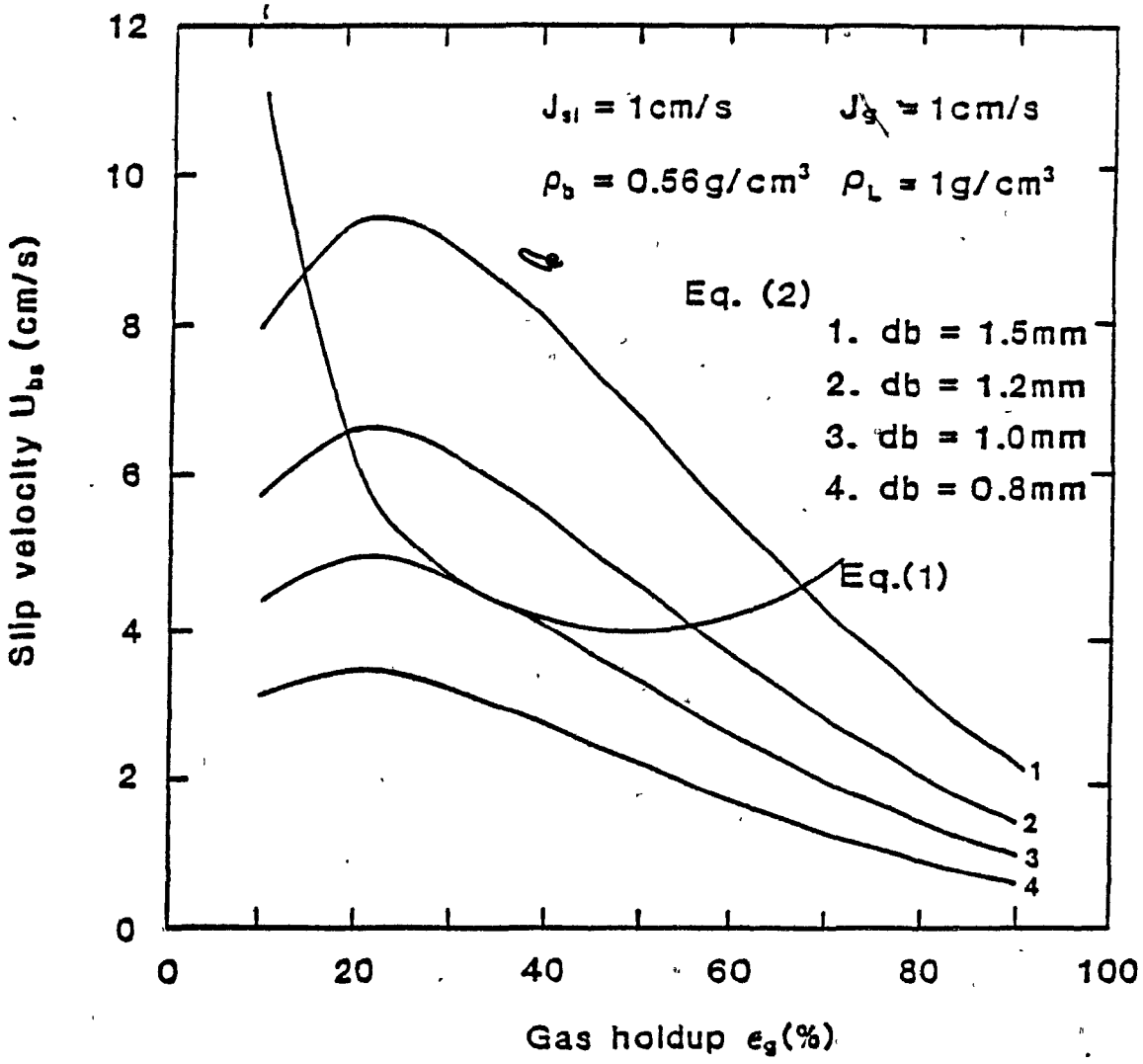

Figure 5 Ubs vs ε_g for various db at ρ_b = 0.56 g/cm³

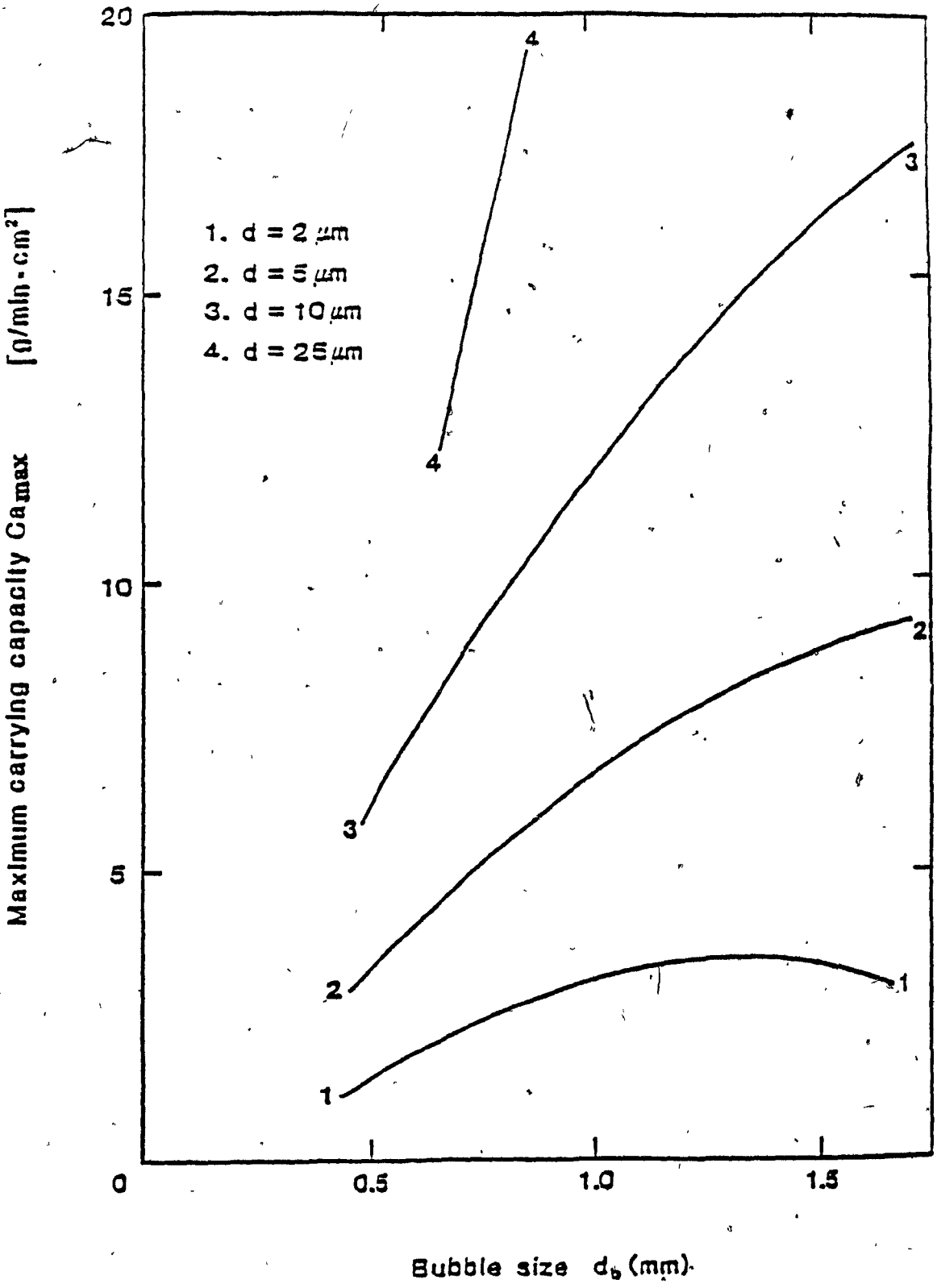

Figure 7 Maximum carrying capacity vs db. Camax occurs at Jgmax for the given db

Table 1

Comparison in Carrying Capacity
Between Measured and Estimated

Meas. Ca	Constraint 1	Ps	d_{80} (*)	Jg	Js
g/min/cm^2		g/cm^3	um	cm/s	
1.97	3.71	4.25	16	2.9	1.21
5.03	6.22	4.55	25	2.7	0.76
1.28	1.35	4.11	6	2.8	0.70
2.24	2.47	4.11	11	2.8	0.70
2.69	4.08	4.98	15	2.9	1.00
3.75	6.24	6.73	17	2.6	1.10

* : $dp = 0.3 \times d_{80}$ (80% passing size)

APPENDIX H

Computer program for the estimation of the maximum bubble/particle aggregate density

```
100  REM    ESTIMATION OF THE MAXIMUM BUBBLE LOADING
110 G = 980
120 UL = 0.01
130  INPUT "ENTER THE DENSITY OF SLURRY PL=";PL
140  INPUT "ENTER THE LIQUID VELOCITY VL(CM/S) VL=";VL
150  INPUT "ENTER THE BUBBLE SIZE (CM) DB=";DB
160  INPUT "ENTER THE GAS VELOCITY VG (CM/S)=";VG
170  PRINT : PRINT : PRINT
180  INPUT "PLOT STEP (0-270) =";D
190  INPUT "PB STEP (0.01-0.1) =";W
200  HCOLOR= 3
210  HGR
220  HPLOT 0,0 TO 270,0 TO 270,150 TO 0,150 TO 0,0
230  HPLOT 0,75 TO 270,75
240  FOR J = 1 TO 100
250 PB = J * W
260  FOR I = 1 TO 270 STEP D
270 EG = I * 3 / 800
280  GOSUB 1170
290 US = 3 * US:UB = 3 * UB
300  IF US > 75 THEN US = 75
310  IF UB > 75 THEN UB = 75
320 FF = US - UB
330  IF FF > 75 THEN FF = 75
340  HPLOT I,(75 - FF)
350  PRINT "US  = ";US / 3; TAB( 20);"UB = ";UB / 3
360  PRINT "EG =";EG; TAB( 20);"PB=";PB
370  NEXT I
380  INPUT "STOP ? (1/0)";Q
390  IF Q = 1 THEN  GOTO 410
400  NEXT J
410  REM  THE SECANT METHOD
420  INPUT "DO YOU WANT TO SOLVE THE ROOT ? (1/0)";A
430  IF A = 0 THEN END
440  INPUT "ENTER THE FIRST EG=";Z1
450  INPUT "ENTER THE SECOND EG=";Z2
460  INPUT "ENTER THE ESTIMATED MAXIMUM PB=";PB
470 PB = PB + 0.0001
480 X1 = Z1:X2 = Z1 * 0.9: GOSUB 640
490 S1 = XN
500 X1 = Z2:X2 = Z2 * 1.1: GOSUB 640
```

```
510 S2 = XN
520 SS =  ABS (S1 - S2)
530  PRINT "S1=";S1; TAB( 20);"S2=";S2
540  IF SS < 0.01 THEN  GOTO 570
550 K = K + 1
560  GOTO 470
570  PRINT "SS= ";SS
580  PRINT "PB= ";PB
590  PRINT "STEP =";K
600  PRINT
610  INPUT "OTHER ROOTS ? (1/0)";PP
620  IF PP = 1 THEN  GOTO 440
630  END
640 I = 1
650 X = X1
660  GOSUB 1160
670 F1 = F
680 X = X2
690  GOSUB 1160
700 F2 = F
710 XN = (X1 * F2 - X2 * F1) / (F2 - F1)
720  IF XN < 0 OR XN > 1 THEN  GOTO 850
730  PRINT "EG=";XN
740  PRINT "PB=";PB
750 X = XN
760  GOSUB 1160
770 F3 = F
780 FD =  ABS (F3)
790  IF FD < 1E - 6 THEN  GOTO 840
800  IF I > 60 THEN  GOTO 880
810 X1 = X2:X2 = XN:F1 = F2:F2 = F3
820 I = I + 1
830  GOTO 710
840  RETURN
850  PRINT "EG=";XN
860  PRINT "PB=";PB
870  END
880  PRINT "PLEASE CHECK INPUT DATA ."
890  PRINT "EG=";XN
900  PRINT "PB=";PB
910  REM  THE SECANT METHOD FOR M
920 M1 = 2.2
930 M2 = 0.9 * M1
940 M = M1
950  GOSUB 1110
960 T1 = FM
970 M = M2
980  GOSUB 1110
990 T2 = FM
1000 MN = (M1 * T2 - M2 * T1) / (T2 - T1)
1010 M = MN
1020  GOSUB 1110
1030 T3 = FM
1040  IF  ABS (T3) < 1E - 6 THEN  GOTO 1100
```

```
1050 M1 = M2
1060 M2 = MN
1070 T1 = T2
1080 T2 = T3
1090  GOTO 1000
1100  RETURN
1110 RE = DB * US * PL * (1 - EG) / UL
1120 CRE = US * DB * PL / (UL * (1 - EG) ^ (M - 1))
1130 Z = 4.45 * CRE ^ ( - 0.1)
1140 FM = Z - M
1150  RETURN
1160 EG = X
1170 US = VG / EG + VL / (1 - EG)
1180  GOSUB 920
1190 UB = G * DB ^ 2 * (1 - EG) ^ (M - 1) * (PL - PB) / (18 * UL * (1 + .15 * RE ^ .68
1200 XI = 1 + 0.55 * EG
1210 UB = UB / XI
1220 F = US - UB
1230  RETURN
```